Temporally and spatially controlled delivery from electrospun biopolyesters

Nicolas Lavielle

UNIVERSITÉ DE STRASBOURG

EMPA
Materials Science & Technology

Thèse présentée pour obtenir le grade de Docteur

de l'Université de Strasbourg en Physique et Chimie Physique

FABRICATION DE NANOFIBRES ET NANOPARTICULES DE BIOPOLYESTERS POUR LA LIBERATION CONTROLEE D'UN COMPOSE MODELE

Présenté par:

Nicolas Lavielle

Soutenue le vendredi 29 Novembre 2013

Membres du jury:

Prof. K. De Clerck (Univeristy of Ghent, Belgium),

Prof. F. Bossard (University of Joseph Fourier, Grenoble, France)

Prof. P. Schaaf (University of Strasbourg, France)

Prof. L. Thöny-Meyer (ETH Zurich, Switzerland)

Dr. R. Rossi (Empa, ETH domain, Switzerland)

Prof. G. Schlatter (University of Strasbourg, France)

OUTLINE

CHAPTER I/

INTRODUCTION: STATE OF THE ART AND PROPOSED STRATEGIES p.13

SUMMARY OF THE PHD THESIS

Electrospinning of biopolyesters in acidic solvent systems – Control of the nanofiber morphology

Electrospinning is widely used for the synthesis of nanofibrous non-woven membranes. The fabricated electrospun membranes have high porosity and high surface to volume ratio; they are thus suitable for many applications such as sensing, tissue engineering or drug delivery.

In the present work, the first focus was on the fabrication of electrospun fibers with controlled morphology and dimension. Thus, a new approach was developed for the controlled fabrication of ultrathin electrospun poly(Ɛ-caprolactone) (PCL) nanofibers, with diameters ranging from 150 to 400 nm, from a solvent system based on a mixture of acetic acid and formic acid [1]. The possibility of tuning the diameter and morphology of the nanofibers by the in-situ modification of the molecular weight of the polymer was demonstrated for the first time, a consequence of the hydrolytic degradation to which the polyester is subjected in aqueous acidic medium. A study of the PCL degradation kinetics enabled precise adjustments of polymer molecular weight and thus of the solution viscosity. Hence, regimes and boundaries of PCL electrospinning in this solvent system could be determined, ranging from electrospraying of nanoparticles to continuous fiber electrospinning (Figure A). This strategy was applied for the electrospinning and electrospraying of polylactic acid (P(D,L)LA) materials from similar acidic solvent systems.

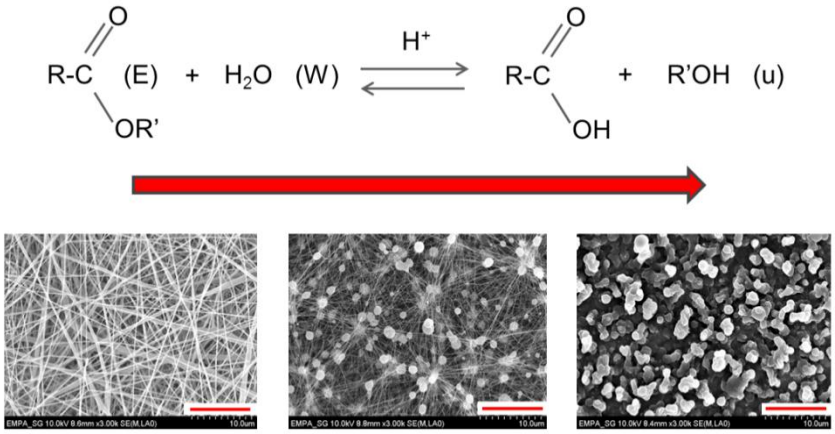

Figure A: *From PCL nanofibers to nanoparticles via hydrolytic degradation - Effect of the solution viscosity. (Scale bar= 10µm)*

Fabrication of hierarchical self-organized composites by combining electrospinning and electospraying technologies

Electrospinning generates nanofibrous membranes with pore sizes in the micron range. Random deposition of the nanofibers results in the fabrication of non-woven membranes. Several strategies have been developed to control the deposition of the nanofibers and thus the structure of the membrane as the use of micropatterned collectors [2] or self-organization of bimodal-sized nanofibers [3,4]. A self-organized honeycomb-like composite made of simultaneously electrosprayed PEG microparticles and PLA electrospun fibers was developed for the first time [5]. The mechanism of self-organization between fibers and particles into growing honeycomb patterns and its evolution as a function of the thickness of the composite was investigated. It was demonstrated that aggregates of particles, leading to a non-uniform distribution of the electrostatic field near the collector, are necessary to form the self-organized composite. Furthermore, it was shown that the specific dimensions of the generated

patterns can be controlled by tuning the flow rate of electrospraying. The obtained composite mat exhibits a hierarchical, porous structure with pore sizes ranging from few microns up to several hundreds of microns (Figure B). This strategy was used with drug-loaded PLA fibers for directional drug delivery.

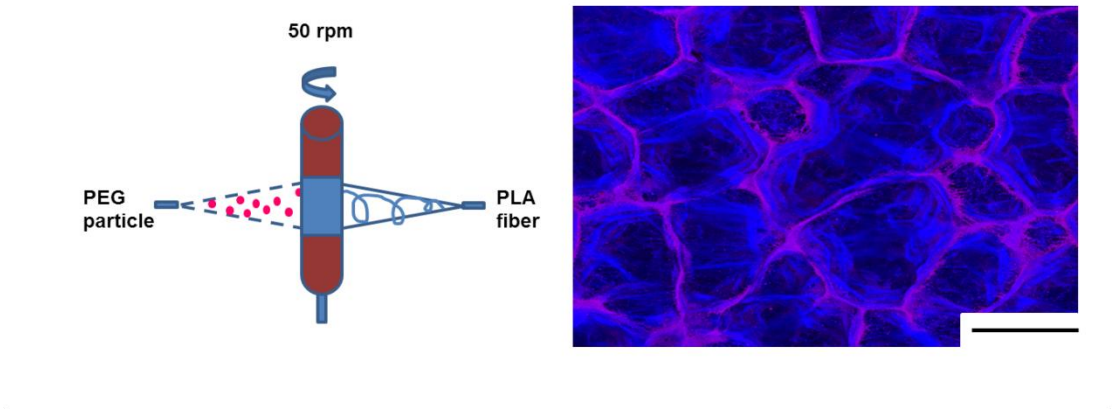

***Figure B**: Fabrication of honeycomb-like structured composites combining electrospinning and electrospraying technologies. (Scale bar = 500µm)*

Temporally and directionally controlled delivery

A method tailoring the hydrophobicity of drug loaded nanofibrous membranes by the incorporation of electrosprayed PEG microparticles was developed [6]. The impact of the hydrophobicity was investigated for drug loaded PLA composite membranes made of nanofibers and nanoparticles. The addition of the PEG microparticles into the nanofibrous mat changed the water contact angle from 132±4° to 24±6° and drastically impacted the drug release profile. This approach was further developed for the fabrication of micropatterned composite membranes with spatially tailored hydrophobicity for spatiotemporally controlled

drug delivery. Indeed, it was demonstrated that an amphiphilic nanofibrous membrane could be engineered for directional delivery (Figure C) and micropatterned sandwich-like membranes for sustained delivery from nanoparticles to a targeted site. Such advanced membrane design with tailored hydrophobicity over the microstructure of the membrane enables spatially and temporally controlled drug delivery suitable for biomedical applications.

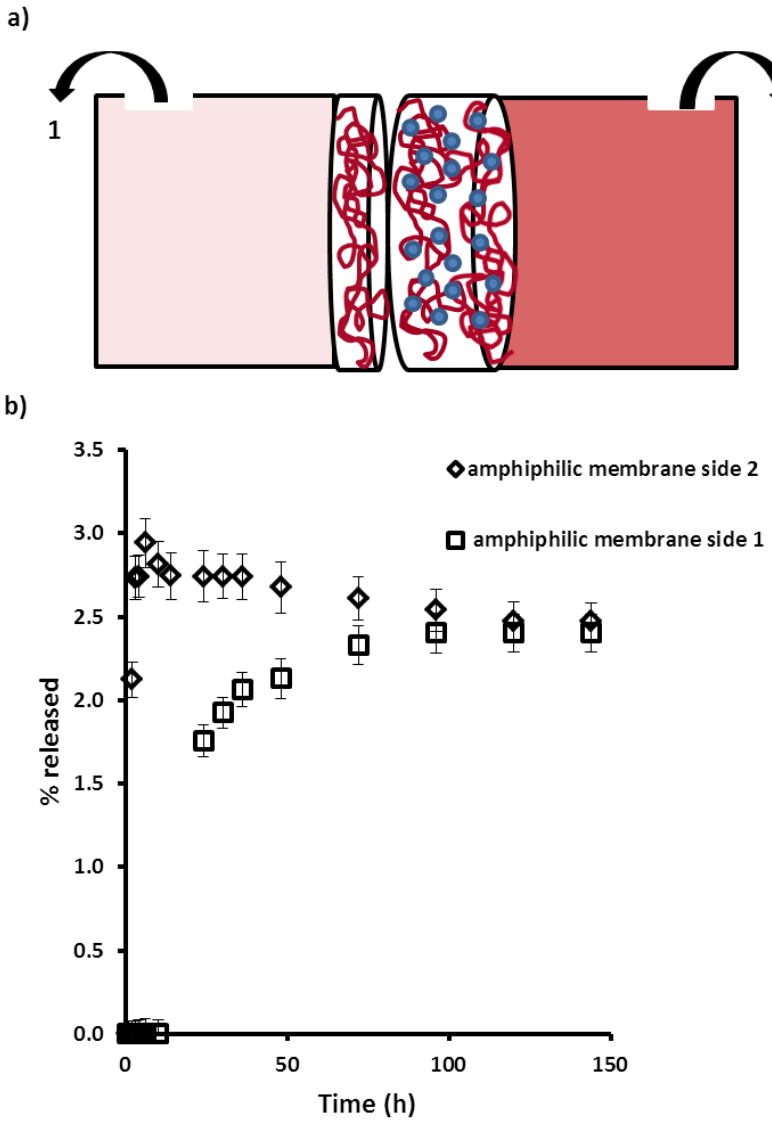

Figure C: *Schematic illustration of the experimental setup using a permeation cell loaded with an amphiphilic membrane (a). Percentage of cumulative release from an amphiphilic nanofibrous membrane in PBS at 25°C as a function of time (b).*

References:

[1] N. Lavielle et al., *Eur. Polymer J.* **2013**, *49*, 1331-1336

[2] N. Lavielle et al., *Macromol. Mater. Eng.* **2012**, *297*, 958-968

[3] D. Ahirwal et al., *Soft Matter* **2013**, DOI: 10.1039/C2SM27543K

[4] N. Lavielle et al., *Langmuir*, manuscript in prep., **2013**

[5] N. Lavielle et al., *ACS Appl. Mater. Interfaces*, manuscript accepted, September, **2013**

[6] N. Lavielle et al., *J. Controlled Release*, manuscript in prep., **2013**

PUBLICATIONS OF THE PHD THESIS

- **In peer-reviewed journals:**

N. Lavielle, A. M. Popa, M. de Geus, A. Hebraud , G. Schlatter, L. Thöny-Meyer, R. M. Rossi, Controlled formation of poly(Ɛ-caprolactone) ultrathin electrospun nanofibers in a hydrolytic degradation-assisted process, ***Eur. Polym. J***., **2013**, 49, 1331-1336

N. Lavielle, A. Hébraud , G. Schlatter, L. Thöny-Meyer, R. M. Rossi, A. M. Popa, Simultaneous electrospinning and electrospraying: A straightforward approach for fabricating hierarchically structured composite membranes, ***ACS Appl. Mater. Interfaces***, **2013**, 5, 10090-10097

N. Lavielle, A. Hébraud , G. Schlatter, L. Thöny-Meyer, R. M. Rossi, A. M. Popa, Tailoring the hydrophobicity of micropatterned electrospun nanofiber and nanoparticle composite membranes for spatially and temporally controlled drug delivery, **in prep. for *J. Controlled Release*, 2013**

- **In international conferences - Oral contributions:**

September 2013: EUROMAT 2013, European Congress and Exhibition on Advanced Materials and Processes, Sevilla, Spain. N. Lavielle. Transversal porosity gradient in electrospun biopolyester nanofibrous membranes for directional drug delivery- Focus on drug delivery

June 2013: EPF 2013, European Polymer Congress, Congress palace, Pisa, Italy. N.Lavielle. Transversal porosity gradient in electrospun biopolyester nanofibrous membranes for directional drug delivery- Focus on composite self-organization

March 2012: Electrospinning: Principles, Possibility and Practice, Institute of Physics, London, UK. N.Lavielle. Controlled formation of polycaprolactone ultrathin electrospun nanofibers in a hydrolytic degradation-assisted process

CHAPTER I/

INTRODUCTION: STATE OF THE ART AND PROPOSED STRATEGIES

Electrospinning of biopolymers can be used to fabricate nanofibers for drug delivery applications. Indeed, a compound can functionalize nanofibers in electrospun membranes and exhibit controlled delivery. Depending on the degree of polymer chain entanglements, electrospinning lead to the fabrication of nanofibers or nanoparticles. In the latter case, the process is called electrospraying, and nanoparticles are known carriers for controlled drug delivery as well. First, the electrospinning and electrospraying process will be described and a review will be performed on the different drug loading strategies, their impact on drug release profiles and the interest of designing advanced membranes for temporally controlled delivery. The strategies used to control the microstructure and architecture of electrospun membranes allowing spatially controlled delivery will be analyzed. Then, in the chapter called "proposed strategies", the reasons for which the different polymers and model drug were chosen will be discussed, the drug loading strategy, the drug release mechanism and my approach for controlling the morphology and microstructure of the electrospun membranes.

A) State of the art

1) Electrospinning and electrospraying process

Electrospinning has been extensively explored during the last decades as a method for the fabrication of micro and nanofibrous nonwovens [1-2]. A typical electrospinning setup, schematically represented in Figure 1a, is composed of a source-electrode-needle through which a polymer solution is injected at a controlled rate, a ground-electrode-collector and a high-voltage power supply. The polymer jet stretches under the action of the electrostatic field (Figure 1b). The jet is elongated due to whipping movements, which favors the rapid evaporation of the solvent and induces the generation of nanofibers (Figure 1c). The nanofibers are collected on a ground-collector as a functional non-woven membrane. Nanofibrous membranes find applications in many fields [3], such as sensing [4], tissue engineering platforms [5] or drug delivery devices [6]. The created membranes possess high surface-to-volume ratio, high porosity, surface for functionalization, small inter-fibrous pore size and high degree of pore interconnection [7-8]. Electrospinning allows the use of a wide range of materials in or on which one can introduce drugs for diffusion or diffusion and degradation drug delivery mechanisms [9]. Compounds such as antibiotics, anti-inflammatories, enzymes, proteins, DNA can functionalize the nanofibers. Strategies for the functionalization of the fibers include coating, embedding and encapsulation [7]. The chosen strategies impact the release kinetics [6].

Electrospraying is a process used for the fabrication of micro and nanoparticles. Electrospraying is very similar to electrospinning and the same setup can be used (Figure 1d) [10]. In the presence of a high difference of voltage, the electrostatic field is responsible for the formation of sprayed particles collected on a substrate (Figure 1e and f). The main

difference between the two processes is the presence and quantity of polymer chain entanglements in the polymer solution. Under identical electrospinning conditions, by simply decreasing the number of polymer chain entanglements in the solution, the morphology can be varied from regular nanofibers to beaded nanofibers and to particles [11-13]. Drug loaded electrosprayed particles have been successfully prepared and the process has shown efficient drug encapsulation [14]. Recently, a review has been published on electrospraying of polymers with therapeutic molecules by Bock et al. [13], showing that temporally controlled release can be achieved with the use of electrosprayed particles.

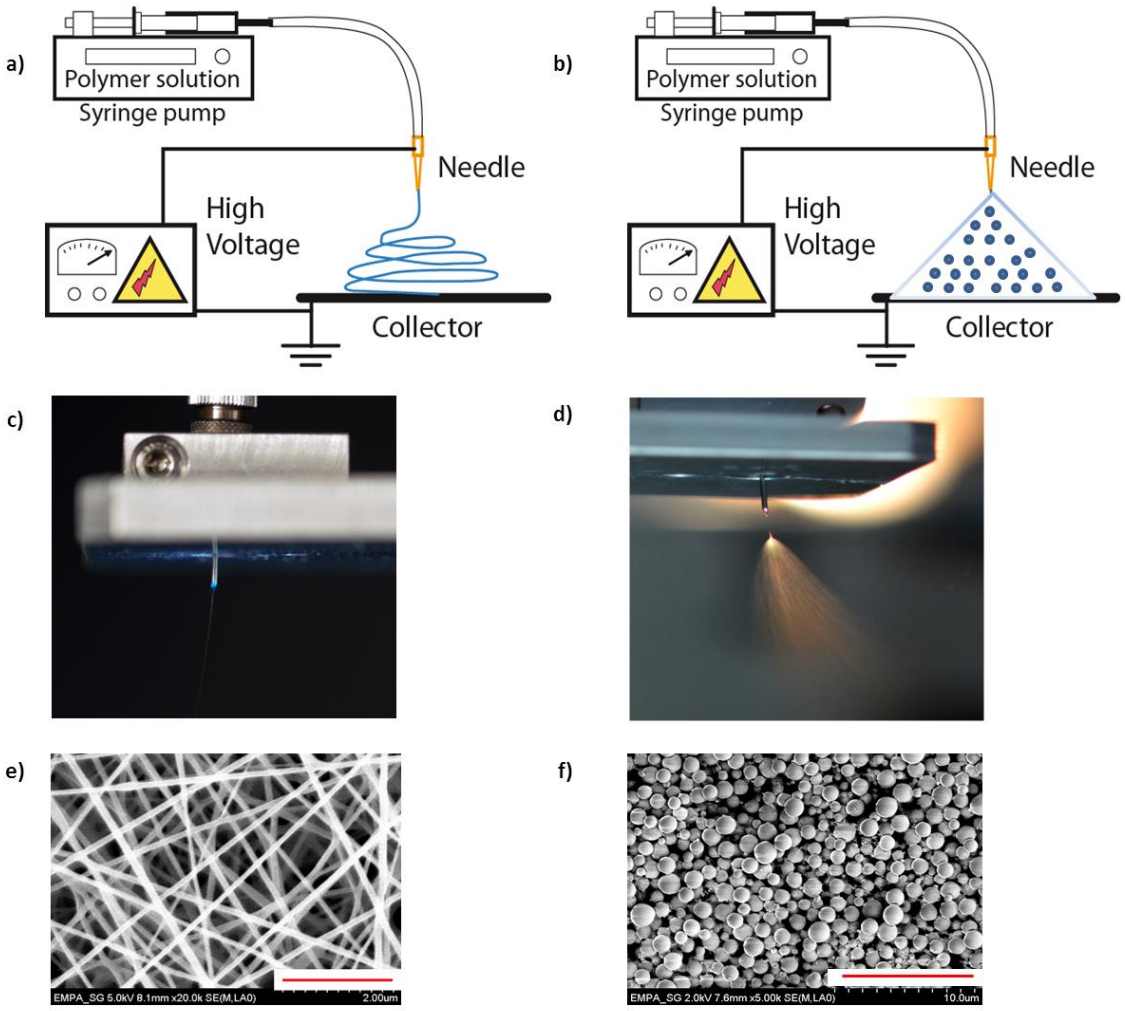

Figure1: Electrospinning versus electrospraying: a) Schematic illustration of the electrospinning (a) and electrospraying (b) setups. Corresponding images of the jet at the exit of the needle (c and d). Corresponding scanning electron microscope (SEM) images of the morphology obtained for PLA of different molecular weights (e and f).

2) Temporally controlled drug release from nanofibrous membranes

Researchers focused on the ability of electrospun nanofibers to release drug in a controlled manner. In this chapter, the first focus will be on the different drug loading strategies, and then will investigate the drug release mechanisms and the impact of electrospinning process on release profile. To conclude this chapter, the release from multicomponent scaffolds and the fabrication of advanced scaffolds for temporally controlled drug delivery will be studied.

a) Drug loading strategies and impact on release profiles

Three main strategies are involved in the functionalization of nanofibrous membrane by insertion of a drug: surface fibers loading, fibers embedding and fibers encapsulation (Figure 2). Surface functionalization, presented in Figure 2a, is possible by physical or chemical post-electrospinning immobilization. Due to high surface to volume ratio, a consequent amount of drug can be loaded on the nanofibrous mat. This strategy often leads to an initial burst release of the compound followed by the delivery of the remaining amount of drug in a short time. To enhance the drug loading capacity or to delay the release, plasma treatment, chemical treatment, or surface graft polymerization can be envisaged [15]. The adsorptions of nanoparticles, layer-by-layer assembly of polyelectrolytes or chemical immobilization of active drugs are also possible to tailor the release profile [9]. Drugs can also be embedded into the fiber by blend electrospinning (Figure 2b). As such, the active ingredient is solubilized in the polymer solution before electrospinning. Commonly used solvents in electrospinning can denature the drug and lead to the loss of its bioactivity. The choice of the solvent is as such primordial to maintain drug efficiency [16-18]. The presence of charged drugs can lead to a non-uniform distribution of the drug within the fiber volume. The drug can also be

encapsulated in the fiber. Fibers encapsulation, the drug is present only in the core of the fiber, can be performed with co-axial electrospinning and emulsion electrospinning. Emulsion electrospinning, presented in Figure 2c, involves the simultaneous spinning of two immiscible solutions. The drug is in a dissolved solution forming the disperse phase. The continuous phase is the polymeric solution. During the electrospinning process, the continuous phase evaporates rapidly in the air with an increase of viscosity, leading to a viscosity gradient that trigers the migration of the droplets to the center of the jet. Mutual dielectrophoresis induces the coalescence of the droplets under the electric field and generates core-shell structured fibers. Dielectrophoresis is the action of coalescence of droplets driven by an electric field, which leads to an arrangement in columns structure. One can also observe a core formed of droplets when coalescence is not occurring because of higher Rayleigh instability. Indeed, it was shown that the surface energy of a particular volume of fluid in the form of a cylindrical jet is higher than the one of the same volume divided into droplets [1]. Viscoelasticity and interfacial tension of the dispersed phase are supposed to regulate this phenomenon [19-21]. Co-axial electrospinning (Figure 2d) involves the use of a co-axial needle in the electrospinning setup. Two solutions are independently pumped through a coaxial nozzle submitted to the electric field. This technique allows a wide range of choice for drug and polymer solvents and permits the fabrication of core-shell nanofibers [22]. The chemical interactions of the two phases are primordial for the electrospinnability of the core-shell. When using two immiscible solvents, one can use a common solvent in the two immiscible solutions to increase electrospinnability. Studies showed that the ratio of the flow rates of the sheath and core solutions is an important parameter to be considered for the electrospinnability [23].

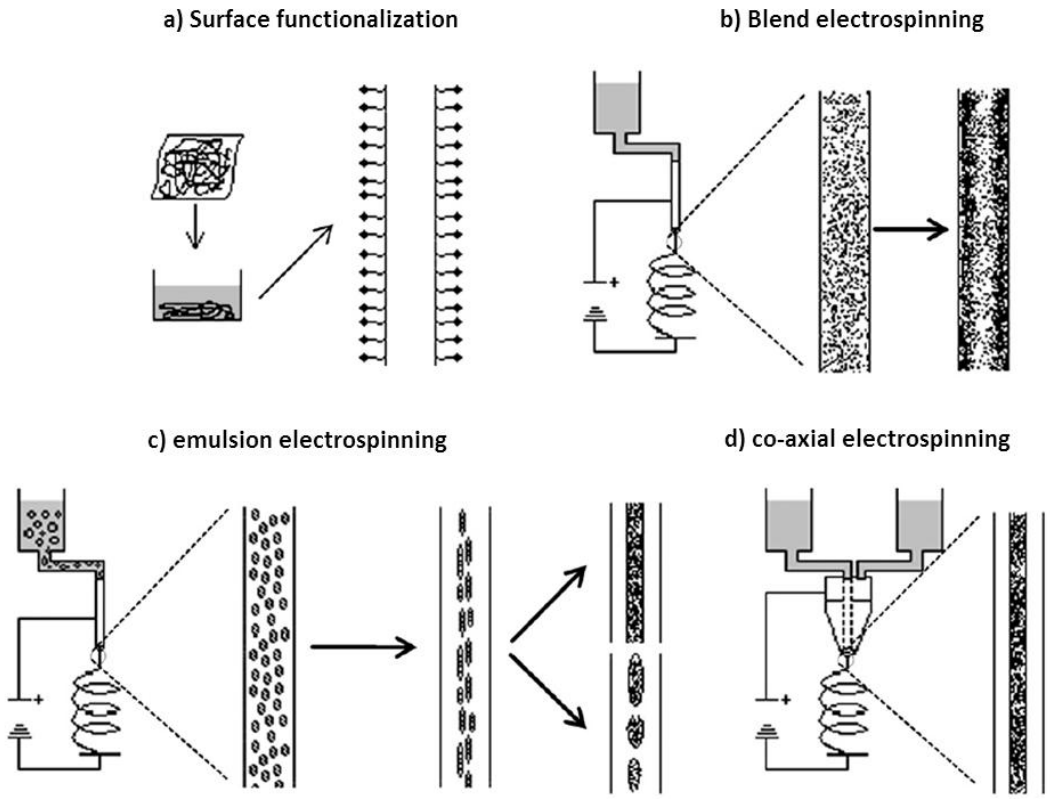

Fig.2: Scheme of electrospinning drug loading strategies and expected redistribution of the drug within the fiber volume (adapted from ref. [9]).

Considering drug spatial distribution within the fibers, some studies showed a radial migration of the drugs to the surface of the fibers, leading to a non-uniform drug distribution in the fibers. Most bioactive molecules are charged molecules that are submitted to charge repulsion during the electrospinning process. This field driven surface migration is governed by charge repulsion leading to surface enrichment of drugs [24-25]. It can occur for blend electrospinning, emulsion electrospinning and co-axial electrospinning. In the case of blend electrospinning, the redistribution of the drug in the fibers impacts the release profile of the compound. In the case of emulsion and co-axial electrospinning, redistribution occurs but the mechanism of release is not the distribution but the diffusivity of the drug through the barrier.

b) Drug release mechanisms from electrospun nanofibers

Drug release from electrospun nanofibers can be governed by three types of release profiles due to diffusion (drug release by diffusion of the drug from the polymer fiber), bulk (release by erosion of the fibrous membrane) and surface erosion (release by erosion of the surface of the fibrous membrane), presented in Figure 3. Diffusive release mechanism is most commonly seen from drug-loaded electrospun nanofibers [9]. Mean diffusion distance, diffusivity of the drug through the polymer fiber and polymer matrix and concentration gradient control the release kinetics from diffusive release mechanism systems. In the case of surface loading, diffusion is taking place and generates a burst release followed by short-period release of the compound. One can also setup a diffusion mechanism through a barrier. This system can be generated by co-axial electrospinning or emulsion electrospinning as discussed previously. The core would contain the drug and act as a reservoir and the shell would be used as the barrier for diffusion. The barrier can also be a layer membrane that the drug would have to cross to reach the release environment. If the diffusion rate through the barrier is sufficiently low compared to the reservoir capacity and the rate of drug clearance in the release environment, one can create a near constant concentration gradient, meaning a constant delivery over time [26]. In such a system, one has to consider the changing parameters over time as barrier erosion in the case of degradable polymer or reservoir depletion. Such systems are not widely studied and promise great opportunities in temporally controlled drug delivery.

One can also setup a system where the drug release will be governed by a matrix degradation and erosion mechanism. Biodegradable polymers are here directly concerned. Crystallinity and molecule orientation can both prevent drug release diffusion [27]. Degradation is defined

by the decrease of average molecular weight. It can be surface or bulk degradation type. Erosion is defined by the decrease of total mass. Erosion and degradation take place in the same time in the case of surface degradation as oligomers are free for environment diffusion. In the case of bulk degradation, erosion is delayed until the average molecular weight of the bulk matrix is low enough to allow diffusive loss of oligomers [27]. In case of bulk erosion, diffusion is the driving mechanism of drug release. In the first stage, release is governed by diffusion mechanism of the drug leading to an initial burst release. In the intermediate stage, a characteristic equilibrium constant release is observed due to diffusive ability of the drug in the fiber matrix and mat. In the last phase, erosion mechanism is important when bulk erosion is advanced enough to allow broader diffusion of the drug; a late burst release is then observed [28]. In case of surface erosion, one can observe a linear release profile correlating with the rate of surface erosion. Indeed, erosion agents are only present on fibers surface, diffusion mechanism can be neglected as the inner polymer matrix is not involved [29]. However, polymers can exhibit a dual surface and bulk eroding behavior, the control over drug delivery has to be tuned by the formulation, the loading strategy or advanced electrospinning technique. Degradation environment, material properties, and dimensions and structure of the scaffold directly impact degradation characteristics.

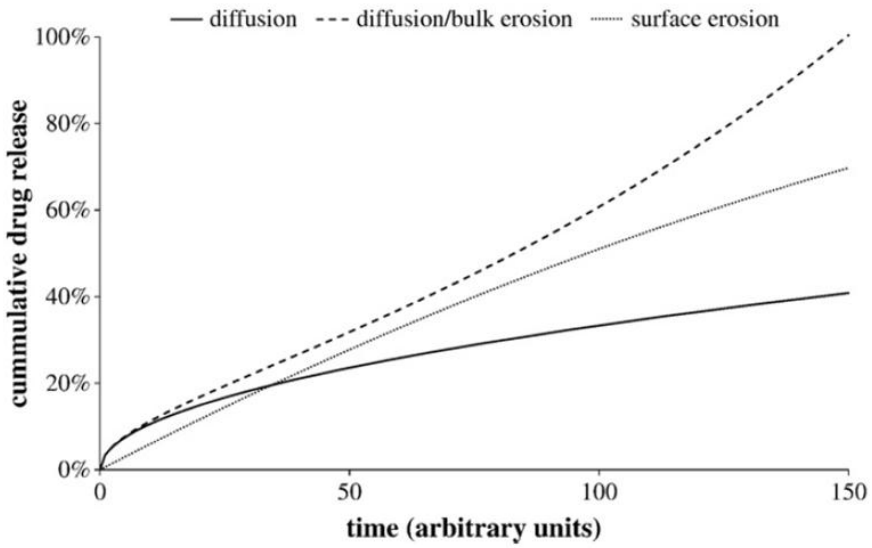

Figure 3: Comparison of different characteristic release profiles due to diffusion, bulk and surface erosion in the case of uniform distribution of drug in the fibers (adapted from ref. [9])

c) Multicomponent release and advanced membrane design

Temporal drug release from nanofibrous membranes depends also on scaffold porosity and fibers dimensions and morphology. Hence, the use of multicomponent scaffolds allows combining different release profiles to create a complex, finely-tuned release profile. Multicomponent membranes multiply possibilities of scaffold design, scaffold structure and characteristics and offer a novel platform for drug delivery. The use of different fibers within a unique scaffold can be performed with a multi-needle electrospinning setup. Indeed, the presence of several needles with the corresponding high voltage supply allows a simultaneous electrospinning of different fibers, fabricating a unique scaffold (Figure 4a) [30]. Scaffold mechanical properties can be tuned with such a setup [31]. Multilayered scaffolds can be useful for tissue engineering applications to reproduce tissue structure and properties (Figure 4b). Each layer can be used to enhance scaffold properties, as a drug loaded layer, a layer for mechanical properties, a barrier layer or a cell specific functionalization layer. For example,

Bottino et al. used a multilayered strategy for the regeneration of alveolar bone using the membrane as an interface implant (Figure 4c) [32].

Some drug delivery systems require the use of several active compounds. Works on those membranes can provide different release profiles from different fibers within a unique scaffold. However, this strategy was under-investigated. Most reports are concerned with the embedding of several compounds within a fiber. Blend electrospinning can be used when two compounds are soluble in a common solvent. However, this method does not allo the production of scaffolds with different release profiles of the two drugs. A simultaneous release is mainly observed [33]. Emulsion electrospinning can generate multiphasic release with different release profiles with the incorporation of one drug in the continuous phase and another in the dispersed phase. However, for separation of the two release phases, a clear difference in time delivery is needed, indeed the chosen strategy has to generate a different release mechanism or an effective difference in diffusivity for a diffusion type mechanism. Low diffusivity is observed for drugs of high molecular weight or for surface eroding mechanism. Simultaneous release is often observed even when using emulsion or co-axial electrospinning. However, it is possible to use multicomponent membranes and separate the drugs. Researchers succeeded to fabricate multilayered scaffolds in which two different layers contained a specific drug, both separated by a barrier layer (Figure 4d) [34]. Such membrane design is appropriate for tailored release of different drugs.

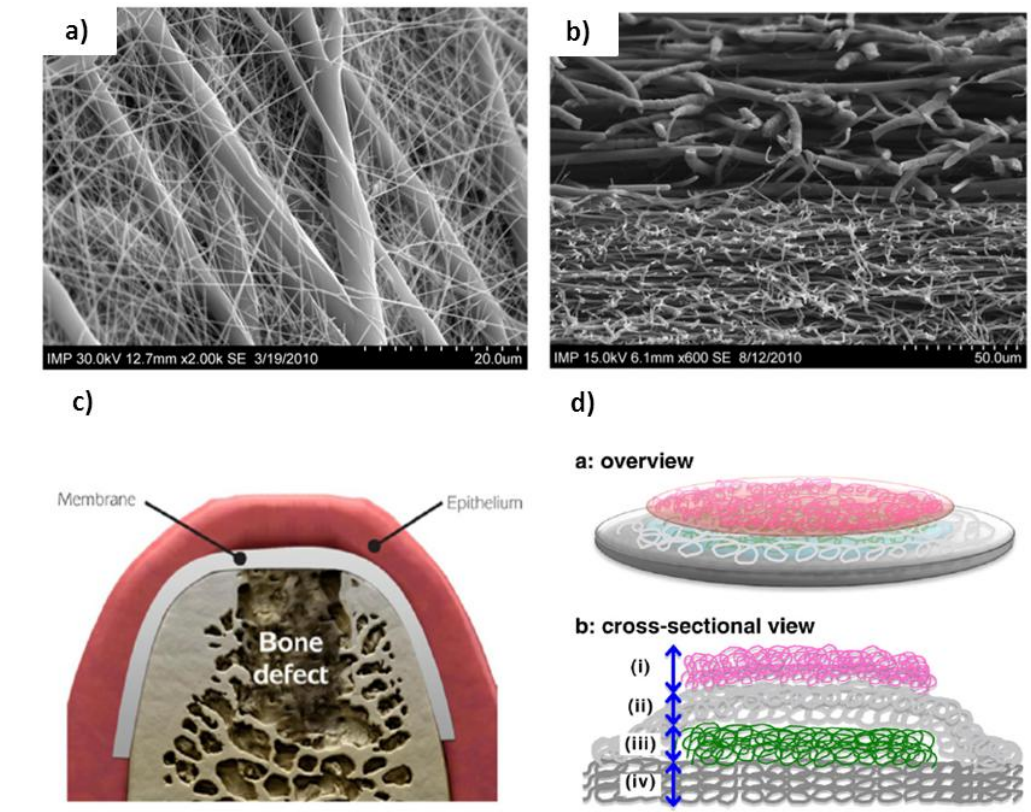

Fig.4: Advanced membranes design: a) Polyethylene oxide (PEO) nanofibers and PCL microfibers forming a unique scaffold; b) Example of bilayered electrospun PCL membrane with different fibers dimension and scaffold porosity (adapted from ref. [9]); c) schematic illustration of a periodontal membrane placed in a guided bone regeneration scenario (adapted from ref. [32]); d) schematical illustration of overview (a) and cross-sectional view (b) of a tetralayered nanofiber mesh composed of (i) the first drug-loaded mesh (top side), (ii) barrier mesh, (iii) the second drug-loaded mesh, and (iv) basement mesh (bottom side) (adapted from ref. [34]).

Work in that perspective can lead to the fabrication of materials that better mimic natural tissues for tissue engineering application and are on the path for spatially and temporally controlled drug. Another aspect of controlled drug delivery is the spatial control. Spatial control of membrane architecture will induce localized drug delivery. Spatial drug delivery control is important for drug delivery devices. Indeed, effective drug delivery systems should incorporate a control of the release kinetics and well-defined localized delivery. Some research has been done to reach controlled drug delivery from electrospun nanofibers; however new electrospun systems still need to be developed to create adequate scaffold properties and achieve a dual spatiotemporally controlled drug delivery.

3) Spatially controlled drug release from nanofibrous membranes

Most of the research performed on drug loaded nanofibrous membranes was focused on the control of the release kinetics achieving sustained or temporally controlled drug delivery. However, the structural aspect of the membrane has not been investigated in details so far [35]. Engineering 3D membranes with well-defined spatial organization of the drug within the mat offering both temporally and spatially controlled release is of great interest [35-36]. A comprehensive review on nanofibers for drug delivery has underlined the need to consider scaffold structure for the fabrication of advanced scaffold design for tissue engineering and drug delivery applications such as multicomponent electrospun membranes or 3D structures with defined porosity [9]. Indeed, electrospun membranes mimic the extracellular matrix of tissues and provide the required structural support for tissue regeneration [37-38]. Additionally, the presence of drug, adding functionality to structural support, is preferred to help the regeneration process, and spatially controlled release is critical for tissue formation [38-40].

a) Mechanism of non-woven mat fabrication

The electrospinning process generates disordered non-woven mats of nanofibers. To explain the generation of non-woven nanofibers, the effect of the main forces applied on the fiber during the electrospinning process has to be analyzed. During the process, the formed fiber is charged on its surface due to high voltage. The fiber is submitted to electrostatic forces due to the presence of an electrostatic field E and of the charges on the fibers. As the electrostatic field is uniform (Figure 5a), only the electric charges located on the surface of the fiber are responsible for the random deposition. Indeed, first of all, a droplet of solution is formed at

the exit of the needle accumulating charges, the Taylor cone. This cone was named the Taylor cone because Taylor studied the conical shape of a droplet under electrification. Then, the droplet is ejected into a fiber due to the accumulation of the charges on which are applied the electrostatic forces overcoming the surface tension forces. Instability of the jet is initially induced by electrical bending instability, amplified by repulsive electrostatic forces. These repulsive forces are responsible for the decrease of fiber diameter until submicron scale and for the jet random deposition [1] (Figure 5b).

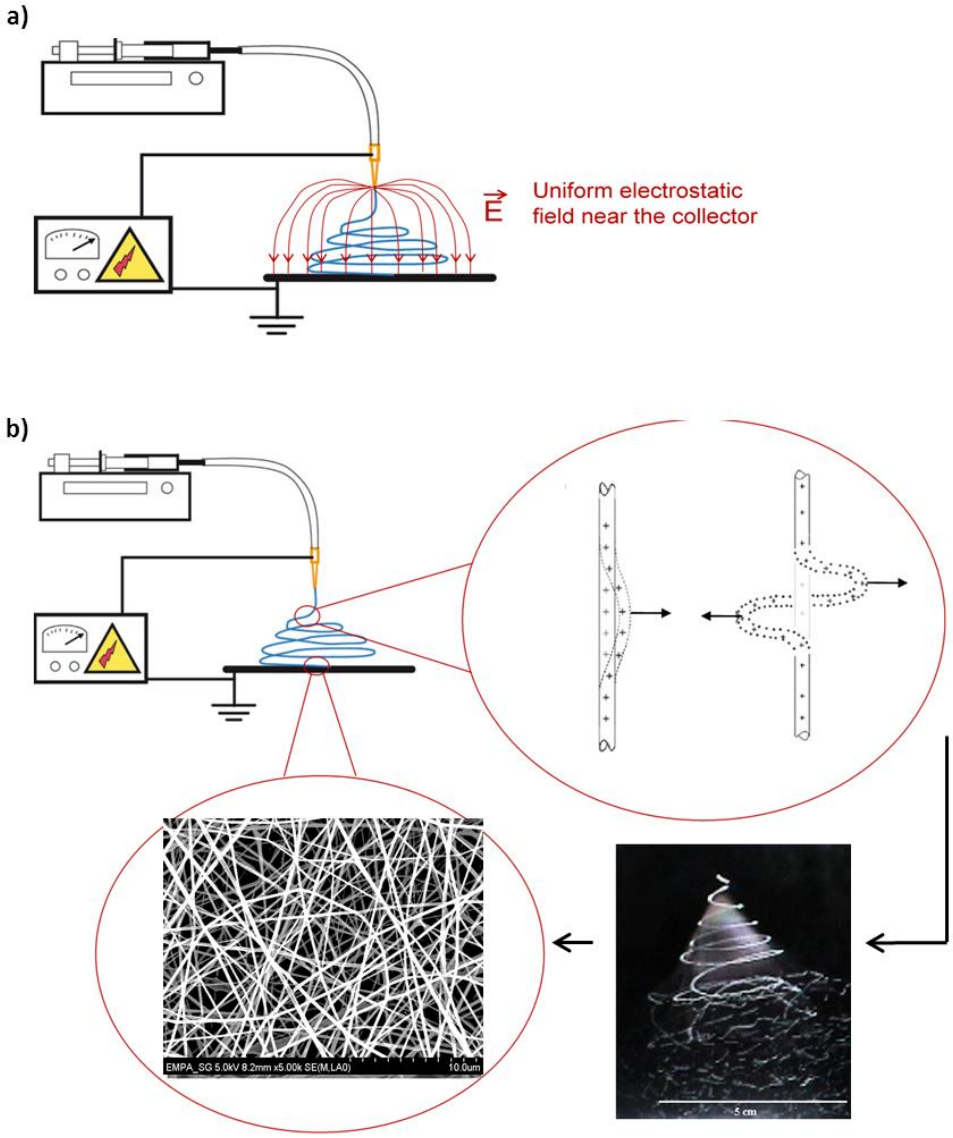

Figure 5: Random deposition of nanofibers in the electrospinning process: a) Electrostatic field generated by electrospinning process; b) From the initial bowing of the nanofiber to the non-woven nanofibrous mat.

Architecture control of the generated membrane is a relevant research field for the global control of electrospinning process and for many applications such as fiber reinforcement, fabrication of nanoscale fluidic, electronic, photonic devices, tissue engineering and drug delivery control. Several studies have been performed to control the deposition of the fibers and thus the structure of the generated mats. Aligned fibers [41-44], deposition control [45-47] and 3D structures [47] have been elaborated based on the control of the electrostatic forces applied on the fiber during electrospinning process. Indeed, as the electrostatic field is uniform during the electrospinning process, one can expect that the deposition of the fiber can be influenced by modulating the electrostatic field near the collector.

b) Deposition and architecture control

The electrospinning process usually leads to non-woven mats by the random deposition of nanofibers. However, the control over the organization of nanofibers in electrospun membranes would provide a great benefit for various applications [9]. Indeed, precise geometric design of multicomponent electrospun membranes or 3D structures with defined porosity and pore sizes are necessary to mimic tissue structure and properties for tissue engineering applications [9, 32] and to achieve spatially and temporally controlled release of different drugs for drug delivery applications [34-35].

A number of methods have been developed to control the deposition of the nanofibers and prepare structured membranes. For example, aligned electrospun fibers have been obtained by electrospinning on a rotating collector [42]. Moreover, one can align nanofibers by modulating the electrostatic field. D. Li and Y. Xia [41] showed that one can influence the nanofibers deposition by using dielectric material to pattern the collector. Indeed, they used a conductive collector (gold layer) with dielectric areas of quartz to modify the electrostatic

forces applied on the nanofibers near the collector and guide the deposition (Figure 6a). H. Yan and Z. Zhang [43] exhibited 3D alignment of the fibers by using the air gap between two conductive surfaces (Figure 6b). The geometry and the dielectric constant of the used materials generate a modified electrostatic field guiding the deposition of the fibers.

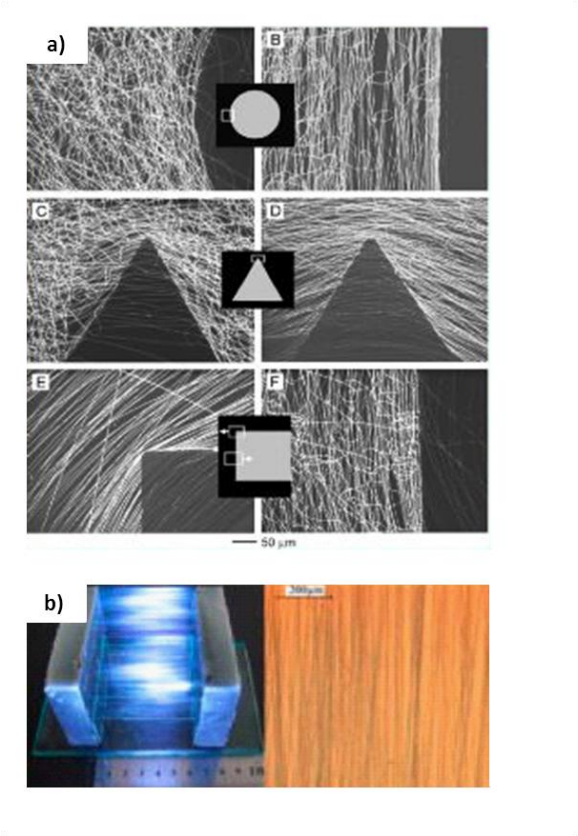

Figure 6: Nanofibers alignment: a) Dark field optical micrographs of nanofibers deposited on gold electrode with quartz dielectric areas. From Ref [41]; b) Electrospun nanofibers collected on an air-gap conductive collector and optical microscope image of the aligned fibers. From Ref [43].

Other complex 2D or 3D structured membranes have also been prepared using electrostatic forces [48-49]. The principle of this approach is the modification of the electrostatic field near the collector, thus guiding the deposition of the charged nanofiber. Deposition control and 3D structures can also be created using 3D structured conductive patterns as a collector (Figure

7a-c) [47]. Another type of structured membranes can be obtained by the self-organization of electrospun nanofibers. They have been first presented by Deitzel et al. [50] for poly(ethylene oxide) and then observed for other polymers [51-54]. Such self-organized mats are very interesting for tissue engineering applications as they can form 3D cm-thick hierarchical foams (Figure 7d) with adequate pore sizes and mechanical properties [54]. It was shown that a bimodal distribution of the fiber diameter is a necessary condition to induce the self-organization. Such irregular fibers, having thick and thin domains, locally impact the electrostatic field and guide the deposition of the fibers into honeycomb-like patterns [54]. In addition, structured membranes were also fabricated using diverse post-electrospinning structuring strategies: direct laser machining [55], wetting of porous template [56] or photopatterning of electrospun membranes [57].

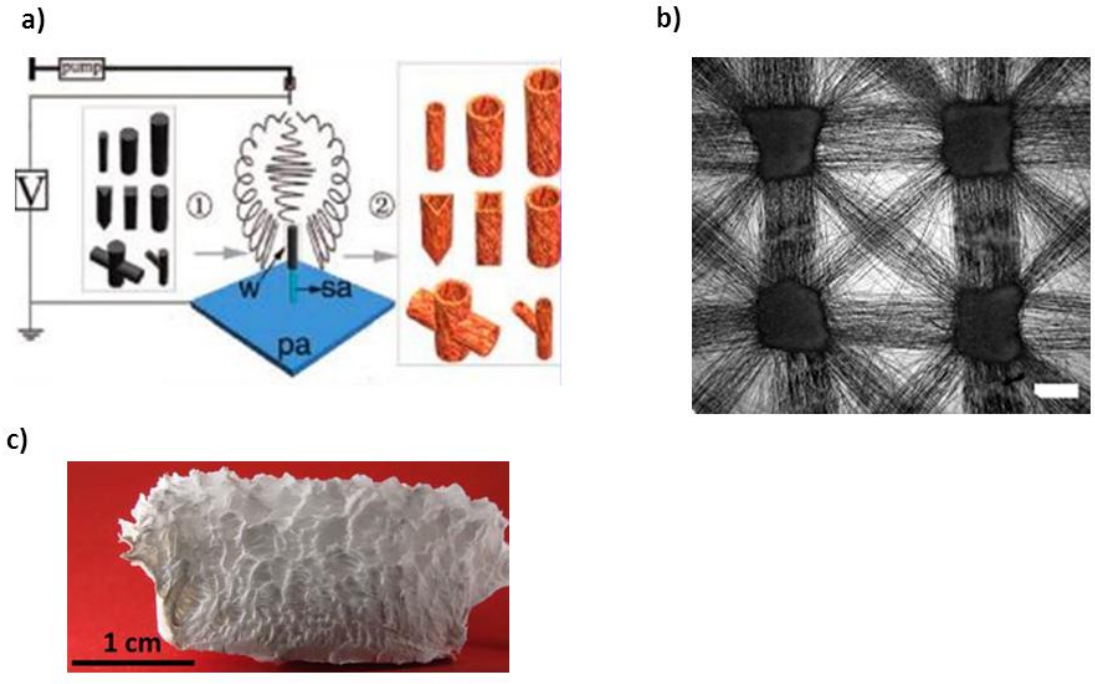

Figure 7: 3D structured membranes: a) Schematic illustration of the fabrication of fibrous tubes using 3D columnar collectors, b) SEM images of patterned architectures (scale bar=

100µm). (adapted from ref. [47]), c) Cross-section image of a 15 mm thick scaffold (adapted from ref.[54]).

B) Choices and strategies

1) Materials, drug loading and drug release mechanism

In this chapter, the materials chosen, the drug loading strategy and the drug release mechanism targeted will be discussed. Once defined, the strategy chosen to control the drug carrier morphology and the microstructure of the membrane for temporally and spatially controlled drug delivery will be presented.

As biomedical applications are targeted, biodegradable and biocompatible materials were considered. Biopolymers are directly concerned and processable with electrospinning. The following biocompatible polyesters were chosen for the study: poly(Ɛ-caprolactone) (PCL) and poly(D,L-lactide) (PLA), presented in Figure 8a and b, respectively. These biopolymers are widely studied for electrospinning, one can easily characterize them and several grades of different molecular weight are commercially available in large quantity. Biodegradable polyesters have been widely studied as electrospun materials, and extensive reviews have been published recently on this subject [58-59]. PCL was used as a starting material because the electrospinning ability of this material was already studied by us. Indeed, a new electrospinning setup was built for this project, and prior knowledge of the used material allowed getting familiar with the specific, new the setup. First, the control of the nanofibers morphology and diameter of PCL was investigated and then transposed to PLA. Indeed, PLA was the chosen material for the drug delivery application. Apart from its biocompatibility and biodegradability, P(D,L)LA , with a (D,L) ratio of 50/50, can be purchased as biomedical

grade and is an amorphous material, as shown in Figure 8c. An amorphous material was chosen because, as discussed previously, crystallinity is known to limit the diffusion of the drug within the polymer matrix. When using semi-crystalline polymers, like PCL, the drug mainly diffuses in the amorphous regions. A simple system was aimed, in which the absence of crystals will not disturb diffusion. Indeed, it was chosen to study the release kinetics of a model compound from the nanofibers by diffusive mechanism only. Once more, this choice was made to simplify the system and to allow studying the direct impact of the membrane morphology and microstructure on the release abilities. Consequently, P(D,L)LA was a good system as it is amorphous and begins to substantially degrade by surface erosion mechanism in our release medium after 2 weeks only. Hence, the drug release study was restricted to 150 hours, in order to have a drug release governed by diffusion mechanism only.

Regarding the solvents used for the electrospinning of PCL and PLA, a solvent system dissolving both materials was needed to enable the transfer of knowledge of one material to the other. PCL is usually dissolved in halogenated solvents and the obtained fibers have diameters in the micrometer or sub-micrometer range [60-62]. As such, much effort was directed towards the development of new systems which allow a more precise control of the PCL nanofiber morphology and diameter [58, 63-64]. Luo et al. recently studied the influence of solubility and dielectric constant of various solvents on the electrospinning of PCL and discussed the impact of the dielectric constant on the diameter of the produced fibers [65]. In a recent report, Van der Schueren et al. [66] showed the steady state formation of PCL fibers with micron-size diameters when electrospun from chloroform and with diameters as low as 270 nm when using formic acid and acetic acid as solvent system. Electrospinnability and fiber morphology of PCL from the acid mixture were studied in details. It was shown that the viscosity of the solutions remained constant up to three hours after solution preparation, a suitable time frame for having stable solution for electrospinning. It was thus decided to work

in the mixture of acetic acid and formic acid offering steady state electrospinning, and to explore the application of these solvents also to the electrospinning of PLA.

The choice of the model compound was influenced by several parameters. The chosen molecule had to be soluble and stable both in the solvents used for electrospinning and the release medium. Then, it was necessary to be able to characterize a low amount of drug using UV-VIS spectroscopy. Then, the strategy chosen to load the drug to the nanofibers was embedding by blend electrospinning. Embedding was chosen because it is easy to implement and the drug is theoretically homogeneously distributed in the volume of the fiber. Moreover, fiber embedding allows the drug to diffuse in the PLA polymer matrix and drug release governed by diffusive mechanism was targeted. To implement blend electrospinning, the chosen model compound had to dissolve in the solvent system of electrospinning, the mixture of acids. The model compound chosen, fulfilling all the above mentioned requirements and commonly used is Rhodamine B, presented in Figure 8d. Rhodamine B is often used as a tracer dye to determine the rate and direction of flow and transport. It was used here as a model compound. Rhodamine B is soluble in the mixture of formic acid and acetic acid and in phosphate buffered saline solution (PBS), the latter being the standard medium used for most drug release studies. Hence, the limit of detection and standard curves of Rhodamine B in PBS and in the mixture of acids at the wavelength of 550 nm were determined. In Figure 8e, the absorbance as a function of the compound concentration in PBS was plotted, as an example. The standard curve in PBS was used to determine the concentration of released drug and the one in acids to obtain the total amount of drug in the membranes in order to reach the percentage of drug released. To conclude, Rhodamine B was chosen to be embedded by blend

electrospinning to an amorphous PLA from a mixture of acids. The release test was performed in PBS over 150 hours allowing diffusive mechanism only.

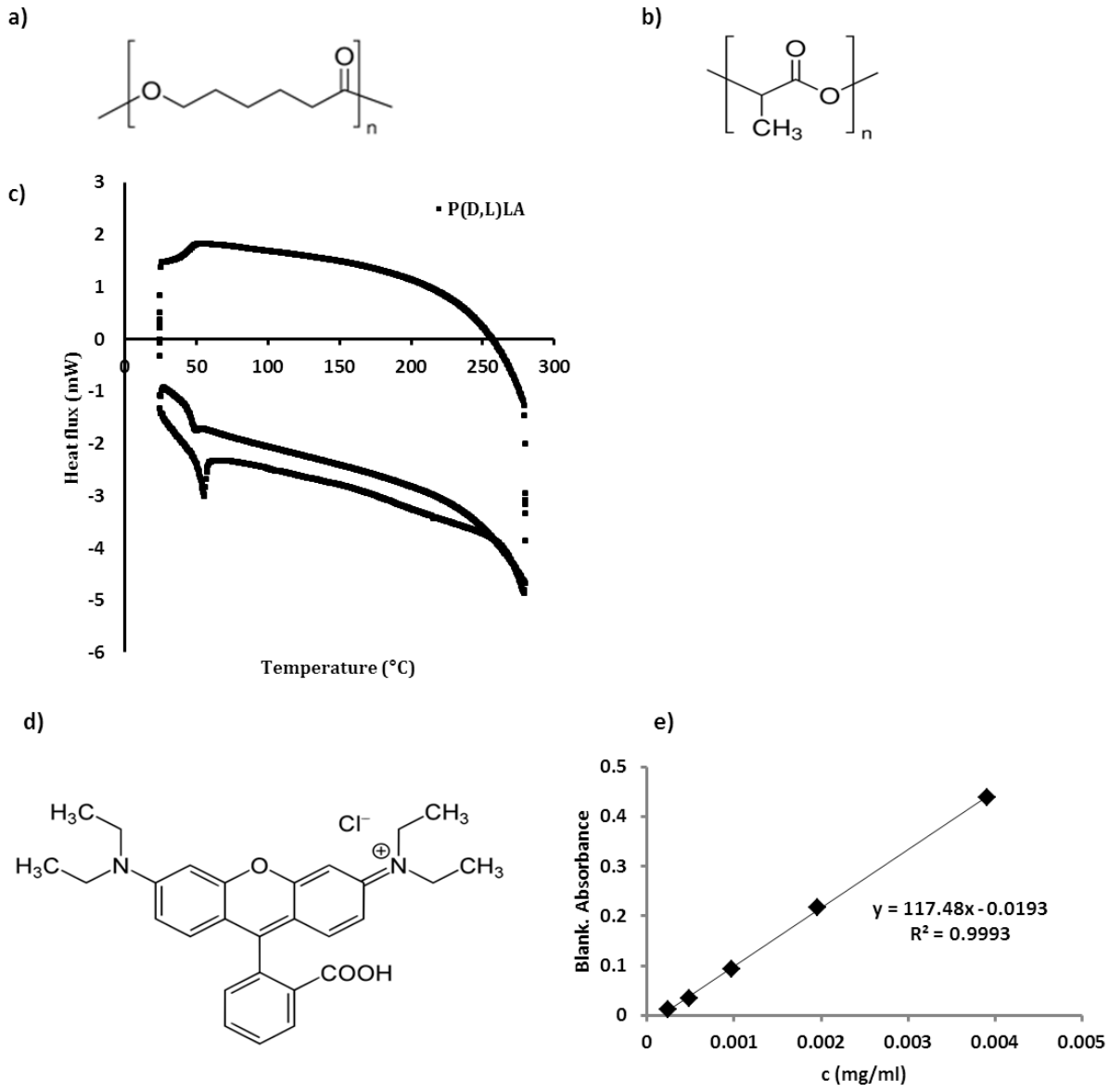

Figure 8: Materials choices and characterization: Chemical structures of PCL (a) and PLA (b). Differential scanning calorimetry (DSC) spectrum of the amorphous PLA (c). Chemical structure of Rhodamine B (d). UV-vis spectroscopy standard curve of Rhodamine B in PBS at 550 nm (e).

2) Control of the morphology and microstructure of the drug loaded membranes

Materials was selected, encapsulation strategy as well, and drug release was restricted to diffusive mechanism in an amorphous matrix. The process used was electrospinning, for the fabrication of nanofibers, and electrospraying, for the one of nanoparticles. The morphology and diameter of the yielded material impacts the drug release kinetics. It is thus primordial to control the morphology and diameter of the nanofibers. To this end, a study was performed on the electrospinning of PCL showing that one can tailor both. Indeed, a new approach for the controlled fabrication of ultrathin PCL electrospun nanofibers was designed, with diameters ranging from 150 to 400 nm, from a solvent system based on a mixture of acetic acid and formic acid. The possibility of tuning the diameter and morphology of the nanofibers by the in-situ modification of the molecular weight of the polymer was demonstrated, a consequence of the hydrolytic degradation to which the polyester is subjected in aqueous acidic medium. A study of the PCL degradation kinetics enabled precise adjustments of polymer molecular weight and thus of the solution viscosity. Hence, regimes and boundaries of PCL electrospinning in this solvent system could be determined, ranging from electrospraying of particles to continuous fiber electrospinning. Morevover, this strategy could be extrapolated to the electrospinning of any polyester which is soluble in the acid mixture. Additionally, the low toxicity of the solvent used makes this system very interesting for the production of scaffolds for biomedical applications. The knowledge on PCL was transposed to PLA successfully.

Once the morphology controlled, the membrane microstructure can be adressed. Nanofibers and nanoparticles morphologies were combined in a unique membrane. Thus, electrospinning and electrospraying were used to fabricate composite membranes with controlled structures.

To this end, a new and versatile electrospinning setup allowing multicomponent fabrication was fabricated (Figure 9). First, a general method for the fabrication of structured electrospun membranes was developed. The self-organization of electrosprayed microparticles and regular thin electrospun nanofibers into growing honeycomb-like patterns was demonstrated. The obtained composites presented a hierarchical porous structure with pore sizes ranging from a few microns up to hundreds of microns. Then, a strategy combining drug loaded hydrophobic nanofibers or nanoparticles with hydrophilic PEG microparticles was developed. The possibility to tailor the hydrophobicity of PLA electrospun nanofibers by the addition of PEG microparticles to impact drug release kinetics was studied and two new strategies based on the hydrophobicity control over the microstructure of the membrane for spatially and temporally controlled delivery were investigated.

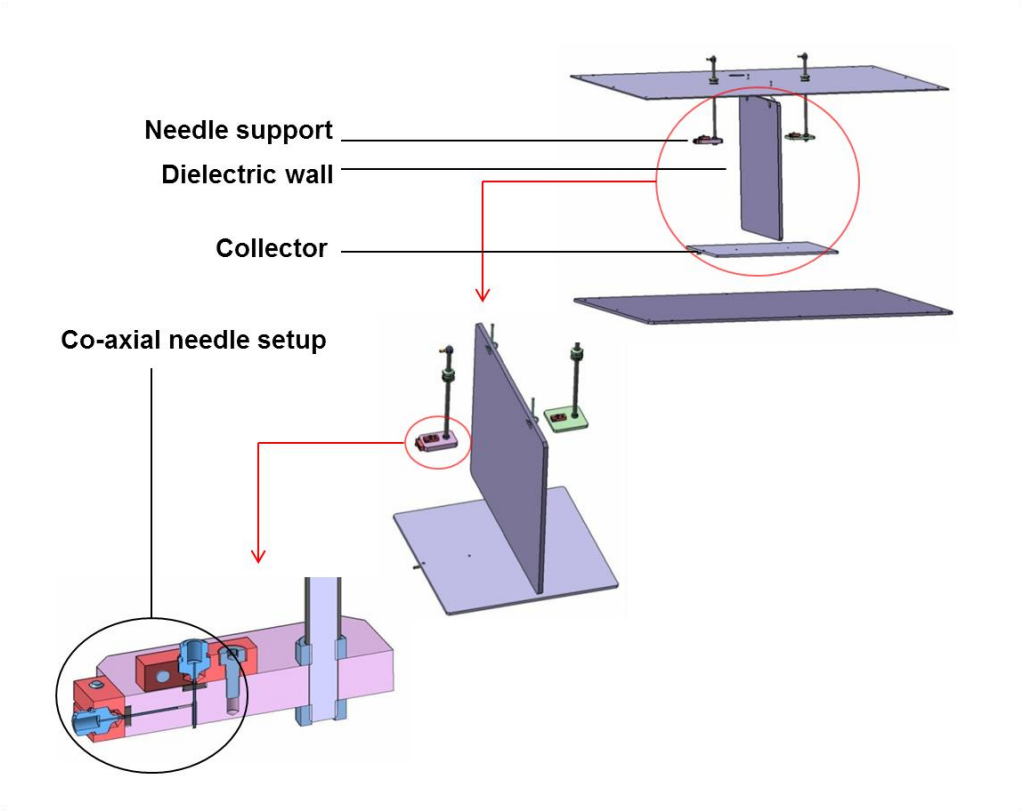

Figure 9: Vertical or horizontal electrospinning setup for multicomponent electrospinning with co-axial possibility. A rotating drum can also be used as collector.

The literature regarding drug loaded nanofibers underlined the need for spatially and temporally controlled delivery from electropun membranes. The choices for the used materials and the strategies were discussed and that the goal of the study was defined: The control of the morphology and microstructure of nanofibrous membranes for spatially and temporally controlled delivery. In chapter 2, the approach for controlling the morphology and dimension of the electrospun material will be discussed. Then, in chapter 3, the method developed for the fabrication of microstructured membranes will be studied. In chapter 4, one will show that multilayered membranes impact spatiotemporal delivery.

C) References

1. Reneker, D. H.; Yarin, A. L., Electrospinning jets and polymer nanofibers. Polymer 2008, 49 (10), 2387-2425.

2. Reneker, D. H.; Chun, I., Nanometre diameter fibres of polymer, produced by electrospinning. Nanotechnology 1996, 7 (3), 216-223.

3. Greiner, A.; Wendorff, J. H., Electrospinning: A fascinating method for the preparation of ultrathin fibres. Angew Chem Int Edit 2007, 46 (30), 5670-5703.

4. Popa, A. M.; Eckert, R.; Crespy, D.; Rupper, P.; Rossi, R. M., A new generation of ultralight thermochromic indicators based on temperature induced gas release. J Mater Chem 2011, 21 (43), 17392-17395.

5. Guex, A. G.; Kocher, F. M.; Fortunato, G.; Korner, E.; Hegemann, D.; Carrel, T. P.; Tevaearai, H. T.; Giraud, M. N., Fine-tuning of substrate architecture and surface chemistry promotes muscle tissue development. Acta Biomater 2012, 8 (4), 1481-1489.

6. Sill, T. J.; von Recum, H. A., Electro spinning: Applications in drug delivery and tissue engineering. Biomaterials 2008, 29 (13), 1989-2006.

7. Wang, B. C.; Wang, Y. Z.; Yin, T. Y.; Yu, Q. S., Applications of Electrospinning Technique in Drug Delivery. Chem Eng Commun 2010, 197 (10), 1315-1338.

8. Huang, S.; Fu, X. B., Naturally derived materials-based cell and drug delivery systems in skin regeneration. J Control Release 2010, 142 (2), 149-159.

9. Szentivanyi, A.; Chakradeo, T.; Zernetsch, H.; Glasmacher, B., Electrospun cellular microenvironments: Understanding controlled release and scaffold structure. Adv Drug Deliver Rev 2011, 63 (4-5), 209-220.

10. Jaworek, A., Electrospray droplet sources for thin film deposition. J Mater Sci 2007, 42 (1), 266-297.

11. Morota, K.; Matsumoto, H.; Mizukoshi, T.; Konosu, Y.; Minagawa, M.; Tanioka, A.; Yamagata, Y.; Inoue, K., Poly(ethylene oxide) thin films produced by electrospray deposition: morphology control and additive effects of alcohols on nanostructure. J Colloid Interf Sci 2004, 279 (2), 484-492.

12. Lavielle, N.; Popa, A. M.; de Geus, M.; Hebraud, A.; Schlatter, G.; Thony-Meyer, L.; Rossi, R. M., Controlled formation of poly(Ɛ-caprolactone) ultrathin electrospun nanofibers in a hydrolytic degradation-assisted process. Eur Polym J 2013, 49 (6), 1331-1336.

13. Bock, N.; Dargaville, T. R.; Woodruff, M. A., Electrospraying of polymers with therapeutic molecules: State of the art. Prog Polym Sci 2012, 37 (11), 1510-1551.

14. Valo, H.; Peltonen, L.; Vehvilainen, S.; Karjalainen, M.; Kostiainen, R.; Laaksonen, T.; Hirvonen, J., Electrospray Encapsulation of Hydrophilic and Hydrophobic Drugs in Poly(L-lactic acid) Nanoparticles. Small 2009, 5 (15), 1791-1798.

15. Yoo, H. S.; Kim, T. G.; Park, T. G., Surface-functionalized electrospun nanofibers for tissue engineering and drug delivery. Adv Drug Deliver Rev 2009, 61 (12), 1033-1042.

16. Martins, A.; Duarte, A. R. C.; Faria, S.; Marques, A. P.; Reis, R. L.; Neves, N. M., Osteogenic induction of hBMSCs by electrospun scaffolds with dexamethasone release functionality. Biomaterials 2010, 31 (22), 5875-5885.

17. Luu, Y. K.; Kim, K.; Hsiao, B. S.; Chu, B.; Hadjiargyrou, M., Development of a nanostructured DNA delivery scaffold via electrospinning of PLGA and PLA-PEG block copolymers. J Control Release 2003, 89 (2), 341-353.

18. Luong-Van, E.; Grondahl, L.; Chua, K. N.; Leong, K. W.; Nurcombe, V.; Cool, S. M., Controlled release of heparin from poly(Ɛ-caprolactone) electrospun fibers. Biomaterials 2006, 27 (9), 2042-2050.

19. Sy, J. C.; Klemm, A. S.; Shastri, V. P., Emulsion as a Means of Controlling Electrospinning of Polymers. Adv Mater 2009, 21 (18), 1814-+.

20. Venugopal, G.; Krause, S.; Wnek, G. E., Morphological Variations in Polymer Blends Made in Electric-Fields. Chem Mater 1992, 4 (6), 1334-1343.

21. Xu, X. L.; Yang, L. X.; Xu, X. Y.; Wang, X.; Chen, X. S.; Liang, Q. Z.; Zeng, J.; Jing, X. B., Ultrafine medicated fibers electrospun from W/O emulsions. J Control Release 2005, 108 (1), 33-42.

22. Wang, C.; Yan, K. W.; Lin, Y. D.; Hsieh, P. C. H., Biodegradable Core/Shell Fibers by Coaxial Electrospinning: Processing, Fiber Characterization, and Its Application in Sustained Drug Release. Macromolecules 2010, 43 (15), 6389-6397.

23. Chakraborty, S.; Liao, I. C.; Adler, A.; Leong, K. W., Electrohydrodynamics: A facile technique to fabricate drug delivery systems. Adv Drug Deliver Rev 2009, 61 (12), 1043-1054.

24. Sun, X. Y.; Shankar, R.; Borner, H. G.; Ghosh, T. K.; Spontak, R. J., Field-driven biofunctionalization of polymer fiber surfaces during electrospinning. Adv Mater 2007, 19 (1), 87-+.

25. Sun, X. Y.; Nobles, L. R.; Borner, H. G.; Spontak, R. J., Field-driven surface segregation of biofunctional species on electrospun PMMA/PEO microfibers. Macromol Rapid Comm 2008, 29 (17), 1455-1460.

26. Huang, Z. M.; He, C. L.; Yang, A. Z.; Zhang, Y. Z.; Hang, X. J.; Yin, J. L.; Wu, Q. S., Encapsulating drugs in biodegradable ultrafine fibers through co-axial electrospinning. J Biomed Mater Res A 2006, 77A (1), 169-179.

27. Cui, W. G.; Li, X. H.; Zhou, S. B.; Weng, J., Degradation patterns and surface wettability of electrospun fibrous mats. Polym Degrad Stabil 2008, 93 (3), 731-738.

28. Cleland, J. L.; Lim, A.; Barron, L.; Duenas, E. T.; Powell, M. F., Development of a single-shot subunit vaccine for HIV-1 .4. Optimizing microencapsulation and pulsatile release of MN rgp120 from biodegradable microspheres. J Control Release 1997, 47 (2), 135-150.

29. Siepmann, J.; Gopferich, A., Mathematical modeling of bioerodible, polymeric drug delivery systems. Adv Drug Deliver Rev 2001, 48 (2-3), 229-247.

30. Liang, D.; Hsiao, B. S.; Chu, B., Functional electrospun nanofibrous scaffolds for biomedical applications. Adv Drug Deliver Rev 2007, 59 (14), 1392-1412.

31. Baker, B. M.; Nerurkar, N. L.; Burdick, J. A.; Elliott, D. M.; Mauck, R. L., Fabrication and Modeling of Dynamic Multipolymer Nanofibrous Scaffolds. J Biomech Eng-T Asme 2009, 131 (10).

32. Bottino, M. C.; Thomas, V.; Janowski, G. M., A novel spatially designed and functionally graded electrospun membrane for periodontal regeneration. Acta Biomater 2011, 7 (1), 216-224.

33. Piras, A. M.; Chiellini, F.; Chiellini, E.; Nikkola, L.; Ashammakhi, N., New multicomponent bioerodible electrospun nanofibers for dual-controlled drug release. J Bioact Compat Pol 2008, 23 (5), 423-443.

34. Okuda, T.; Tominaga, K.; Kidoaki, S., Time-programmed dual release formulation by multilayered drug-loaded nanofiber meshes. J Control Release 2010, 143 (2), 258-264.

35. Bonani, W.; Motta, A.; Migliaresi, C.; Tan, W., Biomolecule Gradient in Micropatterned Nanofibrous Scaffold for Spatiotemporal Release. Langmuir 2012, 28 (38), 13675-13687.

36. Wylie, R. G.; Ahsan, S.; Aizawa, Y.; Maxwell, K. L.; Morshead, C. M.; Shoichet, M. S., Spatially controlled simultaneous patterning of multiple growth factors in three-dimensional hydrogels. Nat Mater 2011, 10 (10), 799-806.

37. Xie, J. W.; Li, X. R.; Xia, Y. N., Putting Electrospun Nanofibers to Work for Biomedical Research. Macromol Rapid Comm 2008, 29 (22), 1775-1792.

38. Biondi, M.; Ungaro, F.; Quaglia, F.; Netti, P. A., Controlled drug delivery in tissue engineering. Adv Drug Deliver Rev 2008, 60 (2), 229-242.

39. Silva, E. A.; Mooney, D. J., Effects of VEGF temporal and spatial presentation on angiogenesis. Biomaterials 2010, 31 (6), 1235-1241.

40. Cao, L.; Mooney, D. J., Spatiotemporal control over growth factor signaling for therapeutic neovascularization. Adv Drug Deliver Rev 2007, 59 (13), 1340-1350.

41. Li, D.; Ouyang, G.; McCann, J. T.; Xia, Y. N., Collecting electrospun nanofibers with patterned electrodes. Nano Lett 2005, 5 (5), 913-916.

42. Katta, P.; Alessandro, M.; Ramsier, R. D.; Chase, G. G., Continuous electrospinning of aligned polymer nanofibers onto a wire drum collector. Nano Lett 2004, 4 (11), 2215-2218.

43. Yan, H.; Liu, L. Q.; Zhang, Z., Alignment of electrospun nanofibers using dielectric materials. Appl Phys Lett 2009, 95 (14).

44. Kuo, C. C.; Wang, C. T.; Chen, W. C., Highly-Aligned Electrospun Luminescent Nanofibers Prepared from Polyfluorene/PMMA Blends: Fabrication, Morphology, Photophysical Properties and Sensory Applications. Macromol Mater Eng 2008, 293 (12), 999-1008.

45. Carnell, L. S.; Siochi, E. J.; Holloway, N. M.; Stephens, R. M.; Rhim, C.; Niklason, L. E.; Clark, R. L., Aligned mats from electrospun single fibers. Macromolecules 2008, 41 (14), 5345-5349.

46. Wu, Y. Q.; Carnell, L. A.; Clark, R. L., Control of electrospun mat width through the use of parallel auxiliary electrodes. Polymer 2007, 48 (19), 5653-5661.

47. Zhang, D. M.; Chang, J., Electrospinning of Three-Dimensional Nanofibrous Tubes with Controllable Architectures. Nano Lett 2008, 8 (10), 3283-3287.

48. Murugan, R.; Ramakrishna, S., Design strategies of tissue engineering scaffolds with controlled fiber orientation. Tissue Eng 2007, 13 (8), 1845-1866.

49. Lavielle, N.; Hebraud, A.; Mendoza-Palomares, C.; Ferrand, A.; Benkirane-Jessel, N.; Schlatter, G., Structuring and Molding of Electrospun Nanofibers: Effect of Electrical and

Topographical Local Properties of Micro-Patterned Collectors. Macromol Mater Eng 2012, 297 (10), 958-968.

50. Deitzel, J. M.; Kleinmeyer, J.; Harris, D.; Tan, N. C. B., The effect of processing variables on the morphology of electrospun nanofibers and textiles. Polymer 2001, 42 (1), 261-272.

51. Thandavamoorthy, S.; Gopinath, N.; Ramkumar, S. S., Self-assembled honeycomb polyurethane nanofibers. J Appl Polym Sci 2006, 101 (5), 3121-3124.

52. Ye, X. Y.; Huang, X. J.; Xu, Z. K., Nanofibrous mats with bird's nest patterns by electrospinning. Chinese J Polym Sci 2012, 30 (1), 130-137.

53. Yan, G. D.; Yu, J.; Qiu, Y. J.; Yi, X. H.; Lu, J.; Zhou, X. S.; Bai, X. D., Self-Assembly of Electrospun Polymer Nanofibers: A General Phenomenon Generating Honeycomb-Patterned Nanofibrous Structures. Langmuir 2011, 27 (8), 4285-4289.

54. Ahirwal, D.; Hebraud, A.; Kadar, R.; Wilhelm, M.; Schlatter, G., From self-assembly of electrospun nanofibers to 3D cm thick hierarchical foams. Soft Matter 2013, 9 (11), 3164-3172.

55. Huaqiong Li, Y. S. W., Feng Wen, Kee Woei Ng, Gary Ka Lai Ng, Subbu S. Venkatraman, Freddy Yin Chiang Boey, Lay Poh Tan, Human Mesenchymal Stem-Cell Behaviour On Direct Laser Micropatterned Electrospun Scaffolds with Hierarchical Structures. Macromol. Biosci. 2013, 13, 299-310.

56. Chen, J. T.; Chen, W. L.; Fan, P. W., Hierarchical Structures by Wetting Porous Templates with Electrospun Polymer Fibers. Acs Macro Lett 2012, 1 (1), 41-46.

57. Sundararaghavan, H. G.; Metter, R. B.; Burdick, J. A., Electrospun Fibrous Scaffolds with Multiscale and Photopatterned Porosity. Macromol Biosci 2010, 10 (3), 265-270.

58. Cipitria, A.; Skelton, A.; Dargaville, T. R.; Dalton, P. D.; Hutmacher, D. W., Design, fabrication and characterization of PCL electrospun scaffolds-a review. J Mater Chem 2011, 21 (26), 9419-9453.

59. Dong, Y. X.; Liao, S.; Ngiam, M.; Chan, C. K.; Ramakrishna, S., Degradation Behaviors of Electrospun Resorbable Polyester Nanofibers. Tissue Eng Part B-Re 2009, 15 (3), 333-351.

60. Rutledge, G. C.; Lowery, J. L.; Datta, N., Effect of fiber diameter, pore size and seeding method on growth of human dermal fibroblasts in electrospun poly(epsilon-caprolactone) fibrous mats. Biomaterials 2010, 31 (3), 491-504.

61. Smith, L. A.; Ma, P. X., Nano-fibrous scaffolds for tissue engineering. Colloid Surface B 2004, 39 (3), 125-131.

62. Del Gaudio, C.; Grigioni, M.; Bianco, A.; De Angelis, G., Electrospun bioresorbable heart valve scaffold for tissue engineering. Int J Artif Organs 2008, 31 (1), 68-75.

63. Lee, K. H.; Kim, H. Y.; Khil, M. S.; Ra, Y. M.; Lee, D. R., Characterization of nano-structured poly(Ɛ-caprolactone) nonwoven mats via electrospinning. Polymer 2003, 44 (4), 1287-1294.

64. Moghe, A. K.; Hufenus, R.; Hudson, S. M.; Gupta, B. S., Effect of the addition of a fugitive salt on electrospinnability of poly(Ɛ-caprolactone). Polymer 2009, 50 (14), 3311-3318.

65. Luo, C. J.; Stride, E.; Edirisinghe, M., Mapping the Influence of Solubility and Dielectric Constant on Electrospinning Polycaprolactone Solutions. Macromolecules 2012, 45 (11), 4669-4680.

66. Van der Schueren, L.; De Schoenmaker, B.; Kalaoglu, O. I.; De Clerck, K., An alternative solvent system for the steady state electrospinning of polycaprolactone. Eur Polym J 2011, 47 (6), 1256-1263.

CHAPTER II/

PUBLICATION N°1: "CONTROLLED FORMATION OF POLY(Ɛ-CAPROLACTONE) ULTRATHIN ELECTROSPUN NANOFIBERS IN A HYDROLYTIC DEGRADATION-ASSISTED PROCESS"

A) Abstract

We describe a new approach for the controlled fabrication of ultrathin poly(Ɛ-caprolactone) (PCL) electrospun nanofibers, with diameters ranging from 150 to 400 nm, from a solvent system based on a mixture of acetic acid and formic acid. We demonstrated for the first time the possibility of tuning the diameter and morphology of the nanofibers by the in-situ modification of the molecular weight of the polymer, a consequence of the hydrolytic degradation to which the polyester is subjected in aqueous acidic medium. A study of the PCL degradation kinetics enabled precise adjustments of polymer molecular weight and thus of the solution viscosity. Hence, regimes and boundaries of PCL electrospinning in this solvent system could be determined, ranging from electrospraying to continuous fiber electrospinning.

B) Introduction

Electrospinning has been extensively explored during the last decades as a method for the fabrication of nanofibrous nonwovens [1, 2]. A typical electrospinning set-up is composed of a source-electrode-needle through which a polymer solution is injected at a controlled rate, a ground-electrode-collector and a high-voltage power supply. The polymer jet stretches under the action of the electric field. The jet is elongated due to whipping movements, which favors the rapid evaporation of the solvent and induces the generation of nanofibers. The nanofibers are collected on a ground-collector as a functional non-woven membrane. Nanofibrous membranes find applications in many fields [3], such as sensing [4], tissue engineering platforms [5] or drug delivery devices [6]. Biodegradable polyesters such as poly(Ɛ-caprolactone) (PCL) have been widely studied as electrospun material, and an extensive review has been recently published on the subject [7]. PCL is usually dissolved in halogenated solvents and the obtained fibers have diameters in the micrometer or sub-micrometer range [8-10]. As such, much effort is directed towards the development of new systems which allow a more precise control of the PCL nanofiber morphology and diameter [7, 11, 12]. Luo et al. recently studied the influence of solubility and dielectric constant of various solvents on the electrospinning of PCL and discussed the impact of the dielectric constant on the diameter of the produced fibers [13]. In a recent report, Van der Schueren et al. [14] showed the steady state formation of PCL fibers with micron-size diameters when electrospun from chloroform and with diameters as low as 270 nm when using formic acid and acetic acid as solvent system. Electrospinnability and fiber morphology of poly(Ɛ-caprolactone) from the acid mixture were studied in details. They showed that the viscosity of the solution remained constant up to three hours after solution preparation, a suitable time frame for having stable solution for electrospinning. Indeed, hydrolytic degradation of PCL is occurring in aqueous acidic medium leading to a decrease of the solution viscosity with time.

In the present work we took advantage of the hydrolytic degradation of PCL in acid solutions containing trace amounts of water, as a straightforward approach for controlling the biopolymer molecular weight and thus the viscosity of the solution. A degradation model was used to understand and predict the evolution of the molecular weight in time as a function of the initial polymer and water concentrations. We described the influence of the molecular weight and concentration of PCL on the fiber morphology and determined the electrospinning regimes and boundaries, ranging from electrospraying to continuous fiber electrospinning.

C) Experimental

1) Materials and electrospinning experiments

PCL (Mw = 105 kg/mol, PDI = 1.6, measured by SEC) was supplied by Perstorp under the commercial name Capa 6800. Acetic acid (purum ≥99.0%, H2O≈0.2%) and formic acid (≈ 98%, H2O ≈ 2%) were provided by Fluka. Content of water was given by Fluka. All products were used as received.

Electrospinning was performed on a home-made vertical electrospinning setup composed of a high voltage power supply (SL30P10, Spellman), a programmable syringe pump from WPI (Aladdin, AL1000), a Luer-Lock metallic needle from BGB (gauge 21), a Luer-Lock plastic syringe from Once (ID = 12 mm), VBM Luer-Lock connectors (CHLLM20, Laubscher), silicon tubes between the connectors and an aluminum plate as collector. The experimental conditions of electrospinning remained the same for all the experiments (ΔV = 26 kV, needle-collector distance = 13.5 cm, pump flow rate = 0.4 mL/h, duration = 4 min, room temperature, 40% RH). PCL solutions were prepared in acetic acid / formic acid 50/50 (v/v) at concentrations of 15%, 20%, 25%, 30% and 35% (w/v) (as an example, a solution of 15% (w/v) was prepared by adding 15 g of polymer in 100 mL of solvent mixture). Electrospinning was performed at 24, 48, 72, 96, 168 and 264 hours after solution preparation. The electrospun membranes were dried and stored in a dried atmosphere.

2) Molecular weight and intrinsic viscosity measurements

Size exclusion chromatography (SEC) was performed on the as-obtained PCL pellets and on all electrospun membranes fabricated as described in section 2.1, using a differential refractive index detector (SEC apparatus: Viscotek, Houston, TX, USA). About 30 mg of each polymer sample were dissolved in 10 mL of tetrahydrofuran (THF). Aliquots of 100 µL of the polymer solution were injected and separated on three sequentially coupled SEC columns (300 mm × 8 mm, pore sizes 103, 105, and 107 Å, PSS, Mainz, Germany) at 35 °C, applying a flow rate of 1 mL/min of THF. Calibration was performed with 10 narrow standard polystyrene (PS) samples from PSS (2 × 103 g/mol to 2.13 × 106 g/mol). We used [η]M as a universal calibration parameter to convert the PS calibration into one for PCL using the Mark–Houwink–Sakurada equations of PCL and PS in THF [15,16].

The specific viscosity (ηsp) was evaluated from 0.5%, 1%, 1.5%, 2% and 2.5% (w/v) PCL solutions in the acidic solvent mixture diluted from a batch solution of 20% (w/v) at different times after dissolution (from 15 to 330 h), in order to cover the time range of the study (from 24 to 264 hours). For this, an Ubbelohde micro-viscometer (K = 0.09241) from VWR was used. By plotting the measured specific viscosity over the PCL concentration (C) as a function of the PCL concentration, we determined the intrinsic viscosity of the solutions ([η]) as [η] = limc→0 (ηsp/C). SEC was performed on a 1 mL sample vacuum dried from the batch solutions (20% (w/v)) in order to correlate the intrinsic viscosity to the molecular weight of PCL for each selected degradation time. (See Figure S1 in the Supplementary data for the calculation of [η] at different molecular weights).

3) Characterization of the fiber morphology

Gold (5 nm) was sputtered on all electrospun membranes using a scanning electron microscope coating unit (E5100) from Polaron Equipment Limited. The fiber morphology was characterized using a scanning electron microscope (SEM, Hitachi S-4800 at Vacc = 10kV, Ie = 10 µA). For each sample, the average nanofiber diameter and standard deviation were calculated from the diameter measured from 12 nanofibers in 3 randomly selected areas. Electrospinning of the PCL solution at 25% concentration was performed in triplicate in order to assess the repeatability of our process. The diameters measured on the SEM micrographs were analyzed through one-way ANOVA using the Origin software ($F=2$, $p<0.1$).

D) Results and Discussion

1) Evolution of the molecular weight of PCL and solution intrinsic viscosity with degradation time

In a first step, we investigated the degradation behavior of PCL in a mixture of acetic acid and formic acid (50/50, v/v), and therefore solutions with concentrations ranging from 15-35% (w/v) in 5% increments were prepared. In this range of concentrations, PCL appeared completely soluble. In order to monitor the hydrolytic degradation of the biopolymer we analyzed the evolution of the number average molecular weight (Mn) of PCL as a function of time. The obtained membranes were dissolved in THF and analyzed by SEC. Within 264 hours, the value of Mn decreased from 65 to 10 kg/mol, while the polydispersity index increased from 1.6 to 2 (Figure 1 and S3). The polydispersity index increases up to a value of 2 due to random chain scission in agreement with the Flory's statistical theory (Yu et al. [17]). The decrease of the molecular weight is due to the hydrolytic degradation of polyester in solution (in-situ), catalyzed by the presence of acids at room temperature. In order to predict the decrease of the molecular weight as a function of the initial solution concentrations and time, we used analytical equations describing degradation of polyesters developed by Pitt et al. [18] and Lyu et al. [19]. The use of this approach was suitable for our system, as PCL was fully solubilized in the acid mixture and thus all ester bonds had the same probability of reacting with water at a given time [20]. We imposed variable water and ester concentrations and a constant acid concentration, which was a realistic hypothesis, because the acid amount largely exceeded the water quantity. The amount of water in the acidic solutions (1.1 wt %) was much higher than the number of alcohol functions at chain ends, even after 264 hours.

Therefore, we considered the equilibrium to be shifted towards the hydrolysis direction and neglected secondary reactions such as transesterification. Antheunis et al. [21] proposed a theoretical model for the autocatalytic hydrolysis of polyester in aqueous medium. In our case, however, we can assume the absence of autocatalysis as the acid concentration is much larger than the ester and water concentrations. We can thus describe the evolution of the newly yielded alcohol concentration, *u*, through a second order equation (eq.1) and from it express theoretical number average molecular weight (M_n) as a function of time (eq.2) (see Supplementary data for calculation details and Figure S2 for the determination of *k*):

$$\frac{du}{dt} = kEW \quad [mol.L^{-1}s^{-1}] \quad (eq.1)$$

$$M_n(t) = \rho \frac{E_0 e^{k(E_0 - W_0)t} - W_0}{(W_0 + u_0)E_0 e^{k(E_0 - W_0)t} - W_0(E_0 + u_0)} \quad [g.mol^{-1}] \quad (eq.2)$$

In which *u* is the concentration of alcohol groups (mol.L^{-1}), *k* is the second-order hydrolysis rate constant (L.mol-1.s^{-1}), *E* is the concentration of ester bonds (mol.L^{-1}), *W* is the concentration of water molecules (mol.L-1) and ρ the weight concentration of polymer (g.L^{-1}).

In Figure 1, the correlation can be observed between the experimental data and theoretical curve of the M_n values as a function of time for 20% (w/v) PCL solution (see Figure S3 in the Supplementary data for the experimental data and theoretical curve of the M_n values for 15%, 25%, 30% and 35% (w/v) PCL solutions). As such, the adapted model allows the prediction of M_n of PCL as a function of degradation time. This model is very useful to predict and control the solution viscosity and thus the fiber morphology, as we will demonstrate below.

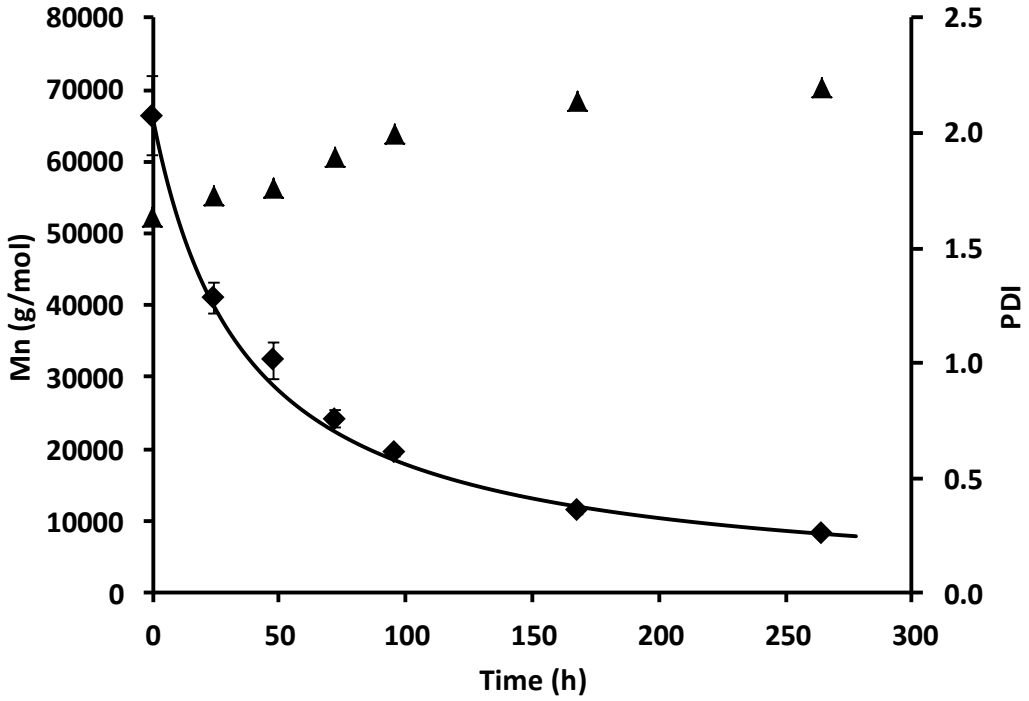

Figure 1: Evolution of M_n (■) and PDI (▲) as a function of degradation time for 20% (w/v) PCL and the corresponding theoretical plot of M_n (—).

Viscosity of the prepared solutions was investigated in order to correlate it to the morphology of the obtained fibers. The dependence between the logarithm of the solution intrinsic viscosity, a key parameter affecting the fiber morphology [22, 23], and the logarithm of the weight average molecular weight (M_w) of PCL is presented in the supporting information. We used the linear regression equation to approximate the intrinsic viscosities of the solutions, from which the electrospun membranes were fabricated.

2) Influence of the molecular weight and concentration of PCL on the electrospun nanofiber morphology

Electrospinning was performed from solutions with different polymer concentrations (15%, 20%, 25%, 30% and 35% (w/v)) after selected degradation times (24, 48, 72, 96, 168 and 264 hours) using identical electrospinning conditions. 24 hours after preparation, PCL solutions with concentrations below 35% (w/v) could be electrospun, whereas at, and above, this concentration no jet formation could be observed due to a very high viscosity.

All membranes were analyzed by SEM. In Figure 2 the micrographs of membranes obtained by electrospinning from a 25% (w/v) solution are presented at various degradation times. In the first 72 hours, bead-free nanofibers were formed (Figure 2a-c). Moreover, a constant decrease of the fiber diameter, from 315 to150 nm, was observed when increasing the degradation time. After 72 hours the viscosity of the solution decreased substantially and as a consequence, beaded fibers were formed as can be observed in Figure 2d and e. As expected, the number of beads per surface area increased and the beads diameter decreased upon reduction of the solution viscosity as a result of hydrolytic degradation, which is in agreement with the results of viscosity impact discussed by Fong et al. [24]. Finally, 264 hours after solution preparation, the electrospinning conditions did not allow further fiber formation and only electrospraying of PCL beads was observed. This morphological evolution - from cylindrical nanofibers to beaded fibers and finally to electrosprayed beads - can be explained by the interplay between the viscoelasticity of the solution and the electrostatic forces applied to the polymer jet. Indeed, the reduction of the molecular weight resulted in a decrease of the viscosity of the solution, whereas the applied electrostatic field remained constant. Consequently, flow instabilities and subsequent beads formation appeared [24].

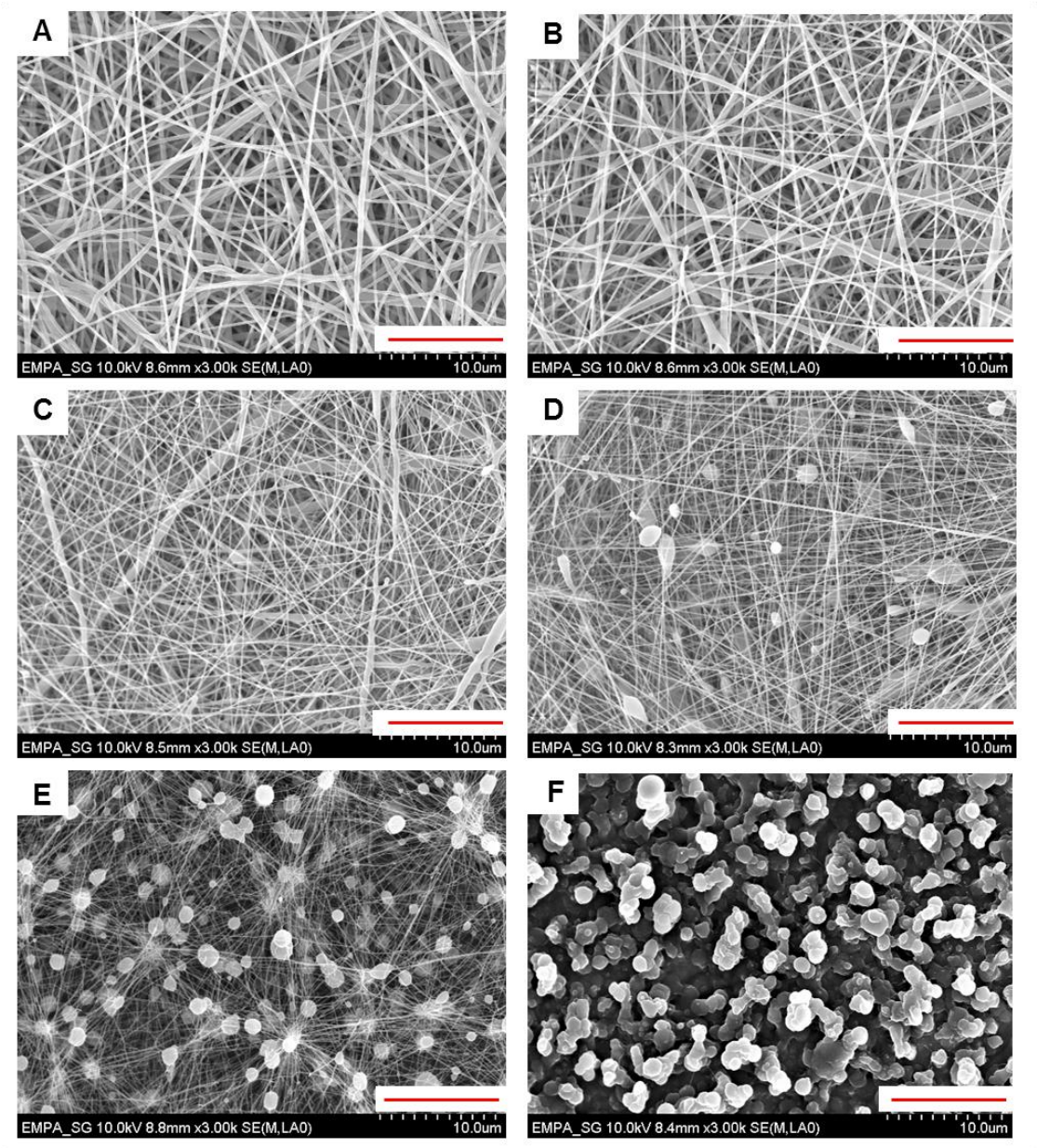

Figure 2: SEM micrographs of the morphology of the electrospun membranes generated from 25% (w/v) PCL solution at different degradation time intervals: A) 24 h, B) 48 h, C) 72 h, D) 96 h, E) 168 h and F) 264 h. Scale bar = 10µm.

We analyzed in detail the evolution of the fiber diameter for all fibers in the concentration range (15-35%) over 264 hours of degradation time. We show in Figure 3 the effect of the respective molecular weights on the fiber diameter for two selected solutions

(concentrations 15 and 30% (w/v)) (see Figure S4 in the Supplementary data for the evolution of the fiber diameter with Mw for the 20%, 25% and 35% (w/v) PCL solutions). At a given concentration, a decrease of molecular weight led to a decrease of solution viscosity, whereas the surface tension and net charge density remained constant [24]. As a consequence, the diameter of the fibers decreased with time for all the concentrations. A similar effect was observed when decreasing the concentration at constant molecular weight. Indeed, a concentration decrease induced a decrease of the solution viscosity leading to a substantial decrease in the diameters of the fibers. The diameters of the nanofibers obtained from the 15% (w/v) solution were smaller in comparison to those obtained from the 30% (w/v) solution.

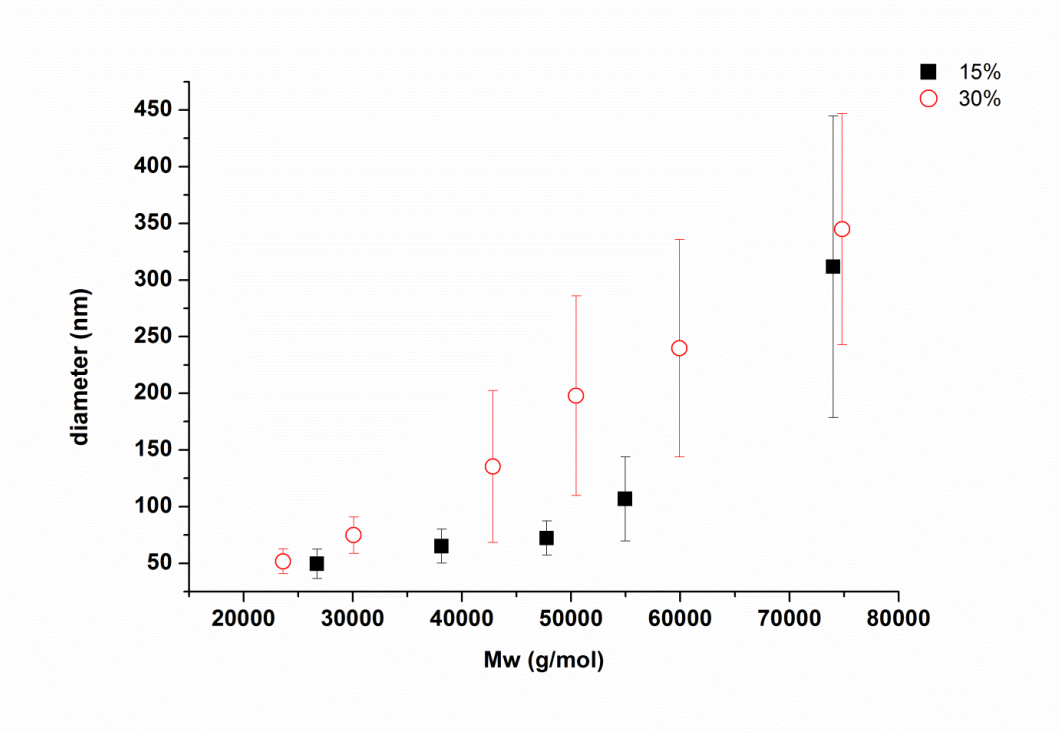

Figure 3: Dependence of the average diameter of electrospun fibers produced from 15% and 30% (w/v) PCL solutions with M_w. The error bars represent the standard deviation of the diameter.

3) Electrospinning regimes and boundaries

In order to determine the different electrospinning regimes, we analyzed the evolution of the fiber diameter as a function of the product of the intrinsic viscosity and the solution concentration, [η]C (Figure 4). The product [η]C is equivalent to the ratio C/C*, where C* is the critical chain overlap concentration, i.e. the crossover concentration between the dilute and the semi-dilute regimes [22]. For [η]C > 21 the solution was too viscous to yield fibers under the applied electrospinning parameters. When the product [η]C was in the interval 10 < [η]C <21, bead-free fibers with diameters ranging from 400±100 nm to 135±70 nm could be formed. A decrease of [η]C directly relates to a decrease of the viscosity of the solution. Hence, when the electrostatic field was maintained constant, higher fiber bending and elongation occurred, and thus a smaller fiber diameter was obtained. When the product [η]C was decreased even further (3 < [η]C < 10), beaded fibers with diameters ranging from 90 ±15 nm to 50±10 nm and bead dimensions ranging from 2500±400 nm to 800±200 nm, respectively, were observed. Finally, when [η]C was lower than 3, only electrospraying occurred. The presented results are in agreement with results reported by Gupta et al. [22] for the electrospinning of PMMA in DMF, in which different possible electrospinning regimes were defined based on the value of the C/C* ratio. In the case of dilute solutions with [η]C < 1, PCL could only be electrosprayed. For 1 < [η]C < 3, the solution was defined as being in the range of the semidilute, unentangled regime. Only for [η]C > 3, which can be considered to be the entrance to the semidilute, entangled domain, fiber formation started. Higher degrees of entanglement were required to form bead-free fibers from [η]C > 10.

A power law fit of the data in Figure 4 allowed the determination of a scaling law for the nanofiber diameter dependency to the concentration and intrinsic viscosity:

$$fiber\ diameter \sim ([\eta]C)^{1.5}$$

Previous studies also correlated the fiber diameter with the C/C* ratio [22,25]. The scaling exponents were 3.1 and 2.6 for PMMA nanofibers and PET-co-PEI nanofibers, respectively. The difference in the scaling exponent was explained by the type of polymer used (linear or branched), but it is also depending on the electrospinning conditions, such as flow rate and applied electrostatic field. Since the flow rate was almost ten times smaller than the one used in the previous reports, and the applied electrostatic field was higher, it was expected that the scaling exponent would be smaller than the ones previously reported. Moreover, it is known that intrinsic parameters (related to the solution properties), such as the dielectric constant, the surface tension and the conductivity, can influence the scaling exponent [11].

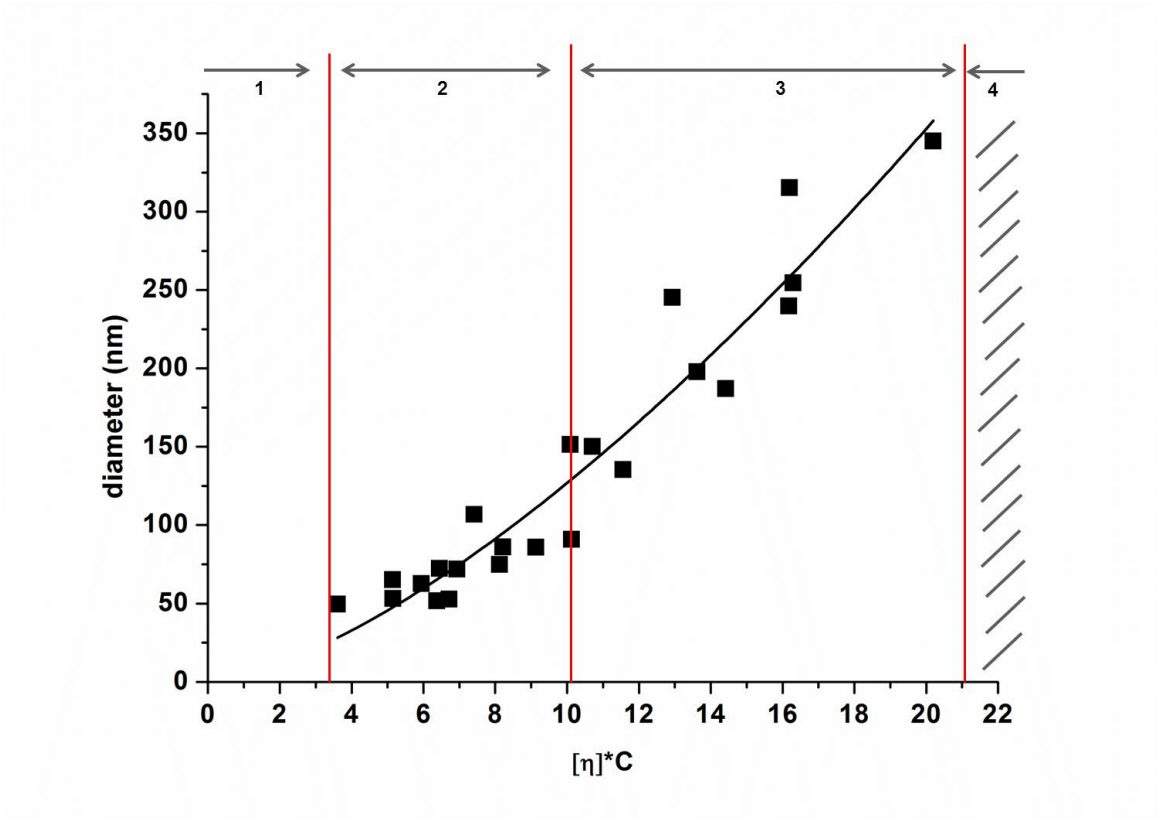

Figure 4: Variation of fibers average diameter with [η]C (■): Zone 1: electrospraying, zone 2: beaded electrospun fibers, zone 3: bead-free electrospun fibers and zone 4: no electrospinning. Equation of power law dependency (▬): diameter = 4.2 $([\eta]C)^{1.5}$. (R^2=0.92).

It is worthy to notice that the bead-free PCL fibers produced from the acidic solvent system had an average diameter of 150±70 nm at 20% (w/v) 48 hours after the preparation of the solution (when M_w=55'000 g/mol) (Figure 5), which is at least ten times smaller than what has been observed when chloroform was used as a solvent and even two times smaller than the diameters obtained from similar acetic acid/formic acid mixtures [14]. Moreover, when beaded fibers were formed, fiber diameters down to 50±10 nm with an average bead diameter of 800±200 nm were measured. The high dielectric constant of formic acid (57.2 at 298K) present at 50% (v/v) in our mixture allowed an increase of net charge density. Therefore, stronger repulsive electrostatic forces acted on the polymer jet, leading to a substantial decrease of the fiber diameter [1].

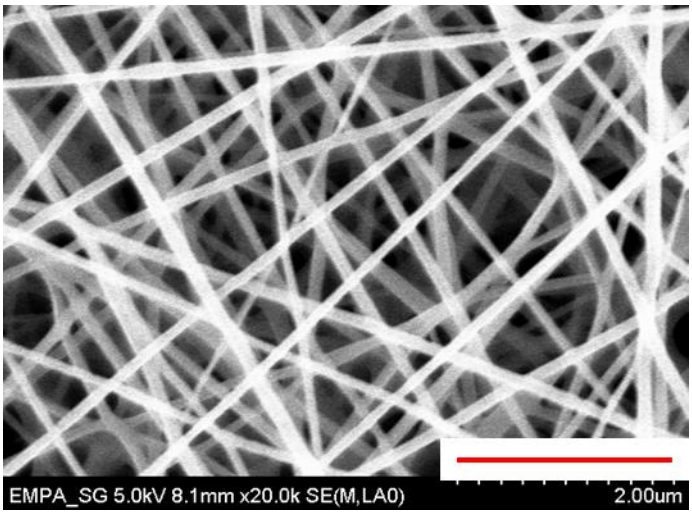

Figure 5: SEM micrograph of bead-free fibers having an average diameter of 150 nm. The fibers were generated at 20% (w/v) PCL at a degradation time of 48 h. Scale bar = 2 µm.

E) Conclusions

We described the production of ultrathin PCL nanofibers by electrospinning formic acid/acetic acid- based biopolymer solutions. The hydrolytic degradation which occurs in these solutions was advantageously used for systematically tuning the length of the polyester chains and consequently the solution viscosity and diameter of the yielded nanofibers. Moreover, a simple model was used for predicting the evolution of the molecular weight as a function of degradation time. The influence of the polymer concentration and molecular weight on the diameter of the nanofiber and its morphology was demonstrated as well. This systematic study allowed the determination of the limits of the electrospinning process as a function of the product between the concentration and the intrinsic viscosity of the feed solution.

The electrospinning of PCL from an acid solution is extremely interesting, as it allows the formation of ultrathin nanofibers with tunable dimensions. This strategy can of course be extrapolated to the electrospinning of any polyester which is soluble in the acid mixture. Additionally, the low toxicity of the solvent used makes this system very interesting for the production of scaffolds for biomedical applications.

F) Supporting information

Calculation details of the degradation model:

We can describe the evolution of the newly yielded alcohol concentration, *u*, through a pseudo-second order equation:

$$\frac{du}{dt} = kEW \qquad \left[\frac{mol}{L.s}\right] \quad (eq.1a)$$

where *u* is the concentration of alcohol groups (mol/L), *k* is the second-order hydrolysis rate constant ($L.mol^{-1}.s^{-1}$), *E* is the concentration of ester bonds (mol/L) and *W* is the concentration of water molecules (mol/L). As *E* and *W* consumption directly depend on the formation of new alcohol groups, equation 1a can be re-written as a function of *u*; u_0, the initial concentration of alcohol groups which is equal to the initial concentration of polymer chains; E_0, the initial concentration of ester bonds and W_0, the initial concentration of water molecules:

$$\frac{du}{dt} = k(E_0 - (u - u_0))(W_0 - (u - u_0)) \qquad \left[\frac{mol}{L.s}\right] \quad (eq.1b)$$

Differential equation 1b can be integrated separating variable *u* from *t*:

$$\frac{1}{E_0 - W_0} \ln \frac{W_0(E_0 - u + u_0)}{E_0(W_0 - u + u_0)} = kt \qquad \left[\frac{L}{mol}\right] \quad (eq.1c)$$

Equation 1c can be re-written to express *u*:

$$u(t) = \frac{(W_0 + u_0)E_0 e^{k(E_0 - W_0)t} - W_0(E_0 + u_0)}{E_0 e^{k(E_0 - W_0)t} - W_0} \qquad \left[\frac{mol}{L}\right] \quad (eq.1d)$$

The number average molecular weight (M_n) can be also related to *P*, the concentration of polymer chains (mol/L), and ρ, the weight concentration of polymer (g/L):

$$M_n(t) = \frac{\rho}{P(t)} \qquad \left[\frac{g}{mol}\right] \quad (eq.2a)$$

As $u(t) =$ P(t), the following expression of M_n as a function of time is obtained:

$$M_n(t) = \rho \frac{E_0 e^{k(E_0 - W_0)t} - W_0}{(W_0 + u_0)E_0 \mathrm{e}^{k(E_0 - W_0)t} - W_0(E_0 + u_0)} \qquad \left[\frac{g}{mol}\right] \quad (eq.2b)$$

Only the second-order hydrolysis rate constant, *k*, needed to be determined in order to plot the theoretical molecular weight *versus* time. *k* was determined experimentally for each studied concentrations by plotting the left term of equation 1c as a function of the selected degradation times (see Figure S2(a)(b)(c)(d)(e) in the Supplementary data for the determination of *k* for 15% , 20%, 25%, 30% and 35% (w/v) PCL solutions, respectively). The values for *u* were calculated from the SEC measurements of M_n and the value for *k* was taken as the slope of the curve. From the five different polymer solutions, we found:

$$k = 1.76.10^{-8} \pm 8.3\% \qquad \left[\frac{L}{mol.s}\right]$$

Determination of the PCL solutions intrinsic viscosity:

Viscosities of the prepared solutions were investigated in order to correlate the viscosity to the morphology of the obtained fibers. We determined the specific viscosity which depends on the polymer molecular weight and concentration. The intrinsic viscosity was calculated from the specific viscosity. Intrinsic viscosity depends on polymer molecular weight only. The dependence between the logarithm of the solution intrinsic viscosity and the logarithm of the weight average molecular weight (M_w) of PCL is presented below. We observed a linear dependence in our working range of weight average molecular weights. We used the linear regression equation to approximate the intrinsic viscosities of the solutions, from which the electrospun membranes were fabricated.

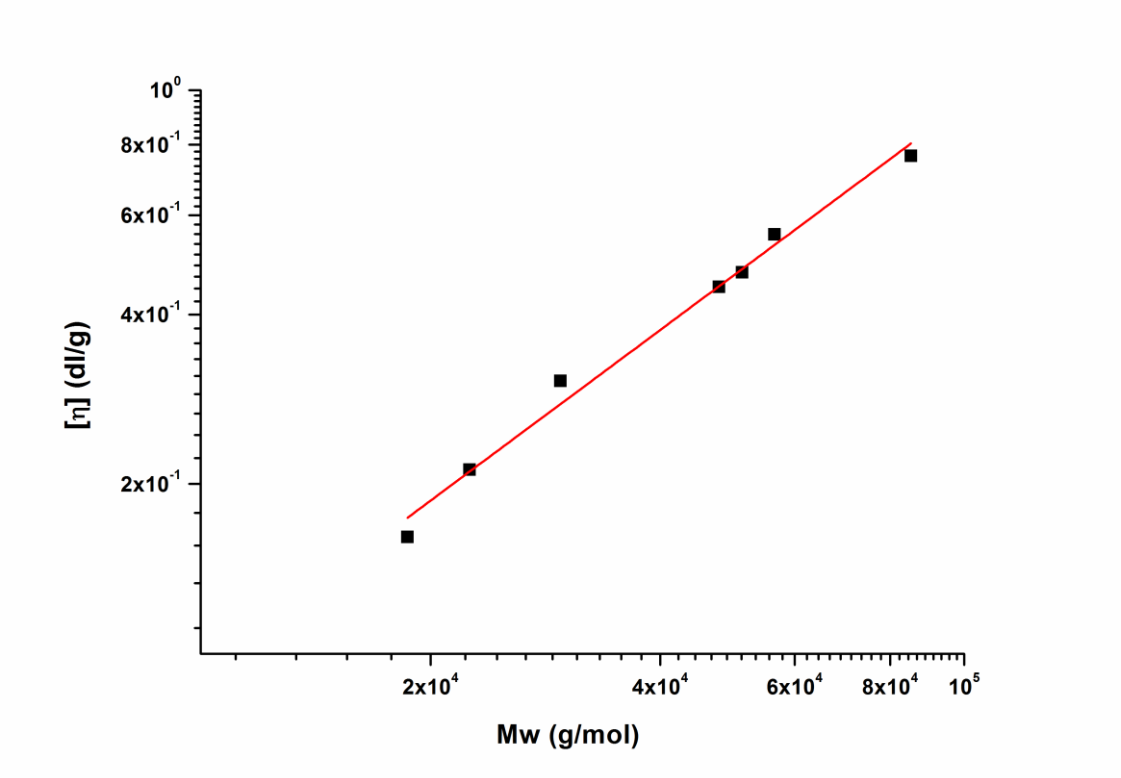

Evolution of the intrinsic viscosity as a function of the weight average molecular weight in logarithmic scale (■). Linear regression equation: $\log[\eta] = 1.007.\log(M_w) - 5.06$ (R^2=0.99), valid for M_w ranging from 18'600g/mol to 85'200g/mol.

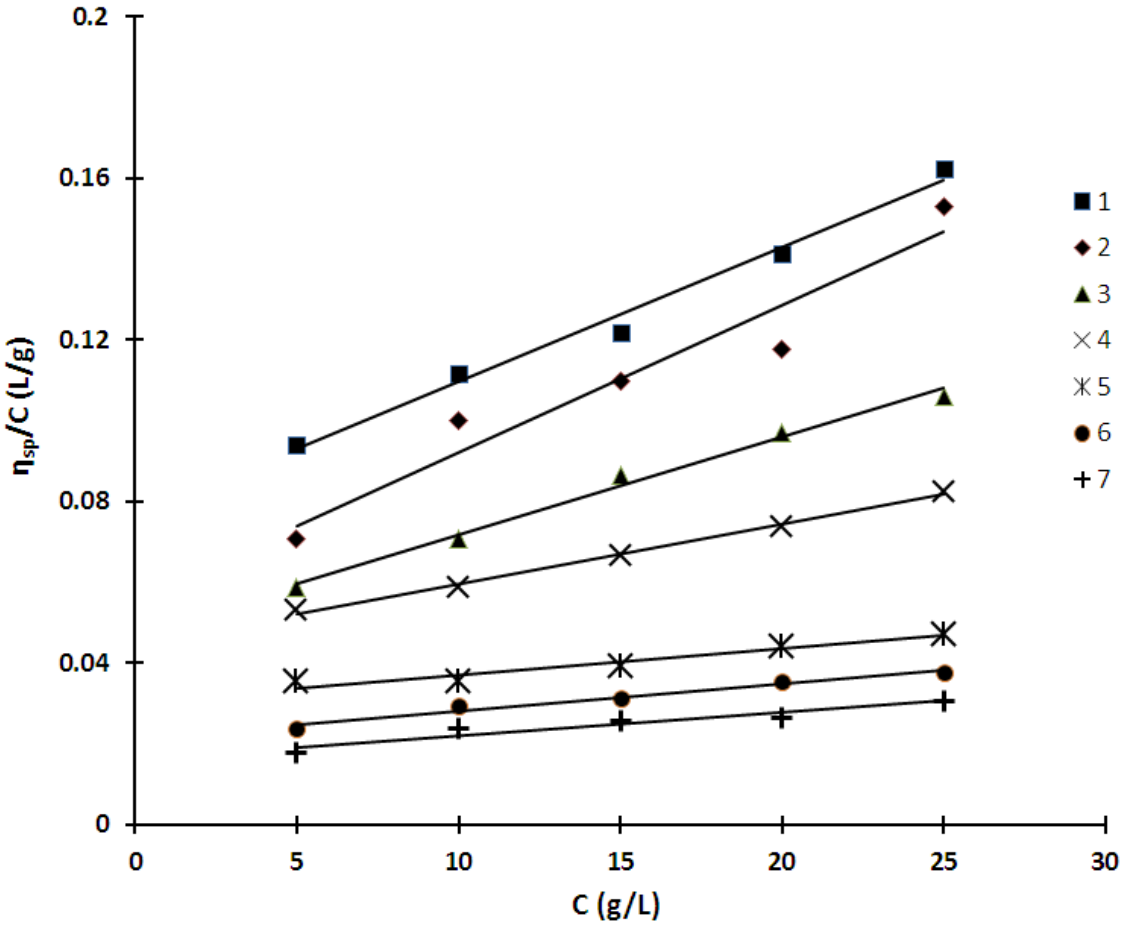

Figure S1: Evolution of η_{sp}/C as a function of C for the determination of [η] at C=0 for different PCL M_w. Linear regression equation and R-squared value are given respectively for **1**: M_w=85200g/mol, y = 0.0033x + 0.0764, R^2 = 0.9861; **2**: M_w=56400g/mol, y = 0.0036x + 0.0555, R^2 = 0.9352; **3**: M_w=51200g/mol, y = 0.0024x + 0.0475, R^2 = 0.9906; **4**: M_w=47700g/mol, y = 0.0015x + 0.0448, R^2 = 0.9959; **5**: M_w=29600g/mol, y = 0.0006x + 0.0305, R^2 = 0.9388; **6**: M_w=22500g/mol, y = 0.0007x + 0.0212, R^2 = 0.9694 and **7**: M_w=18600g/mol, y = 0.0006x + 0.0161, R^2 = 0.9279.

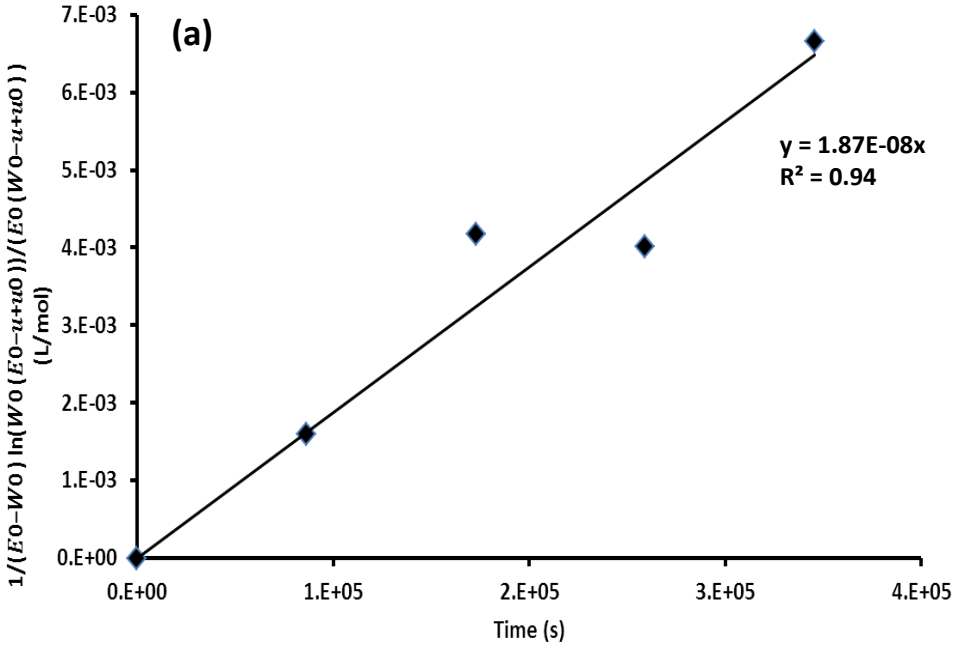
(a)
y = 1.87E-08x
R² = 0.94
7.E-03
6.E-03
5.E-03
4.E-03
3.E-03
2.E-03
1.E-03
0.E+00
0.E+00
1.E+05
2.E+05
3.E+05
4.E+05
Time (s)
1/(EO−WO) ln(WO(EO−u+u0))/(EO(WO−u+u0))
(L/mol)

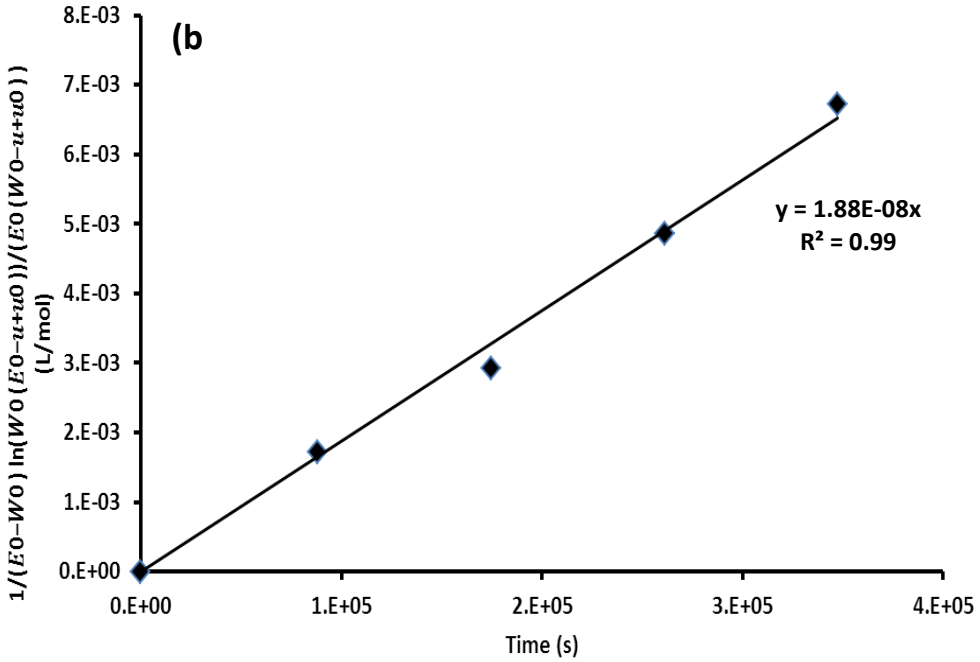
(b)
y = 1.88E-08x
R² = 0.99
8.E-03
7.E-03
6.E-03
5.E-03
4.E-03
3.E-03
2.E-03
1.E-03
0.E+00
0.E+00
1.E+05
2.E+05
3.E+05
4.E+05
Time (s)
1/(EO−WO) ln(WO(EO−u+u0))/(EO(WO−u+u0))
(L/mol)

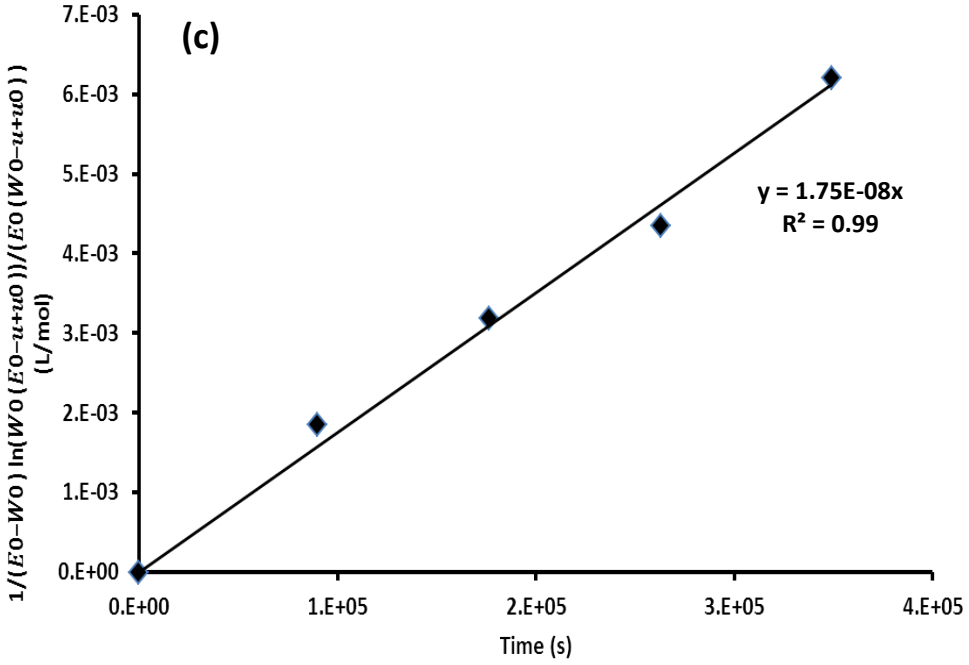
(c)
7.E-03
6.E-03
5.E-03
4.E-03
3.E-03
2.E-03
1.E-03
0.E+00
0.E+00
1.E+05
2.E+05
3.E+05
4.E+05
Time (s)
1/(E0−W0) ln(W0(E0−u+u0))/(E0(W0−u+u0))
(L/mol)
y = 1.75E-08x
R² = 0.99

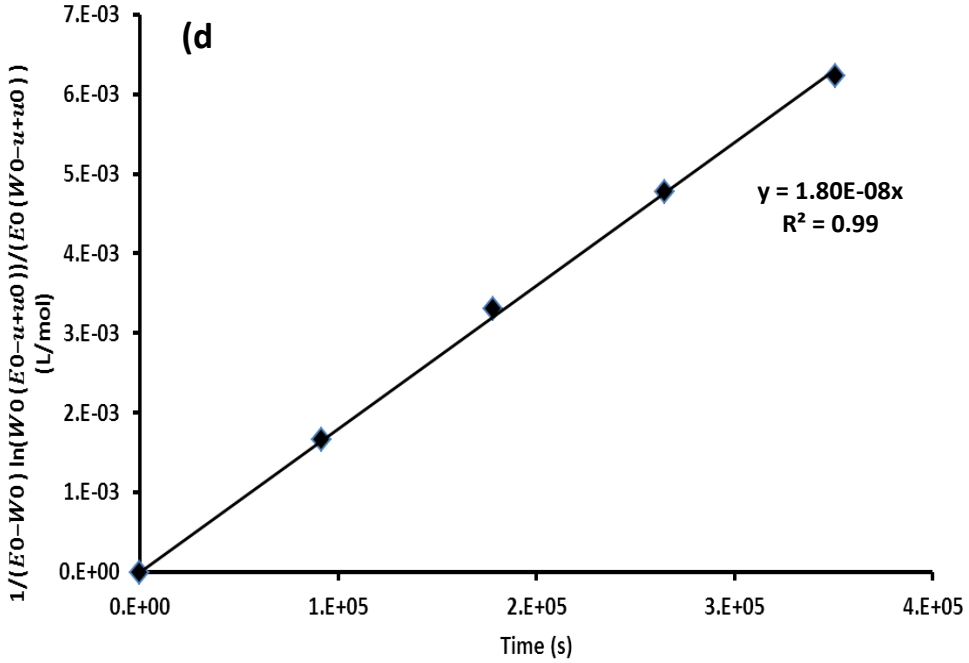
(d
7.E-03
6.E-03
5.E-03
4.E-03
3.E-03
2.E-03
1.E-03
0.E+00
0.E+00
1.E+05
2.E+05
3.E+05
4.E+05
Time (s)
1/(E0−W0) ln(W0(E0−u+u0))/(E0(W0−u+u0))
(L/mol)
y = 1.80E-08x
R² = 0.99

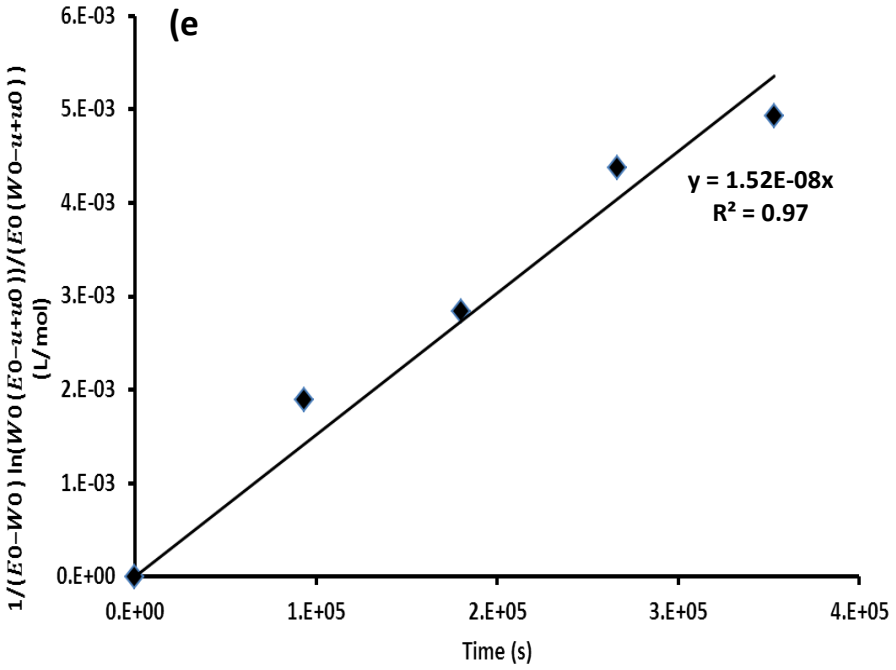

Figure S2 (a)(b)(c)(d)(e): Determination of k for 15% , 20%, 25%, 30% and 35% (w/v) PCL solutions, respectively.

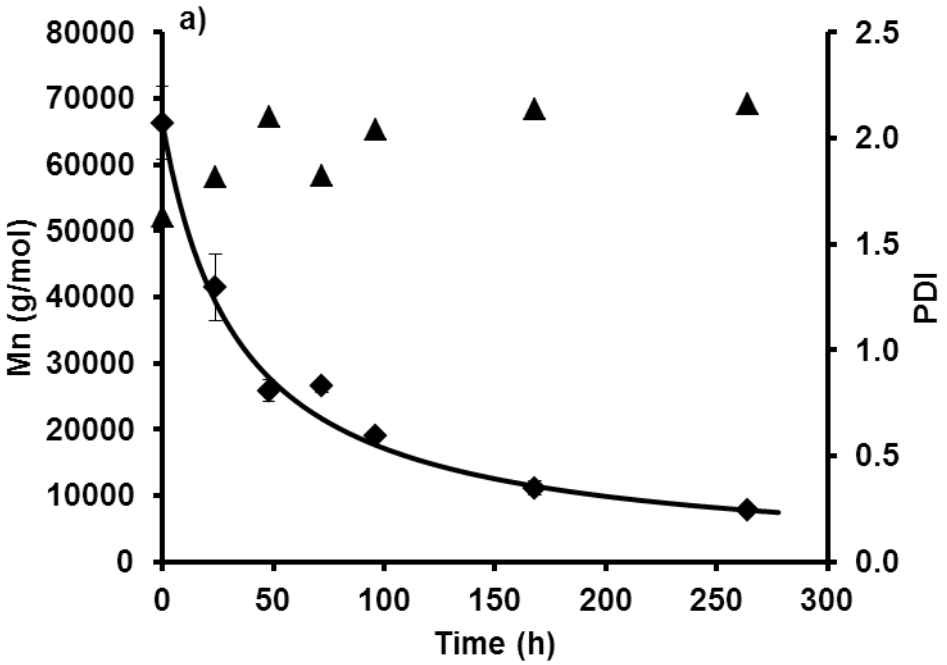
a)
80000
70000
60000
50000
40000
30000
20000
10000
0
Mn (g/mol)
2.5
2.0
1.5
1.0
0.5
0.0
PDI
0
50
100
150
200
250
300
Time (h)

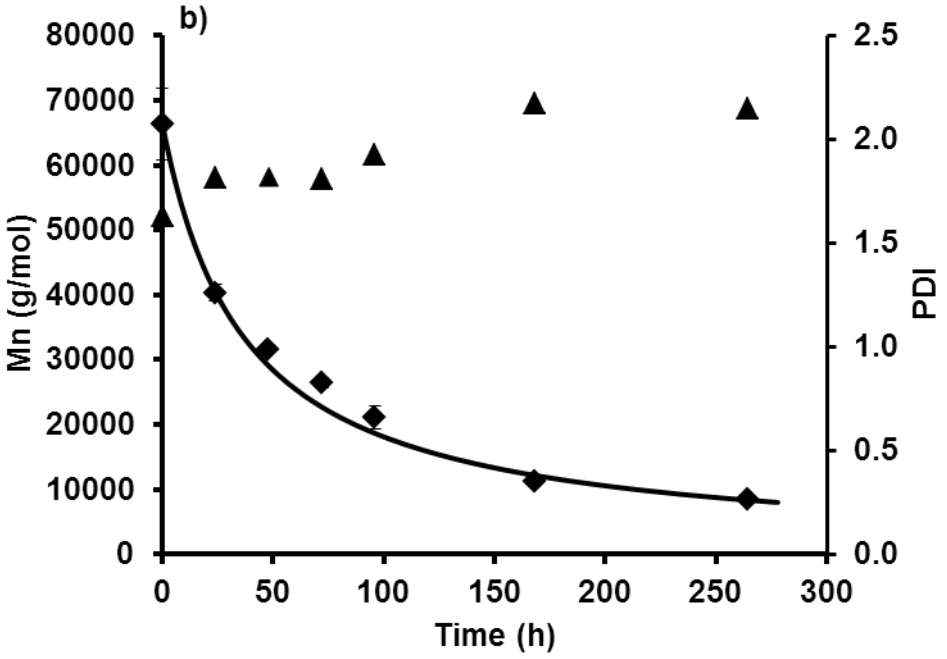
b)
80000
70000
60000
50000
40000
30000
20000
10000
0
Mn (g/mol)
2.5
2.0
1.5
1.0
0.5
0.0
PDI
0
50
100
150
200
250
300
Time (h)

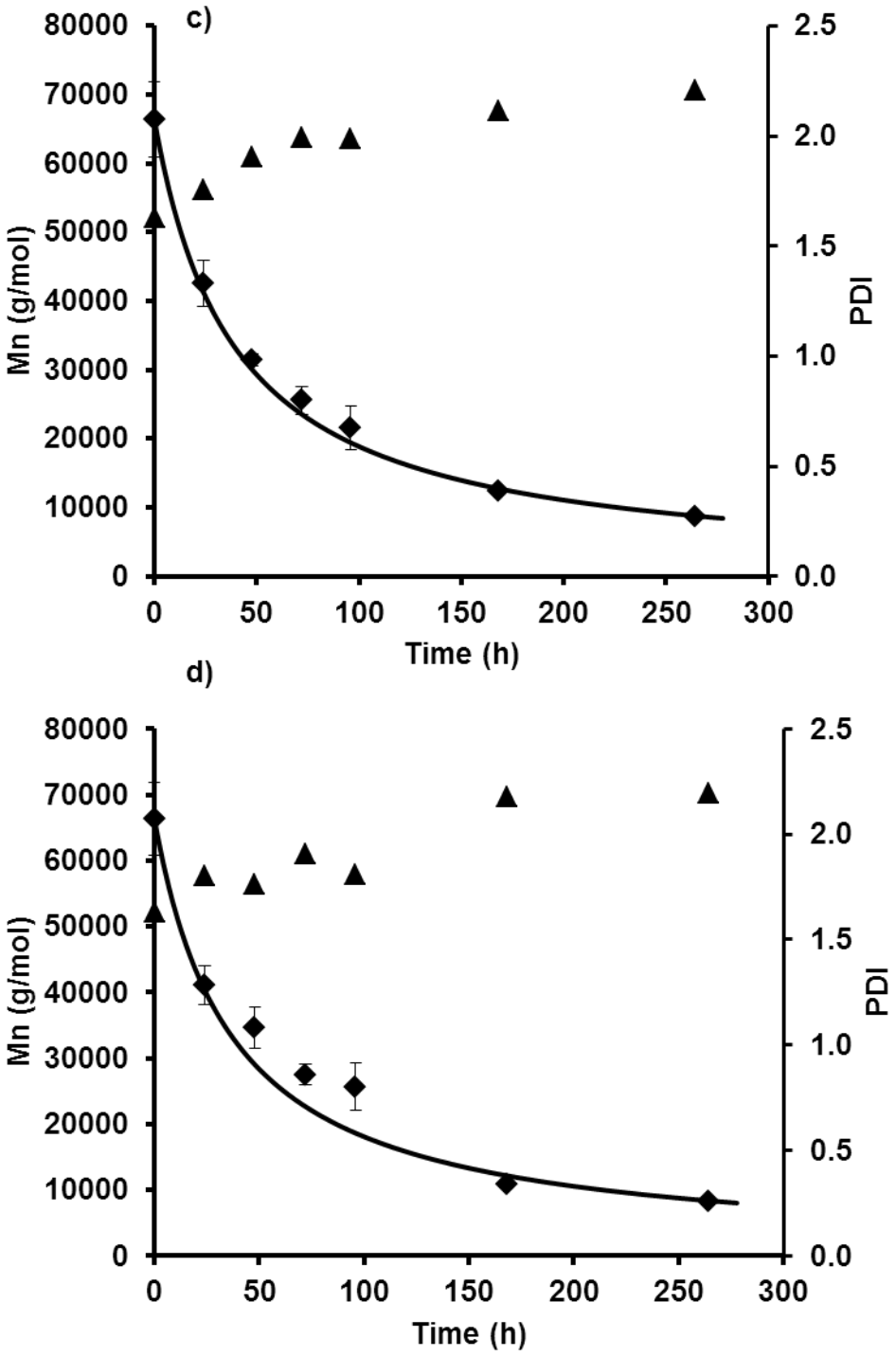

Figure S3 (a)(b)(c)(d): Evolution of M_n (■) and PDI (▲) as a function of degradation time for 15%, 25%, 30% and 35% (w/v) PCL and the corresponding plot of the theoretical model (—), respectively.

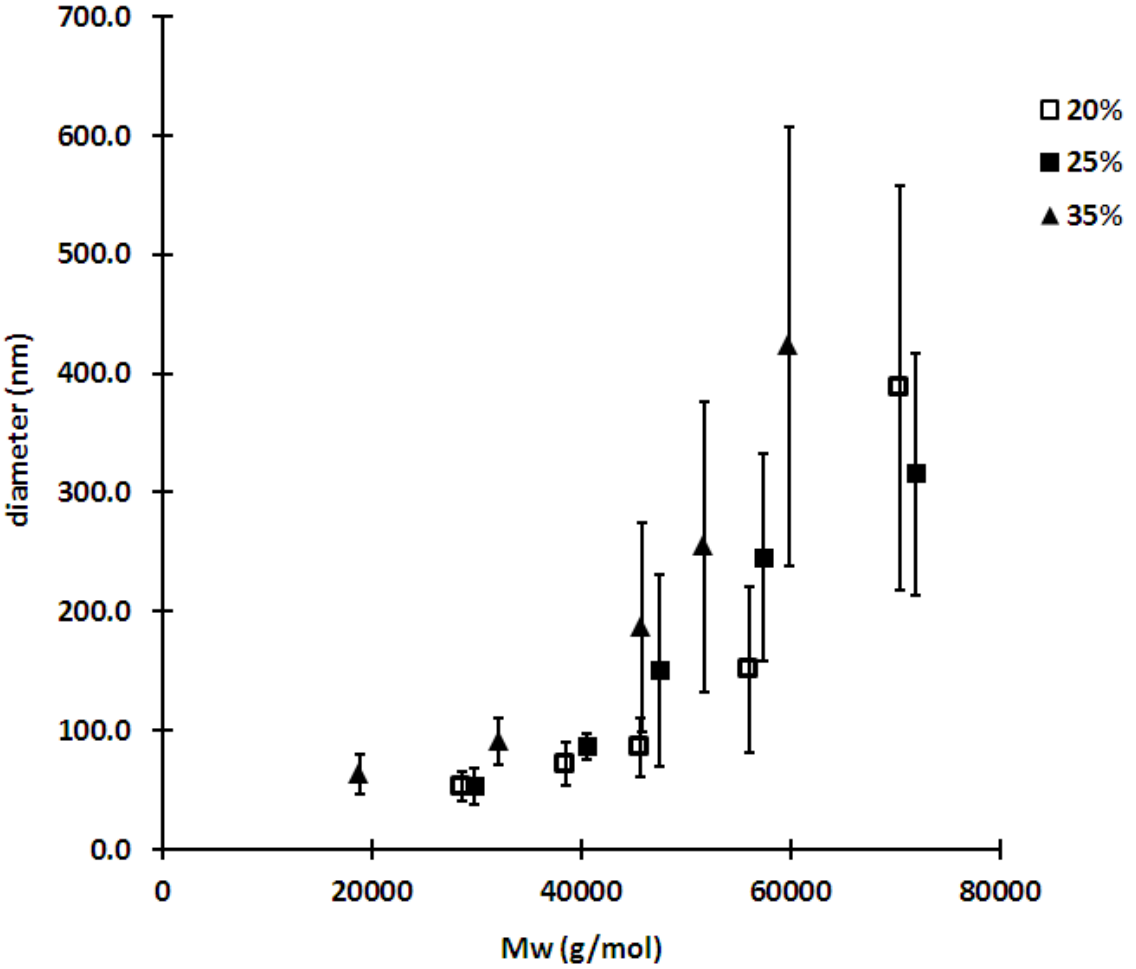

Figure S4: Variation of the average diameter of electrospun fibers produced from 20%, 25% and 35% (w/v) PCL solutions with M_w. The error bars represent the standard deviations of fiber diameter.

G) From fiber morphology to microstructure control of the membrane

We showed in Chapter 2 that the morphology of the electrospun biopolyesters can be tuned from nanofibers, to beaded-nanofibers and to nanoparticles. Moreover, we demonstrated that their diameters can be varied. Indeed, the viscosity of the used solution impacts the morphology and the dimension of the yielded materials. The use of acidic solvent mixture of acetic acid and formic acid enabled the hydrolytic degradation of the polyesters in solution impacting the degree of entanglement between the chains of polymers via the decrease of their molecular weight and thus of the viscosity. We also highlighted that the concentration of polymer in solution influences the morphology and dimension of the nanofibers as it changes its viscosity. Thanks to this approach, we could perform electrospinning for the fabrication of the nanofibers and electrospraying for the nanoparticles. We underlined that the viscosity is a key parameter for the controlled fabrication of the nanofibers. Molecular weight and concentration of the polymer were two key parameters considered for the work achieved, in order to obtain the desired morphologies.

We have shown that we can control to a certain extent the fiber dimensions and morphology. We can now focus on the structural aspect of the electrospun membrane and investigate the control over its architecture, microstructure and porosity. To this end, we have decided to combine electrospinning and electrospraying processing methods to design unique membranes composed of fibers and particles. The addition of particles into the fiber mat can be used to add properties, intrinsic to the particles, and to control the structure of the membrane. Indeed, the simultaneous electrospinning and electrospraying can allow electrostatic interactions between the fibers and the particles to form microstructures. We will now focus on the fabrication of hierarchical self-organized composite by the combination of

two technologies. We will show that particles and fibers can interact together to form structures by self-organization. The fabricated structures are interesting for biomedical applications as they allow the production of 3D membranes with controlled porosity and porosity gradient.

H) References

1. Reneker DH, Yarin AL. Electrospinning jets and polymer nanofibers. Polymer 2008;49(10): 2387-2425.

2. Reneker DH, Chun I. Nanometre diameter fibres of polymer, produced by electrospinning. Nanotechnology 1996;7(3): 216-223.

3. Greiner A, Wendorff JH. Electrospinning: A Fascinating Method for the Preparation of Ultrathin Fibers. Angew Chem Int Edit 2007;46(30): 5670-5703.

4. Popa AM, Eckert R, Crespy D, Rupper P, Rossi RM. A new generation of ultralight thermochromic indicators based on temperature induced gas release. J Mater Chem 2011;21(43): 17392-17395.

5. Guex AG, Kocher FM, Fortunato G, Körner E, Hegemann D, Carrel TP, Tevaearai HT, Giraud MN. Fine-tuning of substrate architecture and surface chemistry promotes muscle tissue development. Acta Biomat 2012;8(4): 1481-1489.

6. Sill TJ, von Recum HA. Electrospinning: Applications in drug delivery and tissue engineering. Biomaterials 2008;29(13): 1989-2006.

7. Cipitria A, Skelton A, Dargaville TR, Dalton PD, Hutmacher DW. Design, fabrication and characterization of PCL electrospun scaffolds - a review. J Mater Chem 2011;21(26): 9419-9453.

8. Lowery JL, Datta N, Rutledge GC. Effect of fiber diameter, pore size and seeding method on growth of human dermal fibroblasts in electrospun poly(ε-caprolactone) fibrous mats. Biomaterials 2010;31(3): 491–504.

9. Smith LA, Ma PX. Nano-fibrous scaffolds for tissue engineering . Colloid Surface B 2004;39(3): 125–131.

10. Del Gaudio C, Grigioni M, Bianco A, De Angelis G. Electrospun bioresorbable heart valve scaffold for tissue engineering. Int J Artif Organs 2008;31(1): 68–75.

11. Lee KH, Kim HY, Khil MS, Ra YM, Lee DR. Characterization of nano-structured poly(e-caprolactone) nonwoven mats via electrospinning. Polymer 2003;44(4): 1287-1294.

12. Moghe AK, Hufenus R, Hudson SM., Gupta BS. Effect of the addition of a fugitive salt on electrospinnability of poly(e-caprolactone). Polymer 2009;50(14): 3311-3318.

13. Luo CJ, Stride E, Edirisinghe M. Mapping the influence of solubility and dielectric constant on electrospinning polycaprolactone solutions. Macromolecules 2012;45(11): 4669-4680.

14. Van der Schueren L, De Schoenmaker B, Kalaoglu OI, De Clerck K. An alternative solvent system for the steady state electrospinning of polycaprolactone. Eur Polym J 2011;47(6): 1256-1263.

15. Grubisic Z, Rempp P, and Benoit H. A universal calibration for gel permeation chromatography. J Polym Sci Pol Phys 1996;34(10): 1707-1713.

16. Schindler A, Hibionada YM, Pitt CG. Aliphatic Polyesters. 111. Molecular Weight and Molecular Weight Distribution in Alcohol-Initiated Polymerizations of e-Caprolactone. J Polym Sci Pol Chem 1982;20(2): 319-326.

17. Yu H, Huang N, Wang C, Tang Z. Modeling of poly(L-lactide) thermal degradation: Theoretical prediction of molecular weight and polydispersity index. J of Appl Polym Sci 2003;88(11): 2557–2562.

18. Pitt CG, Gu Z. Modification of the rates of chain cleavage of poly(ϵ-caprolactone) and related polyesters in the solid state. J Controlled Release 1987;4(4): 283-292.

19. Lyu S, Sparer R, Untereker D. Analytical solutions to mathematical models of the surface and bulk erosion of solid polymers. J Polym Sci Polym Phys 2005;43(4): 383-397.

20. Simha R. Kinetics of Degradation and Size Distribution of Long Chain Polymers. J Appl Phys 1941;12(7): 569-578.

21. Antheunis H, Van der Meer JC, De Geus M, Heise A, Koning CE. Autocatalytic Equation Describing the Change in Molecular Weight during Hydrolytic Degradation of Aliphatic Polyesters. Biomacromolecules 2010;11(4): 1118-1124.

22. Gupta P, Elkins C, Long TE, Wilkes GL. Electrospinning of linear homopolymers of poly(methyl methacrylate): exploring relationships between fiber formation, viscosity, molecular weight and concentration in a good solvent. Polymer 2005;46(13): 4799-4810.

23. Koski A, Yim K, Shivkumar S. Effect of molecular weight on fibrous PVA produced by electrospinning. Mater Lett 2004;58(3-4): 493-497.

24. Fong H, Chun I, Reneker DH. Beaded nanofibers formed during electrospinning. Polymer 1999;40(16): 4585-4592.

25. McKee MG, Wilkes GL, Colby RH, Long TE. Correlations of Solution Rheology with Electrospun Fiber Formation of Linear and Branched Polyesters. Macromolecules 2004;37(5): 1760-1767.

CHAPTER III/

PUBLICATION N°2: "SIMULTANEOUS ELECTROSPINNING AND ELECTROSPRAYING: A STRAIGHTFORWARD APPROACH FOR FABRICATING HIERARCHICALLY STRUCTURED COMPOSITE MEMBRANES"

A) Abstract

We present here for the first time a simple method for micropatterning non-woven composite membranes. The approach is based on the simultaneous electrospraying of microparticles and electrospinning of nanofibers from different polymer solution feeds (polyethylene glycol and poly(D,L-lactide)) on a common support. The mechanism of self-organization between fibers and particles into hierarchical honeycomb-like structures, as well as the evolution of the later as a function of the thickness of the composite, is investigated. We demonstrate that aggregates of particles, leading to a non-uniform distribution of the electrostatic field near the collector, are necessary to form the self-organized composite. Furthermore, it is shown that the specific dimensions of the generated patterns can be controlled by tuning the flow rate of electrospraying. The obtained composite mat exhibits a multi-level porous structure, with pore sizes ranging from few up to several hundreds of microns. Finally it is shown that the microparticles can be selectively leached, allowing the production of a monocomponent membrane and retaining the hierarchical organization of the nanofibers suitable for biomedical and filtration applications.

B) Introduction

Electrospinning is widely used for the synthesis of nanofibrous non-woven membranes [1, 2]. The fabricated electrospun membranes have high porosities and high surface to volume ratio ; they are thus suitable for many applications [3] such as sensing [4], tissue engineering [5] or drug delivery [6]. The electrospinning process usually leads to non-woven mats by the random deposition of nanofibers. However, the control over the organization of nanofibers in electrospun membranes would provide a great benefit for various applications [7]. Indeed, precise geometric design of multicomponent electrospun membranes or 3D structures with defined porosity and pore sizes are necessary to mimic tissue structure and properties for tissue engineering applications [7, 8] and to achieve spatially and temporally controlled release of different drugs for drug delivery applications [9, 10].

A number of methods have been developed to control the deposition of the nanofibers and prepare structured membranes. For example, aligned electrospun fibers have been obtained by electrospinning on a rotating collector [11]. More complex 2D or 3D structured membranes have also been prepared using electrostatic forces [12-15]. The principle of this approach is the modification of the electrostatic field near the collector, thus guiding the deposition of the charged nanofiber. In addition, structured membranes were also fabricated using diverse post-electrospinning structuring strategies: direct laser machining [16], wetting of porous template [17] or photo-patterning of electrospun membranes [18].

Another type of structured membranes can be obtained by the self-organization of electrospun nanofibers. They have been first presented by Deitzel et al. [19] for poly(ethylene oxide) and then observed for other polymers [20-23]. Such self-organized mats are very interesting for tissue engineering applications as they can form 3D cm-thick hierarchical foams with adequate pore sizes and mechanical properties [23]. It was shown that a bimodal distribution

of the fiber diameter is a necessary condition to induce the self-organization. Such irregular fibers, having thick and thin domains, locally impact the electrostatic field and guide the deposition of the fibers into honeycomb-like patterns [23]. However, a bimodal distribution of fiber diameters, leading to self-organization in the mat, is observed only in specific electrospinning conditions and is not easily transposable to every polymers. A solution to this problem could be the combination of electrospun monodisperse thin fibers with electrosprayed larger particles. This more versatile process results in composite membranes, in which fibers and particles of different polymers are combined, thus leading to added functionalities.

The fabrication of composite membranes has already been performed using dual or co-electrospinning [24-26] which allows the combination of properties from different nanofibers within one membrane. Co-electrospinning has inspired the combination of electrospinning and electrospraying technologies to form a composite membrane made of electrospun fibers and electrosprayed particles. Electrospraying is very similar to electrospinning [27]. The main difference between these two processes is the presence and quantity of polymer chain entanglements in the polymer solution. Under identical electrospinning conditions, by simply decreasing the number of polymer chain entanglements in the solution, the morphology can be varied from regular nanofibers to beaded nanofibers and to particles [28-30]. Electrospinning and electrospraying can be performed simultaneously using a rotating mandrel and two capillaries through which the respective polymer solutions are fed; the yielded nano- and micro-objects are collected in a unique membrane. Hydrogels [31], hydroxyapatite [32] or even cells [33] have been simultaneously electrosprayed into electrospun scaffolds for tissue engineering and drug delivery applications. Finally, electrospraying is an efficient way for drug encapsulation into particles [34]. A comprehensive review on electrospraying of polymers with therapeutic molecules was recently published by N. Bock et al [30].

In the present work, we develop a general method for the fabrication of structured electrospun composites. We demonstrate for the first time the self-organization of electrosprayed microparticles and regular thin electrospun nanofibers into growing honeycomb-like patterns. The obtained composites present a hierarchical porous structure with pore sizes ranging from a few microns up to hundreds of microns. The conditions allowing the formation of a structured or a random composite are discussed. The origin of the mechanism of the self-organization of fibers and particles, as well as the evolution of the generated patterns with the thickness of the composite are then investigated. Finally, we show the possibility of further varying the morphology of the composite membrane by the selective leaching of the particles.

C) Experimental section

1) Materials

Poly(D,L-lactide) (PLA) of a molecular weight of 75 kg/mol and 15 kg/mol (values given by the supplier) were respectively supplied by Purac under the commercial names Purasorb PDL 0.6 and Purasorb PDL 0.2A. Acetic acid (purum ≥99.0%, H2O≈0.2%), formic acid (≈ 98%, H2O ≈ 2%) and polyethylene glycol (PEG) of a molecular weight of 15 kg/mol were provided by Fluka (Sigma-Aldrich). The fluorescent dyes Lumogen F Pink 285 and Lumogen F Blue 650 were supplied by BASF. All products were used as received.

2) Electrospinning and electrospraying conditions

PLA nanofibers (75 kg/mol) was electrospun (ΔV = 24.5 kV, needle-collector distance = 13.5 cm, pump flow rate = 0.3 mL/h, room temperature, 40% RH) from a solution of acetic acid / formic acid 50/50 (v/v) at the concentration of 22% (wt.) 24 hours after the preparation of the solution. PLA microparticles (15 kg/mol) was electrosprayed (Vneedle = +28.5 kV, Vcollector = -1kV, needle-collector distance = 13.5 cm, pump flow rate = 0.3 mL/h, room temperature, 40% RH) from a solution of acetic acid / formic acid 50/50 (v/v) at the concentration of 17% (wt.) 24 hours after the preparation of the solution for the fabrication of non-aggregated PLA particles and 48 hours later for the fabrication of aggregated PLA particles. Indeed, after 48 hours of solution preparation the yielded particles were bigger (from 540 ± 170 nm to 1.0 ± 0.2 µm) and permitted aggregation [35]. PEG microparticles was electrosprayed (Vneedle = +27 kV, Vcollector = -1kV, needle-collector distance = 12 cm, pump flow rate = 0.08, 0.1 and 0.2 mL/h, 25°C, 40% RH) from a solution of acetic acid /

formic acid 10/90 (v/v) at the concentration of 55% (wt.). The solvent mixture and the electrospinning – electrospraying conditions were optimized to obtain steady state formation of bead-free PLA nanofibers and spherical PLA and PEG microparticles. Fibers and particles were co-electrospun into a vertical rotating drum as represented in Figure 1a. The rotation speed of the drum was 50 rpm and its diameter 4 cm. Indeed, a low velocity avoids mechanical fiber alignment which could inhibit the spontaneous formation of patterns. Moreover, in order to obtain a homogeneous mixture of the particles within the fibers, a dielectric tape was attached to the rotating collector to delimit the deposition area (5 cm) (Figure S3a and b). Indeed, without the dielectric tape and in the case of a larger deposition area of the particles than the one of the fibers, the charged electrosprayed particles will be deposited preferentially outside the dielectric nanofibrous mat, leading to an inhomogeneous or non-existing composite. Charged electrosprayed particles are very sensitive to the electrostatic field and can be confined with a dielectric tape as shown in Figure S3c. The components of the electrospinning setup have been described previously [29]. The fabricated composites were dried and stored in a dried atmosphere.

3) Characterization of the composites

The morphology of the fibers, particles and composites was characterized using a scanning electron microscope (SEM, Hitachi S-4800 at Vacc = 5kV, Ie = 10 µA). Gold (5 nm) was sputtered on all membranes using a scanning electron microscope coating unit (E5100) from Polaron Equipment Limited. For each sample, the average nanofiber/microparticle diameter and standard deviation were calculated from the diameter measured from 12 nanofibers/microparticles in 3 randomly selected areas. A LSM 710-780 confocal fluorescent microscope from Zeiss was used to localize Lumogen Blue-loaded PLA fibers and Lumogen

Pink-loaded PEG particles in the composite for Figure 1f. An optical microscope from Keyence was used to analyze the dimensions of the self-organized patterns and ImageJ software was used for the analysis of images. The average linear pattern size (L) and the maximum pattern size (L_{max}) were calculated from three randomly selected areas per sample. Two lines were perpendiculary drawn on the images of the micropatterned membranes. The ratio between the length of the line and the number of crossed patterns is equal to L. Perpendicular lines were drawn to assess the orientation degree of the patterns. Lmax was calculated as the average of the maximum pattern length measured from at least twenty patterns. Membranes thickness (h) was assessed using a profilometer (Dektak 150 from Veeco). To this end, composites were deposited when needed on Si wafers previously coated with 100 nm of aluminum and 10 nm of gold with an electron beam evaporator to ensure conductivity of the wafers. Otherwise, the composites were deposited on aluminum foils. Apparent density and porosity were determined gravimetrically using the following formulas, with m, the mass of the membrane and S, the membrane area:

$$apparent\ density\ \left(\frac{g}{cm^3}\right) = \frac{m}{h * S}$$

$$porosity = \left(1 - \frac{apparent\ density}{bulk\ density}\right) * 100$$

Transversal cut with Gillette blades at room temperature was performed to visualize cross-sections of the composites (Figures 5 and 6).

D) Resutlts and discussion

1) Self-organization of microparticles and nanofibers

PEG particles and PLA fibers were electrosprayed and electrospun to generate a composite membrane. Figure 1a shows the setup used for the fabrication of the composite. PEG particles were electrosprayed on one side of the rotating collector and PLA fibers were electrospun on the opposite side. This configuration is optimal for the co-electrospinning [36]. The process parameters were optimized in order to allow the steady state formation of bead-free PLA nanofibers and spherical PEG microparticles. PLA fibers (Figure S1a) and PEG particles (Figure S1b) had an average diameter of 200 ±20 nm and 1.6 ±0.4 µm, respectively. Both polymers were processed from an acetic acid and formic acid solvent mixture. This solvent system has been studied for the electrospinning of PCL [37] and as a tool to control the morphology of the yielded PCL electrospun fibers [29], and it is successfully used for the production of PLA nanofibers and PEG microparticles.

In Figure S1a, when only fibers are deposited, a non-woven electrospun mat with randomly placed PLA nanofibers can be observed. On the other hand, as shown in Figure 1b, the simultaneous electrospinning of PLA fibers and electrospraying of PEG particles leads to a uniquely, structured composite membrane with a honeycomb-like pattern. Indeed, after one hour of deposition, honeycomb-like patterns with polydisperse sizes are observed. Such structures with honeycomb-like patterns have already been observed in simple electrospinning [20-22]. Ahirwal et al. [23] have shown that a bimodal distribution of fiber diameter was necessary to form these honeycomb-like patterns. The electrospinning of a fiber having thick and thin domains leads to the formation of a heterogeneous, rough surface that is non-

uniformly charged. Indeed, thick domains, in contact with the collector, are areas where the electric charges can efficiently dissipate, while between these domains suspended thin fibers remain charged. These heterogeneities modulate the electrostatic field near the collector and act as a template for the formation of honeycomb-like patterns [23]. In our case, the electrosprayed PEG particles play the role of the thick domains whereas the regular PLA fibers play the role of the thin domains. As such, the respective morphologies of the thick or micron size domains and the thin or sub-micron size domains can be independently controlled. Figure 1c shows an elementary domain of the honeycomb-like pattern. We notice that the particles are mainly located in the walls forming the borders of the patterns. In order to confirm this observation, a membrane with stained fibers and particles was fabricated. Lumogen blue fluorescent dye was added to the PLA solution feed and Lumogen pink dye to the PEG solution feed. Confocal fluorescence microscopy (Figure 1d) confirmed that particles and fibers are preferentially deposited in the walls of the honeycomb-like pattern whereas, between the walls, only stretched nanofibers are present. This result is in agreement with the observations made with the self-organization of irregular fibers [23]. Indeed, particles are independent entities, whereas an electrospun fiber can be viewed as a continuous cylinder. To cross the repulsive area formed by the charged fibers inside a pattern from one wall to another, the next particle will just deposit directly on the next wall, whereas the fiber has the possibility of crossing the pattern to reach the next wall or to align along the wall as a consequence of the confinement effect [12,14].

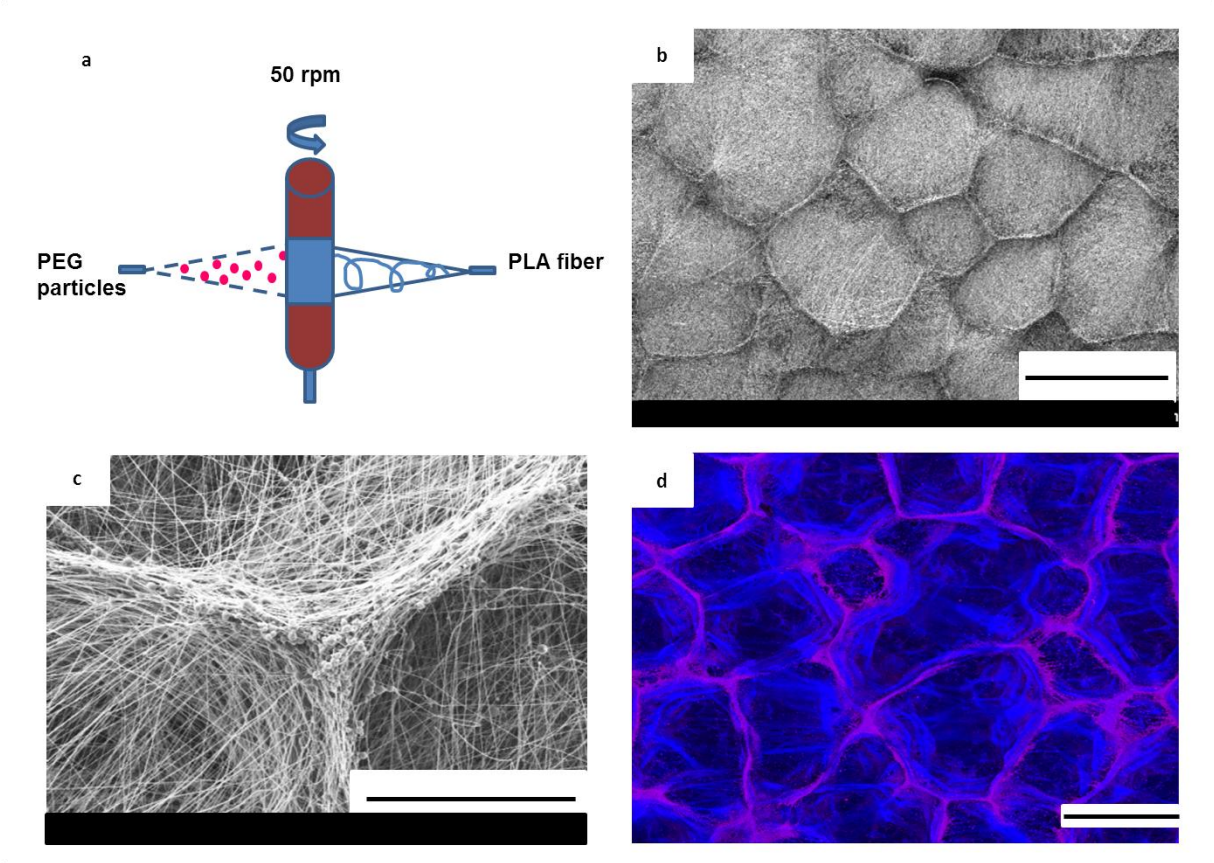

Figure 1: (a) Schematic illustration of the experimental setup. (b) SEM micrograph showing honeycomb-like patterns of the composite after 60 minutes of deposition (scale bar = 1mm); (c) SEM micrograph of an elementary domain of a honeycomb-like pattern formed by the simultaneous electrospinning of PLA nanofibers and electrospraying of PEG microparticles after 60 minutes of deposition (scale bar = 50µm); (d) Confocal fluorescent microscopy image of Lumogen Blue-loaded PLA nanofibers and Lumogen Pink-loaded PEG microparticles composite after 60 minutes of deposition (scale bar = 500µm).

The patterns are formed by the self-organization of the fibers and the particles. In the first moments of the deposition, particles and fibers form a non-uniform, rough surface. This heterogeneous surface is used as a template for the deposition of the following particles and fibers. In Figure S1b, (supporting information) we observe that when only electrospraying is

carried out the particles are not deposited homogeneously over the surface, but are aggregated and form a heterogeneous surface with randomly distributed domains of high and low densities of particles. Again, this observation can be compared with the first moments of the deposition of irregular fibers where some locations showed aggregated thick fiber domains and others thin fiber domains [23]. As discussed before, the non-uniform surface would be the basis for the self-organization of the composite. We thus hypothesize that aggregated particles (or larger particles) are necessary to form the patterns generating a non-uniform electrostatic field. To confirm this hypothesis, we investigated the influence of the aggregation of the microparticles on the self-organization process. Dielectric particles of the same electric charge can be attracted to one another depending on the range of particle size and charge ratios [35, 38 - 39]. As the particle size increases, the attractive force becomes stronger [35]. Unfortunately, we were not able to produce non-aggregated PEG particles because we could not decrease their sizes sufficiently with the used solvent system. Thus, for this demonstration only, PLA was used to produce the particles. Indeed, we found similar conditions (i.e. in the same solvent system) allowing electrospraying of non-aggregated PLA particles (Figure 2a) and aggregated PLA particles (Figure 2d).. Aggregated and non-aggregated particles of PLA were fabricated because their individual size could be tuned from few hundred of nanometers in diameter (540 ± 170 nm) up to micron size (1.0 ± 0.2 µm). When non-aggregated particles were electrosprayed in combination with PLA nanofibers, a uniform distribution of them within the fiber mesh was observed (Figure 2b) leading to a composite membrane with randomly deposited particles and fibers (Figure 2c). On the contrary, for aggregated electrosprayed particles (Figure 2d), their combination with electrospun nanofibers resulted in a heterogeneous distribution of the particles within the membrane (Figure 2e). As a consequence, a non-uniform charge distribution was formed over the surface. The deposition of the incoming fibers was then guided by these heterogeneities in the electric field and micrometric patterns were generated (Figure 2f).

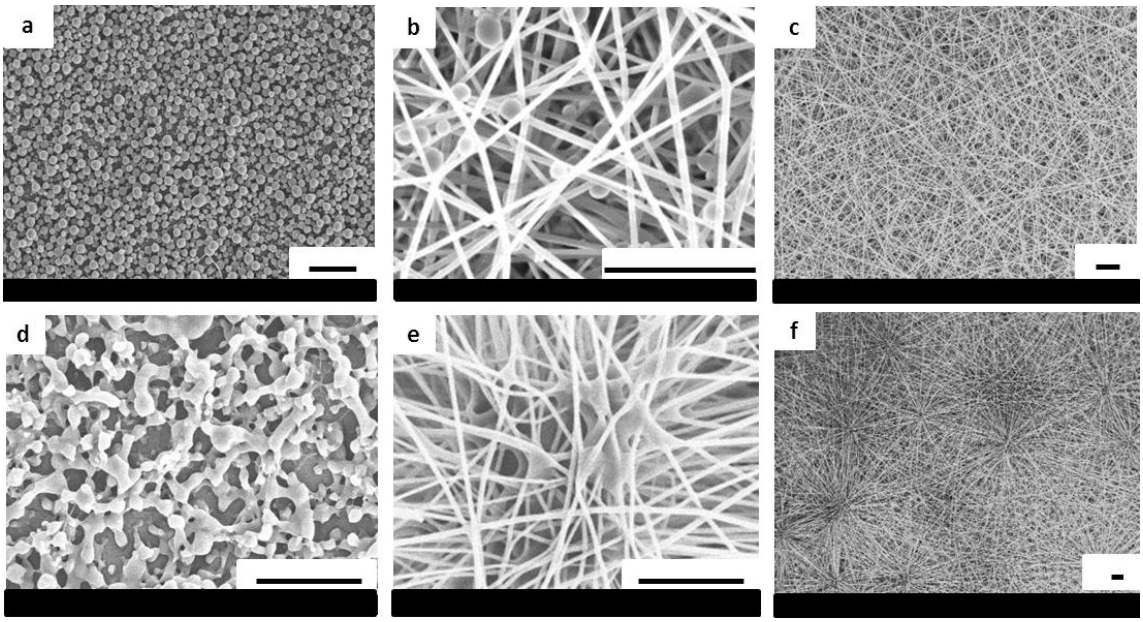

Figure 2: SEM micrographs of non-aggregated electrosprayed PLA particles (a); in the composite with PLA fibers at high (b) and low (c) magnifications; SEM micrographs of aggregated electrosprayed PLA particles (d); in the composite with PLA fibers at high (e) and low (f) magnifications. (scale bar = 5 µm).

It is thus clear that the aggregation degree plays a major role in the formation of patterned composites. We can make the assumption that by varying the size of the aggregated domains one can fine-tune the self-organization of the incoming fibers. To verify this hypothesis, a PEG solution was electrosprayed at different flow rates. This led to the formation of particles of different sizes and quantities. Figures 3a, 3c and 3e show that aggregated PEG particles with average diameters D = 1.3 ±0.2 µm, 1.6 ±0.4 µm and 2.4 ±0.5 µm can be obtained with flow rates q of 0.08 mL/h (PEG 0.08), 0.1 mL/h (PEG 0.1) and 0.2 mL/h (PEG 0.2) respectively. All particles were found to be aggregated on the surface of the collector after simple electrospraying. Because the deposition area was the same for the three kinds of

particles and the PEG solution was the same for all experiments, one can assume that the number of particles produced during a given time is proportional to q/D^3. Thus, the lowest flow rate leads to the production of the highest number of the smallest particles. More precisely, PEG 0.08 yielded 1.5 times more particles than PEG 0.1, which yielded 1.7 times more particles than PEG 0.2. The variation of the flow rate is thus a straightforward manner to modulate the number and the size of the particles but unfortunately not independently. As a consequence, the size of the aggregated particles domains (plain white circles in Figure 3) and the empty domains (dashed white circles in Figure 3) can also be tuned. A higher number of smaller particles lead to smaller particle aggregates and to smaller neighbouring empty domains. Looking at the corresponding self-organized composites made of the particles and the nanofibers (Figure 3 b, d and f), we can observe the influence of the electrospraying flow rate on the pattern size for the same production time (15 minutes). The differences in the pattern sizes can be quantified. We can define *L*, the average characteristic pattern size, defined as $L = L_0/N$, with *N*, the number of patterns crossed by a line of length L_0. We also define *p*, a polydispersity index of the size distribution of the patterns with $p = p'/L_{max}$, where L_{max} is the average of the maximum length of the patterns and *p'* its standard deviation. We found (L= 290 µm; p= 0.4) when PEG 0.08 was used, (L= 345 µm; p= 0.4) with PEG 0.1 and (L= 410 µm; p= 0.5) with PEG 0.2.

In conclusion, by increasing the particle flow rate one can obtain larger aggregate sizes and thus increase the characteristic size *L* of the honeycomb-like patterns. Consequently, the independent production of particles and nanofibers allows the control over the size of the honeycomb-like pattern by varying a simple experimental parameter. This is not possible in the case of the self-organization induced by bimodal nanofibers.

However, one can notice in Figure 3 that the size of the aggregated and related empty domains, in the range of 10 µm, is much smaller than the size L of the patterns, in the range of

few hundreds of microns, obtained after 15 minutes of deposition. A closer observation of the samples shows an increasing pattern size from the edges to the center of the membrane. Indeed, the deposition is not exactly uniform as more fibers and particles are deposited in the center of the collector than on the edges. Moreover, the pattern sizes appear to increase with deposition times until becoming visible on a macroscopic scale.

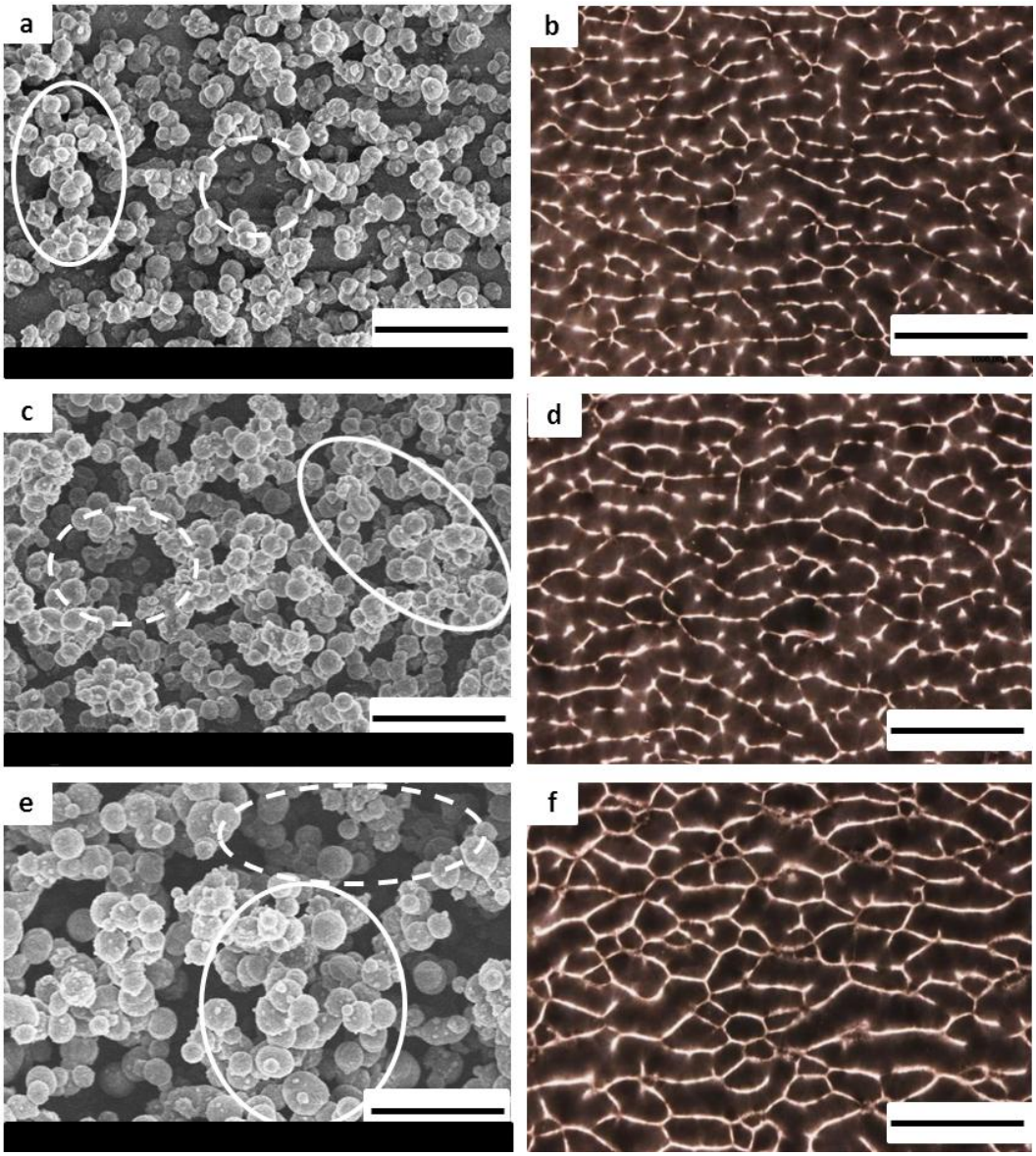

Figure 3: SEM micrographs of aggregated electrosprayed PEG particles at a flow rate of 0.08 mL/h (a), 0.1 mL/h (c) and 0.2 mL/h (e) after two minutes of deposition. Dashed and plain circles are showing empty and aggregated domains, respectively (scale bar = 10 µm); Optical microscopy images of the corresponding self-organized composites with PLA nanofibers obtained by simultaneous electrospraying and electrospinning (b), (d) and (f) after 15 minutes of deposition (scale bar = 1 mm).

2) Evolution of pattern size with the thickness of the sample

In order to understand how the self-organized pattern can grow from a few microns to several hundred of microns and characterize the structure of the membranes, the evolution of pattern size with thickness of the membrane was investigated. For this purpose, electrosprayed PEG 0.1 particles and electrospun PLA fibers were deposited simultaneously on conductive wafers clamped on the rotating collector and observed at the deposition times of 5, 10, 20, 40 and 60 minutes.

For each sample, the thickness profile of the composite was analyzed by profilometry. Figure 4a shows the typical thickness profile of the membrane after 40 minutes of deposition from the edge of the wafer (x=0) toward its center (x=20mm). The growing of the patterns as a function of the thickness can be clearly observed on the optical microscopy image of the sample superimposed with the profile. The average linear pattern size (L) of the membrane was measured for (x= 5, 10, 15, 20) mm (Figure 4a, black vertical lines) and plotted as a function of h, the membrane thickness (Figure 4b). The additional points on the graph of Figure 4b correspond to measurements taken from the center of samples obtained after the different deposition times (optical microscopy images in Figure S2, supporting information). All measurements are in good agreement with each other and fit to the same curve. An increase of the size of the patterns with the thickness has also been observed and explained by Ahirwal et al. [23] for the self-organization of bimodal fibers. It originates from the broad size distribution of the first generated patterns. Electrostatics numerical simulation on such a surface show a higher vertical component of the electrostatic field over the walls of larger patterns, leading to the preferential deposition on the bigger patterns and the progressive disappearance of the smaller ones. In our case also, a size polydispersity of aggregates and patterns can be observed (Figure 3c and d) and thus the evolution of the patterns can be

explained by a similar mechanism. The fabricated composites thus exhibit a hierarchical structure with patterns gradually growing with the thickness of the composite.

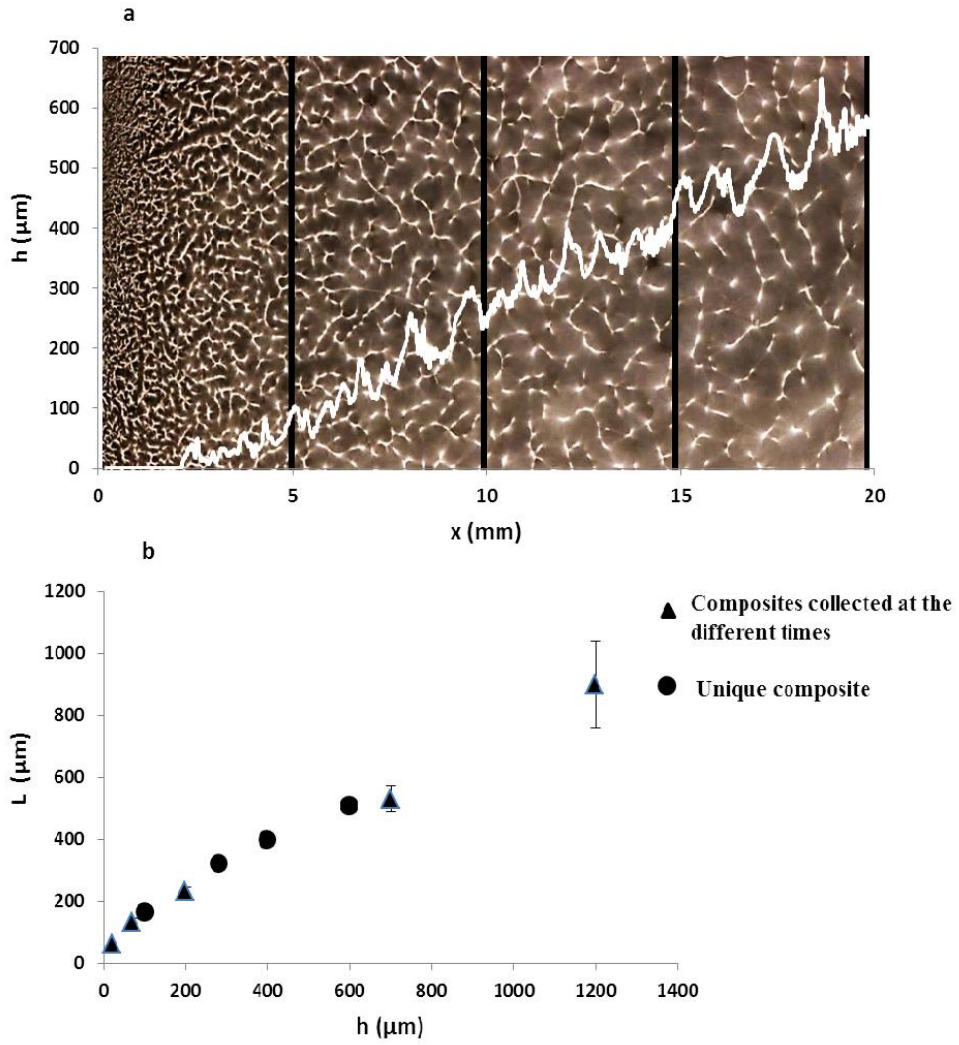

Figure 4: (a) Evolution of the membrane thickness (*h*) as a function of the distance (x) and optical microscopy image of the corresponding membrane. L was determined for *x* equal to 5, 10, 15 and 20 mm represented by the black vertical lanes. (b) Evolution of the average linear pattern size (*L*) with standard deviation as a function of the membrane thickness (*h*)

Figure 5 shows a SEM micrograph of the cross-section of a 1 mm-thick composite membrane made of electrosprayed PEG 0.1 particles and PLA nanofibers after one hour of deposition. Additionally to the pores formed by the inter-fiber distance, we can observe larger pores

formed between the walls of the patterns and directly related to the pattern size *L* [23]. The size of the large pores increases with the thickness of the sample, as the size (*L*) of the formed patterns is growing. In Figure 5a, the main central pattern (black arrows) has pore sizes ranging from few microns at the bottom part up to around one millimeter at the top part of the membrane. Furthermore, on both sides of the image two walls merging into a unique one (white arrows) can be seen, showing the pattern growth as discussed previously. The self-organization of particles and fibers into growing honeycomb-like patterns results in a hierarchical porosity and a global increase of the pore size within the thickness of the membrane. Figure 5b presents the evolution of the apparent density of the membrane as a function of its thickness. We can observe that the apparent density decreases with h and the value is divided by ten over the thickness of the membrane. The corresponding porosity varies from 85 to 98% over the thickness.

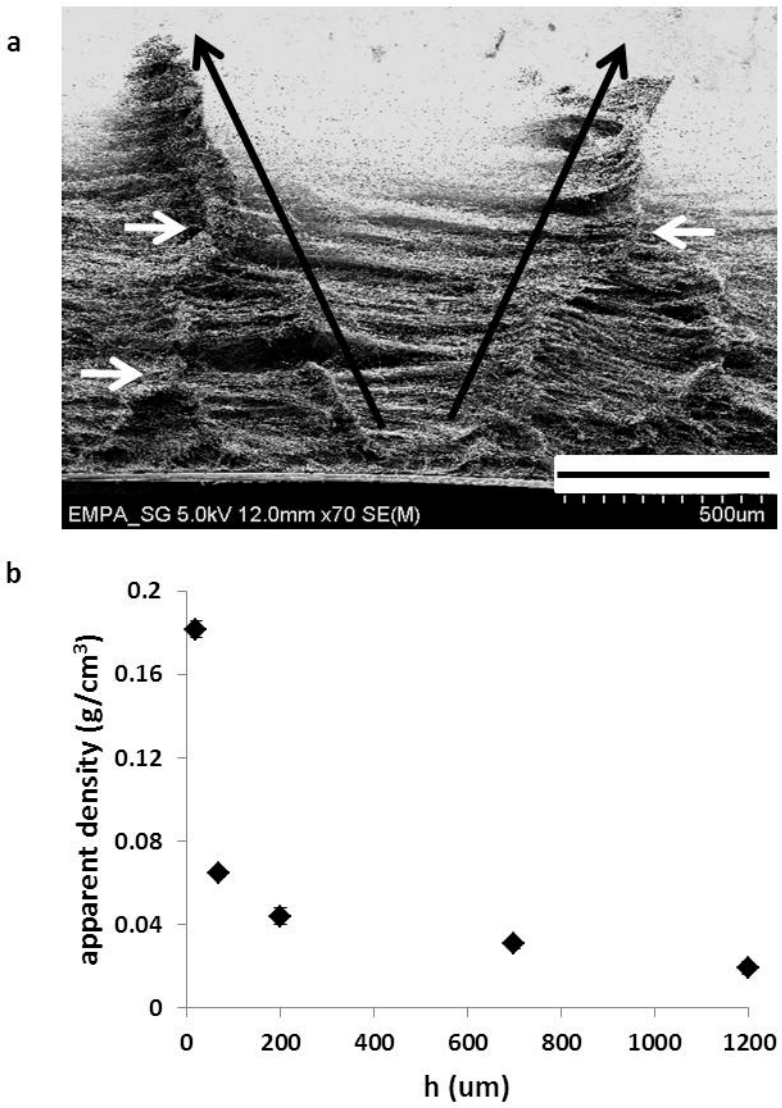

Figure 5: (a) SEM micrograph of a cross-section of the self-organized (scale bar = 500 µm) composite made of PLA nanofibers and PEG 0.1 microparticles after one hour of deposition, showing in the center a growing pattern (black arrows) and on the two sides patterns merging into a unique one (white arrows). (b) Evolution of the apparent density of the composite membrane as a function of its thickness (*h*).

3) Application to the fabrication of hierarchical porous membranes by the selective leaching of the electrosprayed particles

The composite presented here has the additional advantage of being formed by two distinct materials. This allows the design of composites with added functionality by choosing appropriate materials for the intended final application. It is moreover possible to remove selectively one of the two materials by selective leaching. Selective leaching is a strategy that has already been used with co-electrospinning. Selective removal of sacrificial fibers was used to improve cell infiltration in electrospun scaffolds [40] or particle-loaded sacrificial fibers were used to deposition the particles into an electrospun mat [41]. In our case, selective leaching of the particles would allow to have an electrospun membrane formed of regular self-organized nanofibers. To this end, the composite membrane made of PEG0.1 microparticles and PLA nanofibers was washed in a 500 mL bath of deionized water during 10 minutes in order to remove the water-soluble PEG and obtain a pure PLA non-woven. Figure 6 presents SEM images of the membrane before (a, c and e) and after washing (b, d and f). Comparing images 6a and 6b, we can notice that the microstructure formed by the patterns is maintained even after the removal of the PEG particles. A closer look to the walls of the patterns, where the particles are located (Figure 6c) confirms the disappearance of the PEG particles (Figure 6d). The same observation can be made on the basis of the cross-sectional images acquired before and after washing (Figures 6e and 6f respectively). Since the particles and fibers can be generated independently from materials with different properties, it is easily possible to generate a monocomponent microstructured membrane from a multicomponent one.

The processing approach described in this work allows the formation of three-dimensional scaffolds, which are of paramount importance for tissue engineering [23]. In particular, the technology presented here is not limited to certain polymer systems and it allows also the combination of inorganic particles with polymeric matrices. The method also allows the fabrication of scaffolds with large pores having diameters in the tens of microns range, sizes which are comparable to different cell types. As a particular application we can cite bone tissue engineering, where an open, multi-level structured support is essential for ensuring cell infiltration and proliferation [42 - 44]. Such hierarchically structured membranes are also very interesting for biological fluids filtration, as they allow the size selective separation of cells, macro- and small molecular components respectively [45].

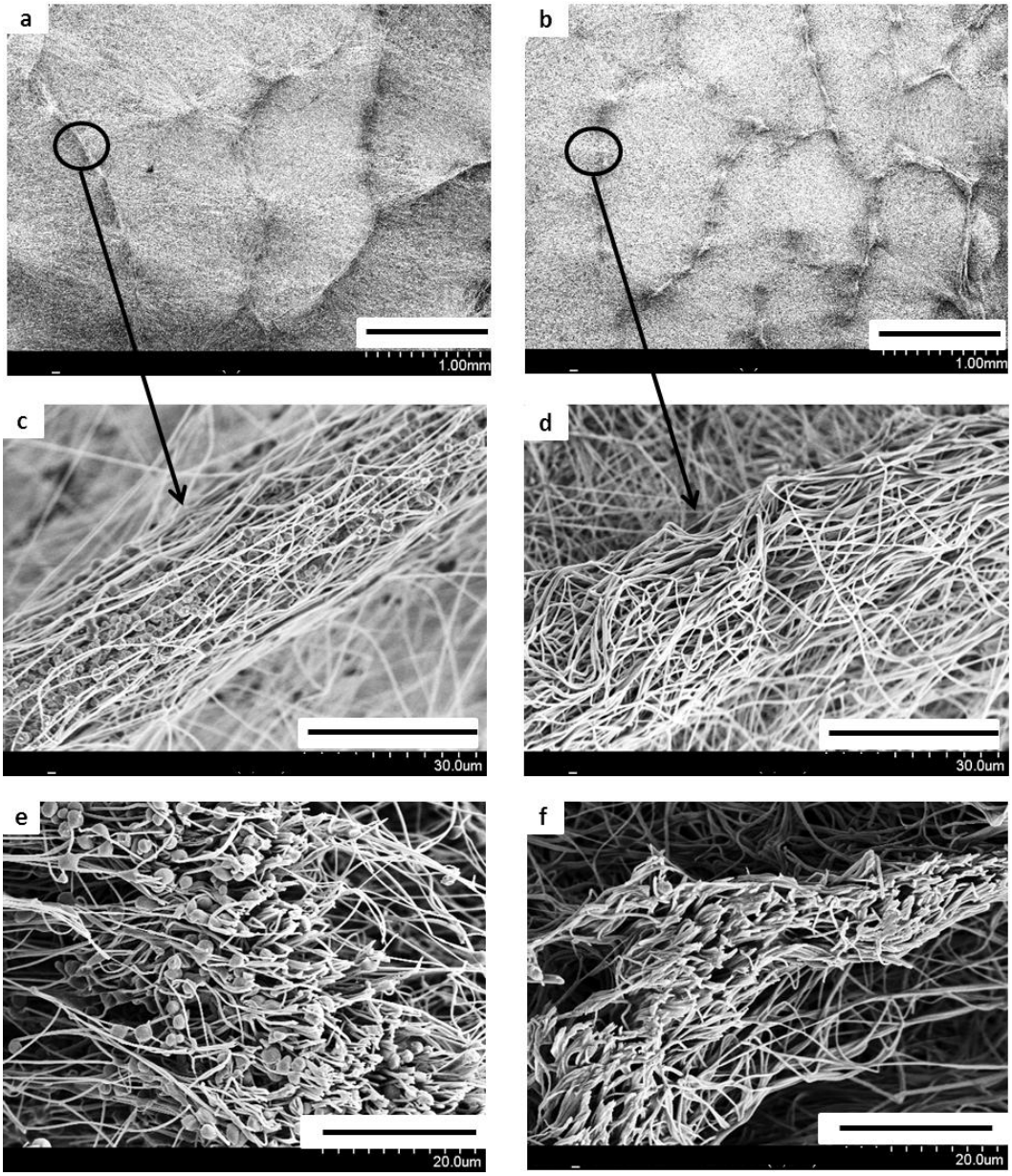

Figure 6: SEM micrographs of the self-organized composite made of PLA nanofibers and PEG0.1 microparticles before (a), (c) and (e) and after (b), (d) and (f) particles leaching. (e) and (f) are cross-section images of the composite.

E) Conclusions

Electrosprayed microparticles and electrospun nanofibers can self-organize to form a unique honeycomb-like composite. The driving force of the organization process is the local variation of the electric field when aggregated particles are used. The specific pattern dimensions can be controlled by varying a simple experimental parameter, the electrospraying flow rate. Moreover, mm-thick samples can be easily prepared with hierarchical porosity and increasing pore sizes that are preserved after selective removal of the particles. This technique is suitable for any other material, as long as aggregated particles are obtained. The combination of electrospinning and electrospraying technologies thus enables the fabrication of new types of structured composite membranes, interesting for a wide range of biomedical applications.

F) Supporting information

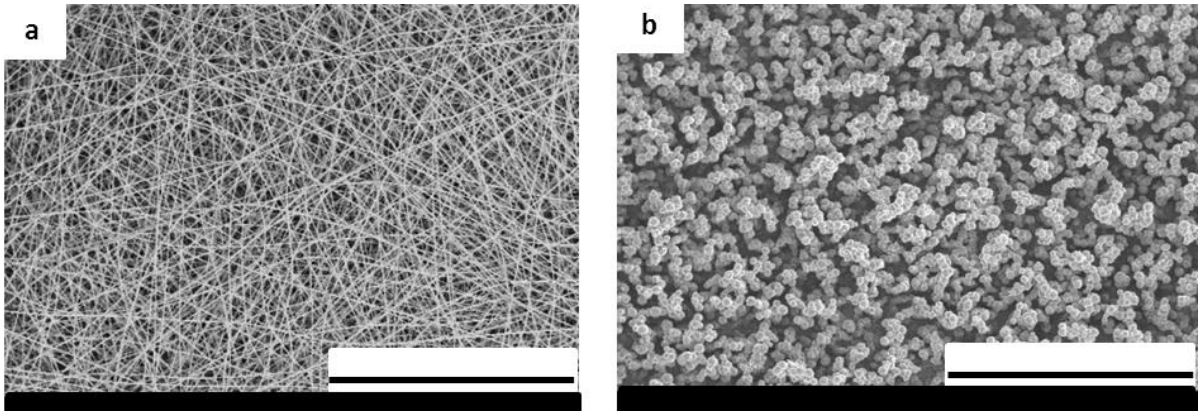

Figure S1: SEM micrographs of (a) PLA fibers after two minutes of electrospinning and of (b) PEG particles after two minutes of electrospraying. (scale bar = 50µm)

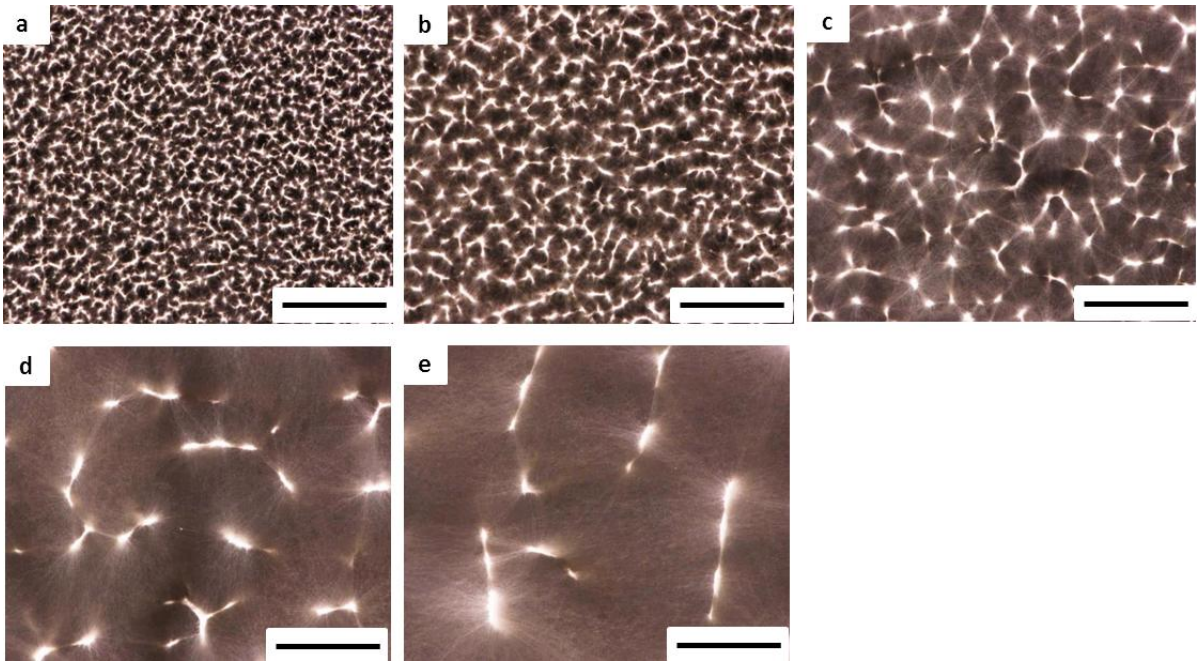

Figure S2: Optical microscopy images of the self-organized at a flow rate of 0.1 ml/h after 5 (a) (*h*= 20µm), 10 (b) (*h*= 70µm), 20 (c) (*h*= 200µm), 40 (d) (*h*= 700µm) and 60 (e) (*h*= 1200µm) minutes of deposition (scale bar = 1 mm).

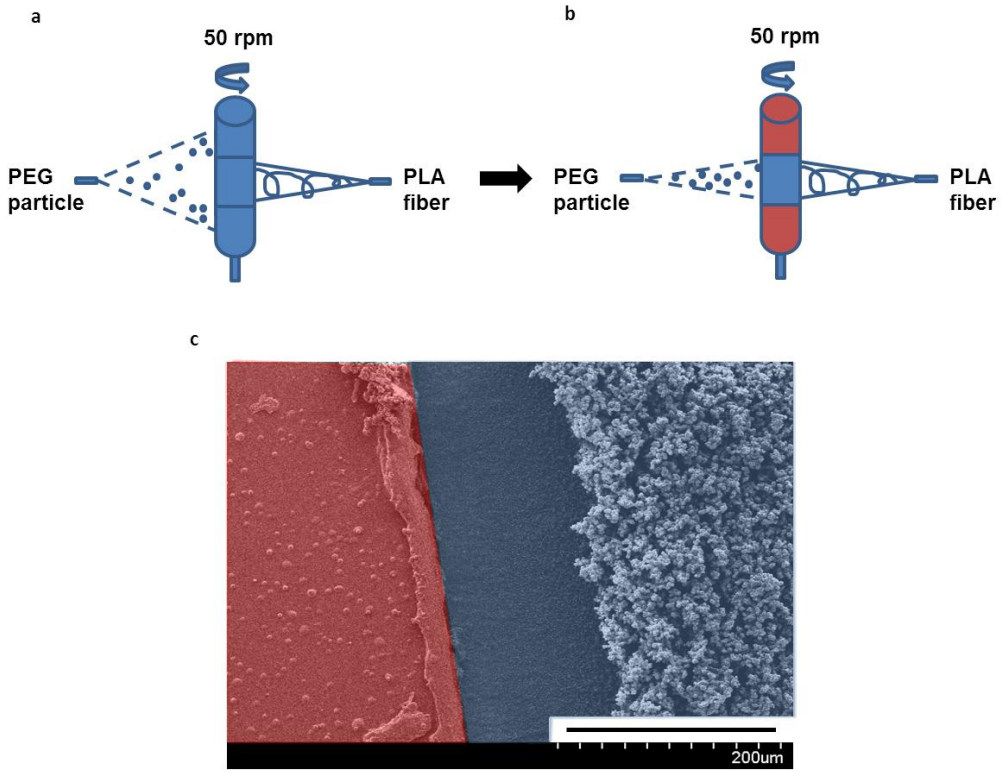

Figure S3: Schematic illustration of the experimental setup without (a) and with (b) dielectric tape (red color). SEM micrograph showing the interface between the dielectric tape (red color) and the conductive aluminum foil (blue color) with simple PEG electrospraying, PEG particles are confined on the conductive blue side (c).

G) From morphology and microstructure control of the membrane to spatiotemporally controlled delivery

In chapter 2, we demonstrated that we can fabricate nanofibers and nanoparticles of defined morphology using electrospinning/spraying process. We will now focus on their potential for temporally and spatially controlled drug delivery. To this end, a model compound was embedded to the nanofibers and nanoparticles by the dissolution of the compound and of the polymer in the electrospinning/spraying solutions. Geometrical impact was investigated for temporal delivery comparing the drug release profile from nanoparticles and nanofibers. Diameter of the nanoparticles/fibers and the concentration of drug are known parameters influencing the drug release kinetics. We focused our interest on the structural aspect of the membrane and its influence on drug release kinetic and direction. To this end, we used the combination of electrospinning and electrospraying technologies.

We showed in chapter 3 that electrosprayed particles can interact with electrospun nanofibers to create growing honeycomb-like structures leading to the fabrication of membranes with a porosity gradient. The yielded porosity gradient was expected to generate directional delivery of the model compound from the nanofibers. Indeed, the porosity gradient is a concentration gradient of fibers within the thickness of the membrane and thus a concentration gradient of drug. Nevertheless, the concentration gradient of drug was not able to preferentially deliver the model compound to a certain direction, based on the release kinetics performed. The directional delivery is probably occurring locally in the membrane because of the presence of the drug concentration gradient; however we could not confirm this hypothesis as the phenomenon is occurring very locally. In order, to perform directional delivery and temporally controlled delivery, we have used again the combination of electrospinning and

electrospraying technologies. However, we focused this time on the chemical properties of the electrosprayed particles to modulate locally the hydrophobicity of the PLA electrospun membrane to potentially impact the spatial and temporal delivery. Using either drug loaded nanofibers or nanoparticles; we fabricated micropatterned membranes with tailored hydrophobicity and performed drug release tests to assess their potential as drug delivery devices for spatially and temporally controlled delivery.

H) References

1. Reneker, D. H.; Yarin, A. L., Electrospinning jets and polymer nanofibers. Polymer 2008, 49 (10), 2387-2425.

2. Reneker, D. H.; Chun, I., Nanometre diameter fibres of polymer, produced by electrospinning. Nanotechnology 1996, 7 (3), 216-223.

3. Greiner, A.; Wendorff, J. H., Electrospinning: A fascinating method for the preparation of ultrathin fibres. Angew Chem Int Edit 2007, 46 (30), 5670-5703.

4. Popa, A. M.; Eckert, R.; Crespy, D.; Rupper, P.; Rossi, R. M., A new generation of ultralight thermochromic indicators based on temperature induced gas release. J Mater Chem 2011, 21 (43), 17392-17395.

5. Guex, A. G.; Kocher, F. M.; Fortunato, G.; Korner, E.; Hegemann, D.; Carrel, T. P.; Tevaearai, H. T.; Giraud, M. N., Fine-tuning of substrate architecture and surface chemistry promotes muscle tissue development. Acta Biomater 2012, 8 (4), 1481-1489.

6. Sill, T. J.; von Recum, H. A., Electro spinning: Applications in drug delivery and tissue engineering. Biomaterials 2008, 29 (13), 1989-2006.

7. Szentivanyi, A.; Chakradeo, T.; Zernetsch, H.; Glasmacher, B., Electrospun cellular microenvironments: Understanding controlled release and scaffold structure. Adv Drug Deliver Rev 2011, 63 (4-5), 209-220.

8. Bottino, M. C.; Thomas, V.; Janowski, G. M., A novel spatially designed and functionally graded electrospun membrane for periodontal regeneration. Acta Biomater 2011, 7 (1), 216-224.

9. Bonani, W.; Motta, A.; Migliaresi, C.; Tan, W., Biomolecule Gradient in Micropatterned Nanofibrous Scaffold for Spatiotemporal Release. Langmuir 2012, 28 (38), 13675-13687.

10. Okuda, T.; Tominaga, K.; Kidoaki, S., Time-programmed dual release formulation by multilayered drug-loaded nanofiber meshes. J Control Release 2010, 143 (2), 258-264.

11. Katta, P.; Alessandro, M.; Ramsier, R. D.; Chase, G. G., Continuous electrospinning of aligned polymer nanofibers onto a wire drum collector. Nano Lett 2004, 4 (11), 2215-2218.

12. Li, D.; Ouyang, G.; McCann, J. T.; Xia, Y. N., Collecting electrospun nanofibers with patterned electrodes. Nano Lett 2005, 5 (5), 913-916.

13. Murugan, R.; Ramakrishna, S., Design strategies of tissue engineering scaffolds with controlled fiber orientation. Tissue Eng 2007, 13 (8), 1845-1866.

14. Lavielle, N.; Hebraud, A.; Mendoza-Palomares, C.; Ferrand, A.; Benkirane-Jessel, N.; Schlatter, G., Structuring and Molding of Electrospun Nanofibers: Effect of Electrical and Topographical Local Properties of Micro-Patterned Collectors. Macromol Mater Eng 2012, 297 (10), 958-968.

15. Zhang, D. M.; Chang, J., Electrospinning of Three-Dimensional Nanofibrous Tubes with Controllable Architectures. Nano Lett 2008, 8 (10), 3283-3287.

16. Huaqiong Li, Y. S. W., Feng Wen, Kee Woei Ng, Gary Ka Lai Ng, Subbu S. Venkatraman, Freddy Yin Chiang Boey, Lay Poh Tan, Human Mesenchymal Stem-Cell

Behaviour On Direct Laser Micropatterned Electrospun Scaffolds with Hierarchical Structures. Macromol. Biosci. 2013, 13, 299-310.

17. Chen, J. T.; Chen, W. L.; Fan, P. W., Hierarchical Structures by Wetting Porous Templates with Electrospun Polymer Fibers. Acs Macro Lett 2012, 1 (1), 41-46.

18. Sundararaghavan, H. G.; Metter, R. B.; Burdick, J. A., Electrospun Fibrous Scaffolds with Multiscale and Photopatterned Porosity. Macromol Biosci 2010, 10 (3), 265-270.

19. Deitzel, J. M.; Kleinmeyer, J.; Harris, D.; Tan, N. C. B., The effect of processing variables on the morphology of electrospun nanofibers and textiles. Polymer 2001, 42 (1), 261-272.

20. Thandavamoorthy, S.; Gopinath, N.; Ramkumar, S. S., Self-assembled honeycomb polyurethane nanofibers. Journal of Applied Polymer Science 2006, 101 (5), 3121-3124.

21. Ye, X. Y.; Huang, X. J.; Xu, Z. K., Nanofibrous mats with bird's nest patterns by electrospinning. Chinese J Polym Sci 2012, 30 (1), 130-137.

22. Yan, G. D.; Yu, J.; Qiu, Y. J.; Yi, X. H.; Lu, J.; Zhou, X. S.; Bai, X. D., Self-Assembly of Electrospun Polymer Nanofibers: A General Phenomenon Generating Honeycomb-Patterned Nanofibrous Structures. Langmuir 2011, 27 (8), 4285-4289.

23. Ahirwal, D.; Hebraud, A.; Kadar, R.; Wilhelm, M.; Schlatter, G., From self-assembly of electrospun nanofibers to 3D cm thick hierarchical foams. Soft Matter 2013, 9 (11), 3164-3172.

24. Ladd, M. R.; Lee, S. J.; Stitzel, J. D.; Atala, A.; Yoo, J. J., Co-electrospun dual scaffolding system with potential for muscle-tendon junction tissue engineering. Biomaterials 2011, 32 (6), 1549-1559.

25. Hong, Y.; Fujimoto, K.; Hashizume, R.; Guan, J. J.; Stankus, J. J.; Tobita, K.; Wagner, W. R., Generating elastic, biodegradable polyurethane/poly(lactide-co-glycolide) fibrous

sheets with controlled antibiotic release via two-stream electrospinning. Biomacromolecules 2008, 9 (4), 1200-1207.

26. Bonani, W.; Maniglio, D.; Motta, A.; Tan, W.; Migliaresi, C., Biohybrid nanofiber constructs with anisotropic biomechanical properties. J Biomed Mater Res B 2011, 96B (2), 276-286.

27. Jaworek, A., Electrospray droplet sources for thin film deposition. J Mater Sci 2007, 42 (1), 266-297.

28. Morota, K.; Matsumoto, H.; Mizukoshi, T.; Konosu, Y.; Minagawa, M.; Tanioka, A.; Yamagata, Y.; Inoue, K., Poly(ethylene oxide) thin films produced by electrospray deposition: morphology control and additive effects of alcohols on nanostructure. J Colloid Interf Sci 2004, 279 (2), 484-492.

29. Lavielle, N.; Popa, AM.; de Geus, M.; Hebraud, A.; Schlatter, G.; Thony-Meyer, L.; Rossi, RM., Controlled formation of poly(Ɛ-caprolactone) ultrathin electrospun nanofibers in a hydrolytic degradation-assisted process. Eur Polym J 2013, 49 (6), 1331-1336.

30. Bock, N.; Dargaville, T. R.; Woodruff, M. A., Electrospraying of polymers with therapeutic molecules: State of the art. Prog Polym Sci 2012, 37 (11), 1510-1551.

31. Ekaputra, A. K.; Prestwich, G. D.; Cool, S. M.; Hutmacher, D. W., Combining electrospun scaffolds with electrosprayed hydrogels leads to three-dimensional cellularization of hybrid constructs. Biomacromolecules 2008, 9 (8), 2097-2103.

32. Gupta, D.; Venugopal, J.; Mitra, S.; Dev, V. R. G.; Ramakrishna, S., Nanostructured biocomposite substrates by electrospinning and electrospraying for the mineralization of osteoblasts. Biomaterials 2009, 30 (11), 2085-2094.

33. Stankus, J. J.; Soletti, L.; Fujimoto, K.; Hong, Y.; Vorp, D. A.; Wagner, W. R., Fabrication of cell microintegrated blood vessel constructs through electrohydrodynamic atomization. Biomaterials 2007, 28 (17), 2738-2746.

34. Valo, H.; Peltonen, L.; Vehvilainen, S.; Karjalainen, M.; Kostiainen, R.; Laaksonen, T.; Hirvonen, J., Electrospray Encapsulation of Hydrophilic and Hydrophobic Drugs in Poly(L-lactic acid) Nanoparticles. Small 2009, 5 (15), 1791-1798.

35. Chu, X. L.; Wasan, D. T., Attractive interaction between similarly charged colloidal particles. J Colloid Interf Sci 1996, 184 (1), 268-278.

36. Stankus, J. J.; Guan, J. J.; Fujimoto, K.; Wagner, W. R., Microintegrating smooth muscle cells into a biodegradable, elastomeric fiber matrix. Biomaterials 2006, 27 (5), 735-744.

37. Van der Schueren, L.; De Schoenmaker, B.; Kalaoglu, O. I.; De Clerck, K., An alternative solvent system for the steady state electrospinning of polycaprolactone. Eur Polym J 2011, 47 (6), 1256-1263.

38. Bichoutskaia, E.; Boatwright, A. L.; Khachatourian, A.; Stace, A. J., Electrostatic analysis of the interactions between charged particles of dielectric materials. J Chem Phys 2010, 133 (2).

39. Stace, A. J.; Boatwright, A. L.; Khachatourian, A.; Bichoutskaia, E., Why like-charged particles of dielectric materials can be attracted to one another. J Colloid Interf Sci 2011, 354 (1), 417-420.

40. Baker, B. M.; Gee, A. O.; Metter, R. B.; Nathan, A. S.; Marklein, R. A.; Burdick, J. A.; Mauck, R. L., The potential to improve cell infiltration in composite fiber-aligned electrospun scaffolds by the selective removal of sacrificial fibers. Biomaterials 2008, 29 (15), 2348-2358.

41. Ionescu, L. C.; Lee, G. C.; Sennett, B. J.; Burdick, J. A.; Mauck, R. L., An anisotropic nanofiber/microsphere composite with controlled release of biomolecules for fibrous tissue engineering. Biomaterials 2010, 31 (14), 4113-4120.

42. Eap, S.; Ferrand, A.; Palomares, C. M.; Hebraud, A.; Stoltz, J. F.; Mainard, D.; Schlatter, G.; Benkirane-Jessel, N., Electrospun nanofibrous 3D scaffold for bone tissue engineering. Bio-Med Mater Eng 2012, 22 (1-3), 137-141.

43. Vitale-Brovarone, C.; Baino, F.; Verne, E., Feasibility and Tailoring of Bioactive Glass-ceramic Scaffolds with Gradient of Porosity for Bone Grafting. J Biomater Appl 2010, 24 (8), 693-712.

44. Karageorgiou, V.; Kaplan, D., Porosity of 3D biornaterial scaffolds and osteogenesis. Biomaterials 2005, 26 (27), 5474-5491.

45. Bruil A, Feijen J, Wenzel-Rejda T. (NPBI Nederlands Produktielaboratorium voor Bloedtransfusieapparatuur en Infusievloeistoffen B.V.). EP0406485 A1, January 9, 1991.

CHAPTER IV/

PUBLICATION N°3: "TAILORING THE HYDROPHOBICITY OF MULTILAYERED ELECTROSPUN NANOFIBER AND NANOPARTICLE COMPOSITE MEMBRANES FOR SPATIALLY AND TEMPORALLY CONTROLLED DELIVERY"

A) Abstract

We present here an approach for tailoring the hydrophobicity of drug loaded nanofibrous membranes by the incorporation of electrosprayed PEG microparticles. The impact of the surface wettability on the release is investigated for PLA composite membranes made of nanofibers and nanoparticles. The addition of the PEG microparticles into the nanofibrous mat lowers the water contact angle from 132±4° to 24±6° and drastically impacts the release profile. Furthermore, we show the fabrication of multilayered composite membranes with tailored hydrophobicity for spatiotemporally controlled delivery of rhodamine B as model compound. We demonstrate that an amphiphilic nanofibrous membrane can be engineered for directional delivery, while multilayered sandwich-like membranes are useful for sustained delivery from nanoparticles to a targeted site. The combination of structural and chemical anisotropy enables a tight control over the spatially and temporally profile of the delivery process.

B) Introduction

Electrospinning is a cost-effective process used to fabricate nanofibrous membranes [1-2]. The fabricated structures have high surface area and high porosity. Thus, they are used in many applications [3] such as sensing [4], tissue engineering [5] or drug delivery [6]. Drug loaded nanofibers have been widely studied as a drug release membrane for controlled drug delivery [7-8]. Most of the research performed on drug loaded nanofibrous membranes was focused on the control of the release kinetics achieving temporally-controlled drug delivery. Drug release kinetics depends on the drug loading strategy. Indeed, impregnation of the membrane in a drug solution after its elaboration leads to adsorbed drug at the surface of the nanofiber, which is responsible for a burst release from the membrane [9]. The drug can also be embedded to the fibers by blend electrospinning leading to a diffusion-like or degradation based release [9]. Acceleration of the diffusion rate of the drug can be obtained by blending a surfactant to the polymer allowing the water to enter and swell the fiber [10]. Delayed release can be achieved by embedding the drug in the core of a core shell structure, the shell acts as a barrier to the drug diffusion [9].

However, for certain application both a spatial and temporal control of the drug release profile is required. It is the case of tissue engineering for which engineering 3D membranes with well-defined spatial organization of the drug within the mat is of great interest [11]. This aspect is essential when a scaffold is placed at an interface between different tissues. For instance, in the case of an occlusive periodontal membrane placed between the bone and epithelial tissue, Bottino et al. [12] proposed a multilayered membrane with hydroxyapatite nanoparticles incorporated on the bone side, while releasing antibiotics on the epithelial tissue side.

Recently, new strategies of membrane structuration have been developed to control spatially and temporally the release of one or several drugs from electrospun membranes. For example,

coelectrospinning of PLA nanofibers containing two drugs with different hydrophilicity was performed, leading to simultaneous release of the two drugs at different rates [13]. Multilayered electrospun constructs of drug loaded nanofibers with different degradation profiles were also elaborated [14]. Other approaches were performed using a multilayer strategy such as the alternation of drug loaded and barrier meshes [15], the fabrication of asymmetric structures [12] and sandwich structures [16]. In most of the cases, a hydrophobic polymer was electrospun, and the release kinetics depended first on the rate of water diffusion inside the hydrophobic membrane, and only after, on the rate of diffusion of the drug out of the wet fibers. The hydrophilicity of the scaffold is thus a very important criterion for temporally controlled release. Lee et al. [17] worked on the control of the hydrophobicity of electrospun membranes by the incorporation of electrosprayed titania nanoparticles activated by UV exposition.

In the present work, we developed a straightforward strategy to tune the hydrophilicity of multilayered scaffolds by the incorporation of electrosprayed PEG particles in order to control the spatiotemporal release of a model molecule. First, we focused on the possibility to tailor the hydrophilicity of PLA electrospun constructs by the addition of PEG microparticles, and showed its impact on the release kinetics. Then, we developed two new strategies based on the hydrophilicity control in the thickness of the membranes. In the first one, the control of the spatial release was demonstrated by the preparation of an amphiphilic nanofibrous membrane, with a hydrophobic and a hydrophilic layer, leading to a directional delivery. In the second approach, sustained delivery was achieved by the confinement of loaded nanoparticles into sandwich-like structure made of hydrophobic or hydrophylic nanofibrous layers. These two strategies demonstrated the potential of the electrospraying/electrospinning process for the fabrication of intelligent drug delivery devices, aimed for therapeutic or tissue engineering applications.

C) Materials and methods

1) Materials

Poly(D,L-lactide) (P(D,L)LA) of a Mw of 75 kg/mol and 15 kg/mol were supplied by Purac under the commercial names Purasorb PDL 0.6 and Purasorb PDL 0.2A. Polyethylene glycol (PEG) of a Mw of 6 kg/mol, acetic acid (purum ≥99.0%, H2O≈0.2%), formic acid (≈ 98%, H2O ≈ 2%), ethanol (≥99.8%) and rhodamine B were purchased from Sigma-Aldrich and used as a model compound. All products were used as received.

2) Fabrication of the membranes

PLA (PDL 0.6) nanofibers was electrospun (ΔV = 24.5 kV, needle-collector distance = 13.5 cm, pump flow rate = 0.3 mL/h, room temperature, 40% RH) from a solution of acetic acid / formic acid 50/50 (v/v) at the concentration of 22% (wt.). Rhodamine B (5% (wt.) to the PLA mass) – loaded PLA (PDL 0.6) nanofibers was electrospun (Vneedle = +23.5 kV, Vcollector = -1kV, needle-collector distance = 14.5 cm, pump flow rate = 0.3 mL/h, room temperature, 40% RH) from a solution of acetic acid / formic acid 50/50 (v/v) at the concentration of 23% (wt.). Rhodamine B (5% (wt.) to the PLA mass) – loaded PLA (PDL 0.2A) nanoparticles was electrosprayed (Vneedle = +28.5 kV, Vcollector = -1kV, needle-collector distance = 13.5 cm, pump flow rate = 0.2 mL/h, room temperature, 40% RH) from a solution of acetic acid / formic acid 50/50 (v/v) at the concentration of 17% (wt.). PEG microparticles was electrosprayed (Vneedle = +25 kV, Vcollector = -1kV, needle-collector distance = 6.5 cm, pump flow rate = 0.1 mL/h, 25°C, 40% RH) from a solution of water / ethanol 80/20 (v/v) at the concentration of 37.5% (wt.). All the solutions were processed 24 hours after their

preparation. We optimized the electrospinning conditions and the solvent mixtures for steady state formation of bead-free PLA nanofibers and spherical PLA and PEG nano and microparticles. The components of the electrospinning setup was described previously [18]. The membranes were deposited on aluminum foils. To fabricate the hydrophilic PLA-PEG membrane, PLA nanofibers and PEG microparticles were co-electrospun into a vertical rotating drum. The rotation speed of the drum was 50 rpm and its diameter 4 cm. Mechanical fiber alignment was avoided by using a low rotation speed and thus allowed random deposition of the fibers. Moreover, to obtain a homogeneous mixture of the particles and the fibers, a dielectric tape was used to delimit the deposition area [19]. The multilayered amphiphilic electrospun membrane was fabricated by the sequential electrospinning of loaded PLA nanofibers for 10 minutes followed by the simultaneous electrospinning of loaded PLA nanofibers and electrospraying of PEG microparticles for 50 minutes. The hydrophobic (/hydrophilic) multilayered sandwich-like membranes were produced by the sequential electrospinning of hydrophobic (/hydrophilic) PLA layer during 10 minutes, followed by one hour electrospraying of the loaded nanoparticles and finally, 10 minutes of hydrophobic (/hydrophilic) PLA layer. The membranes were dried and stored in a dry, dark atmosphere.

3) Characterization of the membranes

The morphology of the membranes were characterized with a scanning electron microscope (SEM, Hitachi S-4800 at Vacc = 5kV, Ie = 10 µA). Gold (5 nm) was sputtered on all membranes using a scanning electron microscope coating unit EM ACE 600 from LEICA. The average nanofiber/nanoparticle/microparticule diameter and standard deviation were calculated from the diameter measured from 10 measurements in 3 randomly selected areas. The membranes thicknesses were estimated from measurements using cross-section SEM

images or a profilometer (Dektak 150 from Veeco) [19]. Transversal cut with Gillette blades at room temperature was performed to visualize the cross-section of the membrane. Static water contact angle measurement was performed on the membranes after 5 minutes immersion in water, using a DSA 25 microsyringe setup, supplied by Kruss. To determine the quantity of rhodamine B in the fabricated membranes, a defined weight of the membranes were dissolved in the mixture of acids and absorbance of the solution was measured at the wavelength of 550 nm by UV-vis spectroscopy (SynergyMx, BioTek). The amount of rhodamine B present in the membranes relative to the membrane weight was determined by comparison with a calibration curve.

Kinetic release tests were performed in triplicate in 25 mL of phosphate buffered saline (PBS, pH=7.4) at 37°C, under stirring at 100 rpm over 150 hours. Aliquots of 400 µL were taken at the different release times, filtered with a 0.22µm filter unit from Millipore and the quantity of released Rhodamine measured by UV-visible spectroscopy. The released percentage was calculated by dividing the released amount in PBS by the total amount present in the membrane. For the directional delivery test, a horizontal permeation cell (Pesce Labs) of 35 mL, schematically represented in Figure 3, was used. The membrane was placed between two cells filled with PBS, with the hydrophobic layer facing cell 1 and the hydrophilic layer facing cell 2. 200 µL aliquots were taken regularly from cell 1 and 2 for the determination of the quantity of rhodamin B released in each cell by UV-visible spectroscopy. Then, differential Scanning Calorimetry (DSC 822 from Mettler-Toledo) was used to analyze the extent of PEG removal from the membranes after 150 hours; performing two heating and cooling cycles from 25 to 100 °C at a rate of 5°C per minute and using an empty capsule as reference. (Figure S2).

D) Results and discussion

1) From hydrophobic to hydrophilic nanofibrous membranes

Our strategy to control the temporal release of a model hydrophilic molecule, rhodamine B, from hydrophobic PLA nanofibers was to tune the hydrophilicity of the membrane by coelectrospraying PEG microparticles inside the membrane. Two types of membranes were fabricated: a hydrophobic PLA and a hydrophilic PLA-PEG membranes. The hydrophobic membrane is a construct of PLA nanofibers loaded with Rhodamine B; the hydrophilic membrane was fabricated by co-electrospinning/electrospraying rhodamine B-loaded PLA nanofibers and pure PEG microparticles. The PLA nanofibers were observed by SEM (Figure 1a) and had an average diameter of 125±20 nm. The PEG microparticles had an average diameter of 2.3±0.4 µm and are presented in a SEM micrograph in Figure S1. The water contact angles of the two membranes were measured as shown in figure 1c and d. The PLA membrane is hydrophobic with a water contact angle of 132±4°. This angle results from the combination of the chemical composition of the PLA material with the nano and microstructure of the surface of the membrane [20-22]. The presence of PEG particles into the nanofibrous membrane changes dramatically the water contact angle which is measured at 24±6°. The composite material becomes hydrophilic due to the homogeneous mixture of PEG particles into the fiber mesh, enabling water penetration into the mat.

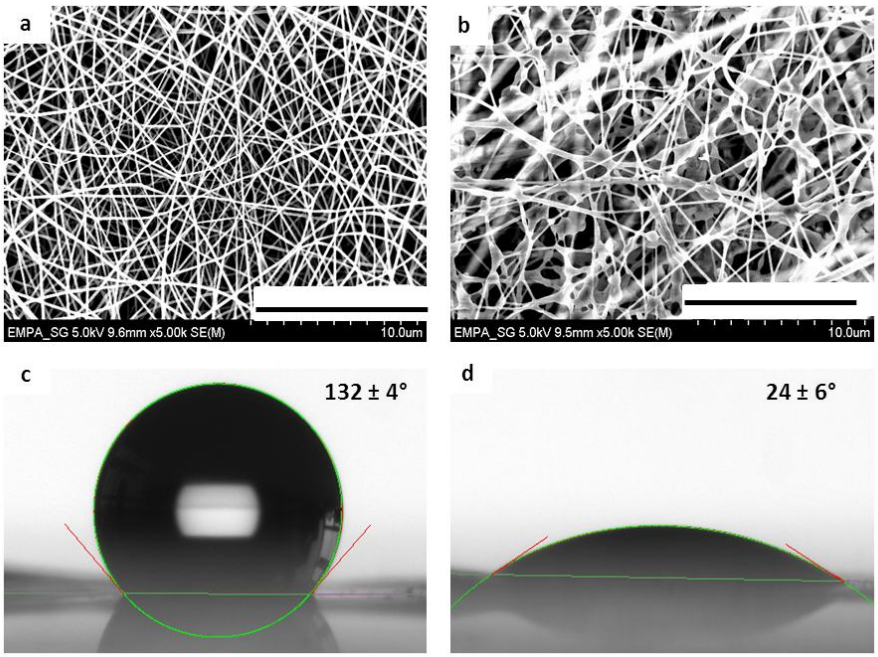

Figure1: SEM micrographs of rhodamine B loaded electrospun PLA nanofibers without (a) or with (b) electrosprayed PEG microparticles (scale bar = 10 µm) and the respective static water contact angles (c,d)

Release kinetics studies have been performed in PBS at 37°C on the two types of membranes presented above. The concentration of the active ingredient in the release media was determined by UV-vis spectroscopy and was plotted versus time. The release profiles are displayed in figure 2. We can observe that less than 5% (detection limit) of rhodamine is released after 150 hours for the hydrophobic PLA membrane. Due to the hydrophobicity of the surface of the hydrophobic membrane, water cannot diffuse in the mat thus hindering the diffusion of the model compound from the fibers to the water. For the PLA-PEG hydrophilic membrane, the initial release is of 15% and 30% are reached within 150 hours. Indeed, the PEG particles lowered the water contact angle and enabled the water to penetrate into the nanofiber mat enabling the release of the compound in water. We hypothesized that the PEG

fraction, having a low molecular weight (6000 g/mol) dissolves rapidly in water and desorbs from the PLA membrane. The monitoring of the thermal behaviour (by DSC) of the membranes before and after the release experiment provided additional support to this hypothesis (figure S2 in Supporting Information). Indeed, we can observe the disappearance of the characteristic melting and crystallization peaks of PEG at 55 and 35°C, respectively, after the release test. The initial release of 14% indicates that a substantial amount of rhodamine B is located on the surface of the fibers. The release profile from this membrane is a diffusion-like profile [9]. Typically, mean diffusion distance, diffusivity of the compound through the polymer matrix and concentration gradient control the release kinetics from delivering systems [9]. The study was limited to the first 150 hours in order to consider the release of the model molecule by diffusive mechanism only. Indeed, degradation by surface erosion of PLA begins significantly after two weeks in PBS [23].

The two release profiles obtained from the two membranes show that the incorporation of the PEG particles plays a major role in the release kinetic. Hydrophobic electrospun membranes can be engineered to allow water penetration into the mat with the incorporation of electrosprayed PEG particles. This method allows us to tailor the hydrophobicity of electrospun membranes and to possibly develop advanced membrane design such as multilayered membranes for spatiotemporal release.

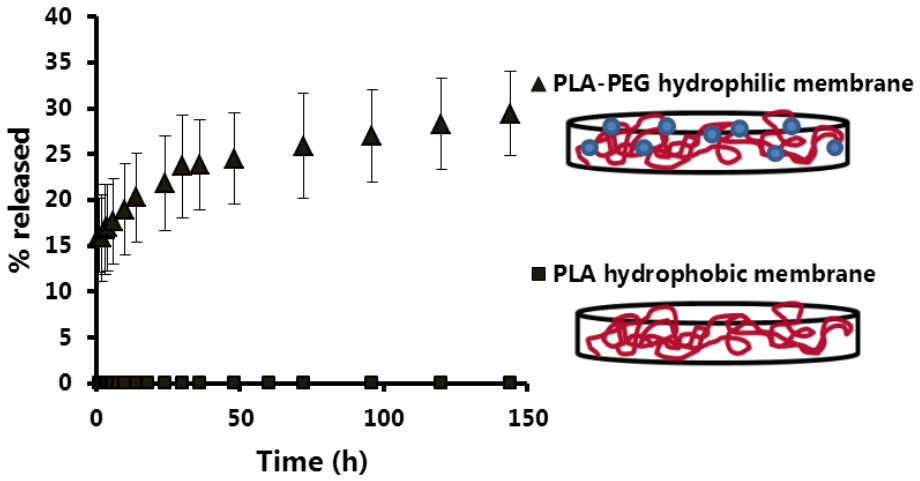

Figure 2: Percentage of cumulative release of rhodamine B from the PLA and the composite membranes in PBS at 37°C and 100 rpm as a function of time, determined by UV vis spectroscopy.

2) Multilayered amphiphilic nanofibrous membrane for directional delivery

Spatially controlled delivery is an important feature of advanced drug delivery systems, as it allows specific targeting of therapeutic sites. To this end, we fabricated an amphiphilic membrane consisting of a hydrophobic layer of PLA nanofibers and a hydrophilic layer composed of PLA nanofibers and PEG microparticles. The membrane was synthesized in a sequential manner, first electrospinning PLA nanofibers for 10 minutes followed by the simultaneous electrospinning of PLA nanofibers and electrospraying of PEG microparticles during 50 minutes. Thus, a bilayered amphiphilic membrane was fabricated with a hydrophobic layer barrier layer with a thickness ≈ 5 μm and a hydrophilic layer of ≈ 25 μm. The release tests were performed in PBS at 37°C in a permeation cell as schematically

represented in figure 3a. The amphiphilic membrane was placed in between the two cells with hydrophobic layer facing cell 1 and hydrophilic layer facing cell 2 and the release profile was determined in the two compartments. The experiments were performed without agitation, as to better mimic the in-vivo situation, where typically no turbulent flow through the membranes is encountered. The results of the release tests are displayed in figure 3b. As expected, the drug concentration preferentially increased in the compartment 2 where the hydrophilic side of the membrane was in contact with the release medium. Indeed, no rhodamine is measured in the compartment 1 of the permeation cell until 24 hours of release; whereas in the compartment 2, over 2% of rhodamine is released after two hours only. The maximum of concentration is reached after six hours in compartment 2. The observed release profile confirms indeed that the presence of the PEG microparticles increases the wettability of the membrane, and thus the contact of the drug-loaded nanofibers with the release media is facilitated. In the cell 1, the hydrophobic layer acts in a first step as a barrier, limiting the diffusion of PBS in the membrane and thus the release of the dye. However, since the pores of the electrospun membrane are orders of magnitude higher than the hydrodynamic radius of the active ingredients, the diffusion of the released rhodamine from one compartment to the other also occurs. Indeed, by analyzing the respective drug concentrations one may notice that after 100 hours the equilibrium of concentration is reached between the two compartments. We can thus conclude that the presence of a hydrophobic layer is sufficient to generate directional delivery for a limited amount of time.

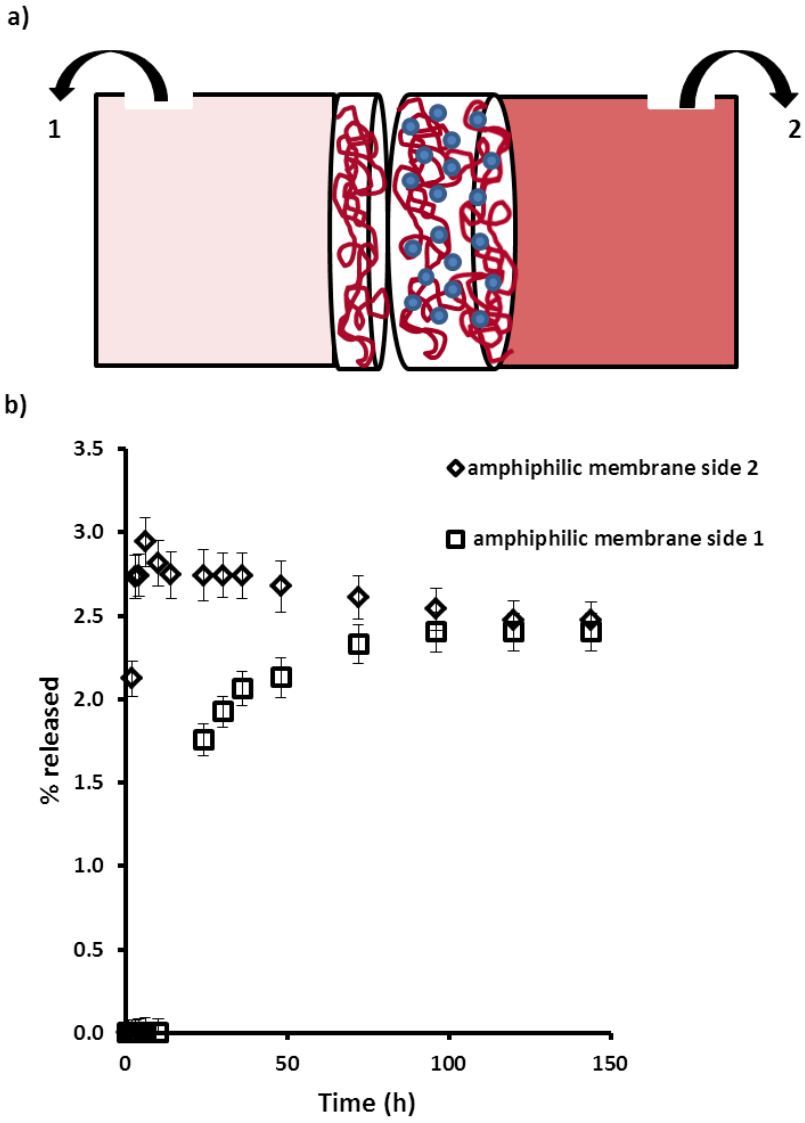

Figure 3: (a) Schematic illustration of the amphiphilic membrane in a permeation unit composed of two cells. (b) Percentage of cumulative release from the amphiphilic membrane to cells 1 and 2 in PBS at 25°C as a function of time.

3) Hydrophobic and hydrophilic multilayered sandwich-like membranes for sustained delivery from nanoparticles

Drug loaded nanoparticles have been widely studied and have shown their potential in the precise adjustment of the release kinetics for drug delivery applications [24-25]. However, one main disadvantage of drug release from particles remains in the fact that they disperse in water. On the other hand, electrospun membranes can be used as scaffolds implanted in a specific site. The mechanical stability of electrospun membranes can be used in combination with drug loaded particles to fabricate scaffolds with precise drug release kinetics from the particles and mechanical stability from the electrospun fibers [26]. A straight-forward approach for tuning the release kinetics of active ingredients from loaded nanoparticles by the use of a sandwich-like structure is described below. Sandwich structures have been successfully constructed with electrospun fibers enveloping drug loaded electropun nanofibers for delayed release [16]. In this work, the strategy was transposed to the encapsulation of a dye-loaded nanoparticle layer and a system based on sandwich-like structures was fabricated. Loaded nanoparticles were deposited between barrier layers of PLA nanofibers. Two types of barrier layers were studied: hydrophobic layers made of PLA nanofibers (hydrophobic sandwich) and hydrophilic layers made by the simultaneous electrospinning of PLA nanofibers and electrospraying of PEG microparticles (hydrophilic sandwich). In this study, no rhodamine B was embedded to the nanofibers. The fabricated nanofibers had an average diameter of 200 ± 20 nm. We sequentially electrospun a hydrophobic (/hydrophilic) PLA layer during 10 minutes, followed by one hour electrospraying of rhodamine B-loaded PLA nanoparticles and finally we electrospun a last hydrophobic (/hydrophilic) layer of PLA nanofibers (schematically represented in figure 4). The PLA nanoparticles had an average diameter of 330±90 nm and they can be observed in the SEM micrograph in figure S3. A cross-section SEM image of the sandwich-like composite (figure 4a), revealed a well-defined

three-layer structure, consisting of a central layer of nanoparticles with a thickness of ≈ 25µm enveloped by two layers of hydrophobic nanofibers having each an estimated thickness of ≈ 10µm. The profile of the dye release as a function of the type of construct and time is shown in figure 4b. Both are displaying a release profile governed by diffusion. A striking difference between the release profiles corresponding to the hydrophilic and hydrophobic constructs respectively can be observed in the first 10 hours of experiment. As such, the hydrophilic sandwich displays a typical burst profile, with 14% of the encapsulated rhodamine being released within minutes from the immersion of the membrane in the release medium. In comparison, no release of the compound is observed within the first 10 hours for the hydrophobic sandwich. The PLA-PEG layers allow the rapid wetting of the membrane and the efficient contact of the dye-loaded nanoparticles with the PBS. However, the hydrophobic PLA layers act as a barrier to water diffusion into the membrane and thus delay both the release of the rhodamine, as well as its diffusion outside the three-layered scaffold. After 150 hours, the hydrophobic sandwich released 20% of rhodamine whereas the hydrophilic one 32%. The differences observed between the release profiles from the two types of sandwich for the initial release concentrations of rhodamine B and the concentration obtained after 150 hours show that the encapsulation of nanoparticles between nanofibrous layer is a valid strategy for avoiding burst-release phenomena and achieving sustained release.

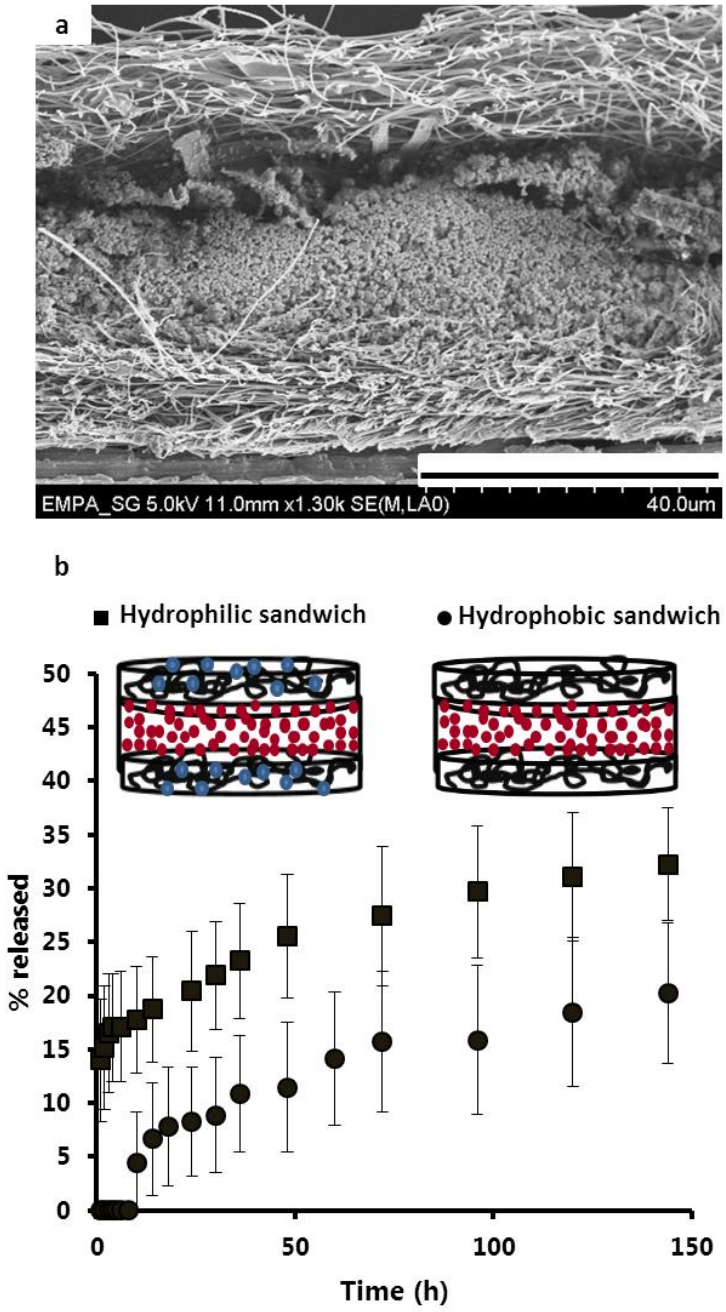

Figure 4: (a) SEM micrograph of a cross-section of the sandwich-like composite composed of a central layer of PLA nanoparticles enveloped by two layers of hydrophobic PLA nanofibrous layers (scale bar = 40 µm). (b) Percentage of cumulative release from the hydrophilic and hydrophobic sandwiches in PBS at 37°C and 100 rpm.

E) Conclusions

We successfully tailored the hydrophobicity of electrospun PLA nanofibrous membrane by the addition of hydrophilic and water soluble electrosprayed PEG. The change in hydrophobicity impacted the release profile allowing water to penetrate into the mat and thus the compound to diffuse from the nanofibers. Using this strategy, we engineered multilayered membranes with spatially tailored hydrophobicity influencing both spatial and temporal delivery. We fabricated amphiphilic multilayered nanofibrous membranes for directional delivery and sandwich-like nanofibrous membranes for a sustained delivery from nanoparticles to a specific site. Release profiles can be tuned by the incorporation of hydrophilic moieties in the barrier layers of multilayered sandwich-like membranes. Further advances could be performed by tuning the size of the hydrophobic/hydrophilic layers to modify the diffusion path length or by modifying the quantity of hydrophilic incorporated moieties. One could even combine it with the amphiphilic strategy to add to the system directionally controlled delivery. Such advanced membrane design giving tailored hydrophobicity over the structure and microstructure of the membrane impacts spatiotemporal release and will enable spatially and temporally controlled delivery for biomedical applications such as tissue engineering.

F) Supporting information

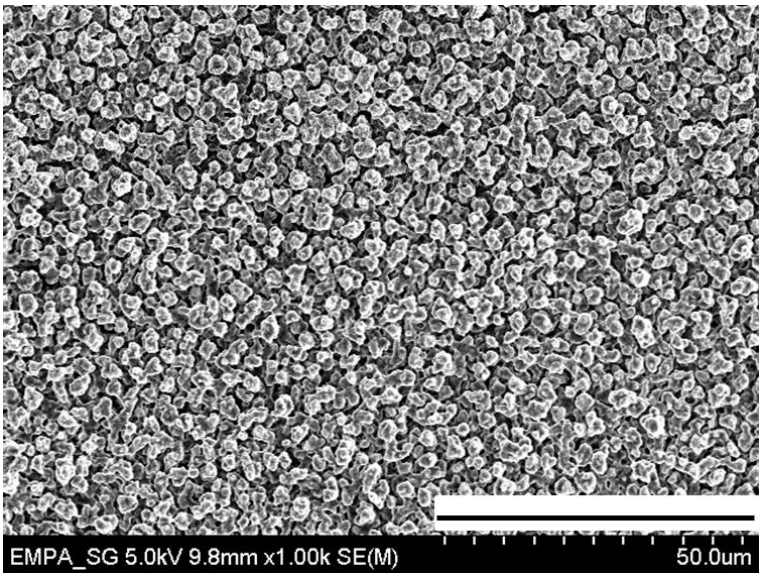

Figure S1: SEM micrograph of the electrosprayed PEG particles after 2 minutes of deposition.

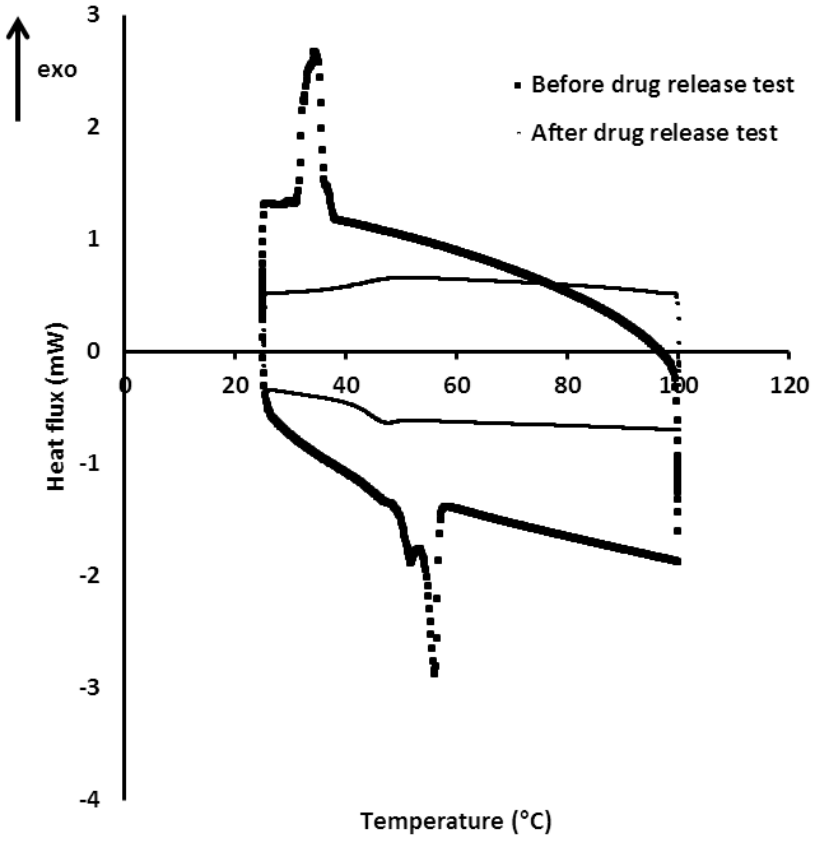

Figure S2: DSC spectra of the composite membrane before and after drug release showing the disappearance of the PEG. The second heating and cooling phase is shown (5°C/minute).

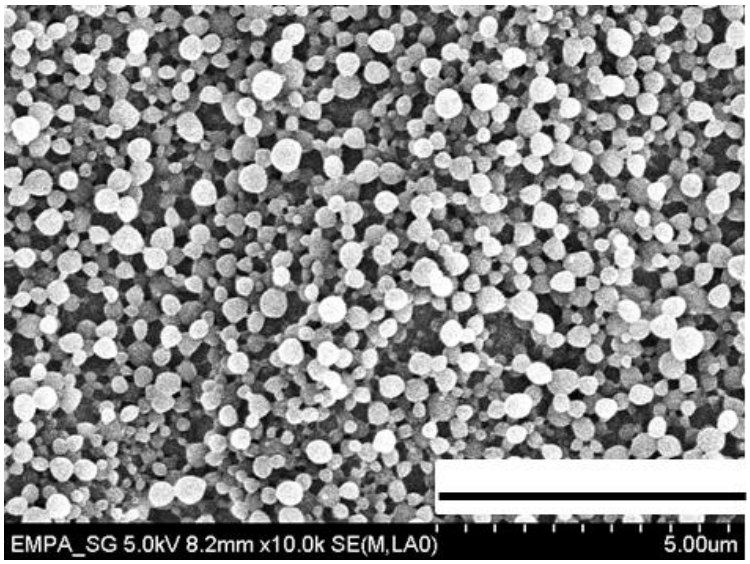

Figure S3: SEM micrograph of rhodamine B loaded nanoparticles after 2 minutes of deposition. (scale bar = 5 µm)

G) References

1. Reneker, D. H.; Chun, I., Nanometre diameter fibres of polymer, produced by electrospinning. Nanotechnology 1996, 7 (3), 216-223.

2. Reneker, D. H.; Yarin, A. L., Electrospinning jets and polymer nanofibers. Polymer 2008, 49 (10), 2387-2425.

3. Greiner, A.; Wendorff, J. H., Electrospinning: A fascinating method for the preparation of ultrathin fibres. Angew Chem Int Edit 2007, 46 (30), 5670-5703.

4. Popa, A. M.; Eckert, R.; Crespy, D.; Rupper, P.; Rossi, R. M., A new generation of ultralight thermochromic indicators based on temperature induced gas release. J Mater Chem 2011, 21 (43), 17392-17395.

5. Guex, A. G.; Kocher, F. M.; Fortunato, G.; Korner, E.; Hegemann, D.; Carrel, T. P.; Tevaearai, H. T.; Giraud, M. N., Fine-tuning of substrate architecture and surface chemistry promotes muscle tissue development. Acta Biomater 2012, 8 (4), 1481-1489.

6. Sill, T. J.; von Recum, H. A., Electro spinning: Applications in drug delivery and tissue engineering. Biomaterials 2008, 29 (13), 1989-2006.

7. Wang, B. C.; Wang, Y. Z.; Yin, T. Y.; Yu, Q. S., Applications of Electrospinning Technique in Drug Delivery. Chem Eng Commun 2010, 197 (10), 1315-1338.

8. Liang, D.; Hsiao, B. S.; Chu, B., Functional electrospun nanofibrous scaffolds for biomedical applications. Adv Drug Deliver Rev 2007, 59 (14), 1392-1412.

9. Szentivanyi, A.; Chakradeo, T.; Zernetsch, H.; Glasmacher, B., Electrospun cellular microenvironments: Understanding controlled release and scaffold structure. Adv Drug Deliver Rev 2011, 63 (4-5), 209-220.

10. Xu, W. J.; Atala, A.; Yoo, J. J.; Lee, S. J., Controllable dual protein delivery through electrospun fibrous scaffolds with different hydrophilicities. Biomed Mater 2013, 8 (1).

11. Biondi, M.; Ungaro, F.; Quaglia, F.; Netti, P. A., Controlled drug delivery in tissue engineering. Adv Drug Deliver Rev 2008, 60 (2), 229-242.

12. Bottino, M. C.; Thomas, V.; Janowski, G. M., A novel spatially designed and functionally graded electrospun membrane for periodontal regeneration. Acta Biomater 2011, 7 (1), 216-224.

13. Thakur, R. A.; Florek, C. A.; Kohn, J.; Michniak, B. B., Electrospun nanofibrous polymeric scaffold with targeted drug release profiles for potential application as wound dressing. Int J Pharmaceut 2008, 364 (1), 87-93.

14. Bonani, W.; Motta, A.; Migliaresi, C.; Tan, W., Biomolecule Gradient in Micropatterned Nanofibrous Scaffold for Spatiotemporal Release. Langmuir 2012, 28 (38), 13675-13687.

15. Okuda, T.; Tominaga, K.; Kidoaki, S., Time-programmed dual release formulation by multilayered drug-loaded nanofiber meshes. J Control Release 2010, 143 (2), 258-264.

16. Chen, D. W. C.; Liao, J. Y.; Liu, S. J.; Chan, E. C., Novel biodegradable sandwich-structured nanofibrous drug-eluting membranes for repair of infected wounds: an in vitro and in vivo study. Int J Nanomed 2012, 7, 763-771.

17. Lee, M. W.; An, S.; Joshi, B.; Latthe, S. S.; Yoon, S. S., Highly Efficient Wettability Control via Three-Dimensional (3D) Suspension of Titania Nanoparticles in Polystyrene Nanofibers. Acs Appl Mater Inter 2013, 5 (4), 1232-1239.

18. Lavielle, N.; Popa, AM.; de Geus, M.; Hebraud, A.; Schlatter, G.; Thony-Meyer, L.; Rossi, RM., Controlled formation of poly(Ɛ-caprolactone) ultrathin electrospun nanofibers in a hydrolytic degradation-assisted process. Eur Polym J 2013, 49 (6), 1331-1336.

19. Lavielle, N.; Hebraud, A.; Schlatter, G.; Thony-Meyer, L.; Rossi, RM., Popa, AM., Simultaneous electrospinning and electrospraying: A straightforward approach for fabricating hierarchically structured composite membranes. Acs Appl Mater Inter 2013, online.

20. Gau, H.; Herminghaus, S.; Lenz, P.; Lipowsky, R., Liquid morphologies on structured surfaces: From microchannels to microchips. Science 1999, 283 (5398), 46-49.

21. Abbott, N. L.; Folkers, J. P.; Whitesides, G. M., Manipulation of the Wettability of Surfaces on the 0.1-Micrometer to 1-Micrometer Scale through Micromachining and Molecular Self-Assembly. Science 1992, 257 (5075), 1380-1382.

22. Shull, K. R.; Karis, T. E., Dewetting Dynamics for Large Equilibrium Contact Angles. Langmuir 1994, 10 (1), 334-339.

23. Cui, W. G.; Li, X. H.; Zhu, X. L.; Yu, G.; Zhou, S. B.; Weng, J., Investigation of drug release and matrix degradation of electrospun poly(DL-lactide) fibers with paracetanol inoculation. Biomacromolecules 2006, 7 (5), 1623-1629.

24. Slowing, I. I.; Vivero-Escoto, J. L.; Wu, C. W.; Lin, V. S. Y., Mesoporous silica nanoparticles as controlled release drug delivery and gene transfection carriers. Adv Drug Deliver Rev 2008, 60 (11), 1278-1288.

25. Elzoghby, A. O.; Samy, W. M.; Elgindy, N. A., Albumin-based nanoparticles as potential controlled release drug delivery systems. J Control Release 2012, 157 (2), 168-182.

26. Wang, F.; Li, Z. Q.; Tamama, K.; Sen, C. K.; Guan, J. J., Fabrication and Characterization of Prosurvival Growth Factor Releasing, Anisotropic Scaffolds for Enhanced Mesenchymal Stem Cell Survival/Growth and Orientation. Biomacromolecules 2009, 10 (9), 2609-2618.

CONCLUSIONS AND OUTLOOK

During the last three years, the work was focused on the fabrication of membranes with drug loaded nanoparticles and nanofibers for controlled drug delivery. To this end, the first eight months of the PhD was spent to elaborate the outline of the PhD project and to build an electrospinning setup allowing multicomponent fabrication. The first focus was on the control of the morphology of the electrospun material. Thus, strategies for the control of the morphology of the nanofibers were investigated, ranging from uniform nanofibers, to beaded nanofibers and to particles. Once the morphology controlled, combination of different morphologies in a unique membrane to control the microstructure of the membrane was aimed. Hence, microstructured composite membranes were developed combining in a unique mat nanofibers and microparticles. Furthermore, by the combination of the different morphologies of different materials, drug loaded membranes with tailored hydrophobicity within the membrane thickness was targeted. To this end, multilayered membranes were elaborated to demonstrate that the structure of the membrane impacts spatially and temporally controlled drug delivery. Three papers were prepared from our work, focused on morphology and structure control for controlled release applications.

First, a new approach was described for the controlled fabrication of biopolyesters electrospun nanofibers from a solvent system based on a mixture of acetic acid and formic acid. For the first time, the possibility of tuning the diameter and morphology of the nanofibers was demonstrated by the in-situ modification of the molecular weight of the polymer, a consequence of the hydrolytic degradation to which the polyester is subjected in aqueous acidic medium. A simple model was used for predicting the evolution of the molecular weight as a function of degradation time. Regimes and boundaries of PCL electrospinning in this

solvent system could be determined, ranging from electrospraying of particles to the electrospinning of nanofibers. The electrospinning of polyesters from an acid solution allows the formation of ultrathin nanofibers with tunable morphology and dimensions. This strategy can be extrapolated to the electrospinning of any polyester which is soluble in the acid mixture. Additionally, the low toxicity of the solvent used makes this system very interesting for the production of membranes for biomedical applications. Acidic solvent systems for the electrospinning of polyesters are expected to be widely used as a replacement for halogenated solvent systems. Indeed, steady-state electrospinning and low toxicity are advantages toward the further development of scaffold for biomedical applications. However, the molecular weight of polyesters decreases in acids in the presence of water; thus one has to be cautious in its use. This decrease of the molecular weight can as well be seen as an advantage for controlling the morphology of the yielded nanofibers as demonstrated before.

Then, a method was presented combining electrospinning and electrospraying technologies for the fabrication of new types of microstructured composite membranes interesting for a wide range of biomedical applications. The approach is based on the simultaneous electrospraying of microparticles and electrospinning of nanofibers from different polymer solution feeds on a common support. The microparticles and the nanofibers can self-organize to form a unique honeycomb-like structured composite. The obtained composite mat exhibits a multi-level porous structure, with pore sizes ranging from few up to several hundreds of microns. The driving force of the organization process is the local variation of the electric field when aggregated particles are used. The specific pattern dimensions can be controlled by varying the electrospraying flow rate. Moreover, mm-thick samples can be prepared with hierarchical porosity and increasing pore sizes that are preserved after selective removal of the particles. Furthermore, this technique is applicable for any material, as long as aggregated

particles are obtained. The fabricated membranes by this technique exhibit a porosity gradient within the thickness of the membrane. The porosity gradient was aimed to be used as a concentration gradient of drug to generate directional delivery of the compound for drug delivery application. However, this strategy did not work; thus others paths for spatially controlled delivery had to be investigated. The main advantage of this method compared with the ones presented in the literature to fabricate honeycomb-like structured membranes stands in the independent fabrication of the nanofibers and the particles responsible for the self-organization. Indeed, the nanofibers can be created independently which allows the tuning of their morphology. Moreover, the particles can be made of different materials enabling further functionalization by the presence of additional properties; as the use of PEG particles presented below. Self-organization between fibers and particles are expected to influence the further development of nanofibrous membranes for the control of the microstructure. For instance, combining different materials of different morphologies could as well be used as advanced membranes for drug delivery applications by the incorporation of several compounds in the particles and in the fibers. Furthermore, this strategy enables the fabrication of cm-thick membranes, necessary for bone tissue engineering for example. Such membranes will find applications in the biomedical and drug delivery fields.

Finally, a method was presented tailoring the hydrophobicity of drug loaded nanofibrous membranes by the incorporation of electrosprayed PEG microparticles. Using this strategy, multilayered membranes of drug-loaded nanofibers or nanoparticles were engineered with spatially tailored hydrophobicity influencing both spatial and temporal delivery. Indeed, an amphiphilic nanofibrous membrane can be engineered for directional delivery and multilayered sandwich-like membranes for sustained delivery from nanoparticles to a targeted site. Usually, in order to tailor the kinetics of release of a drug from nanofibers and

nanoparticles, the strategies developed deal with the amount of drug incorporated or with the dimensions of the carrier. Here, the focus was on the control of the structure of the membrane to influence the release profiles. These membranes propose another path for controlled drug delivery. Such alternative strategies are important for the development of drug delivering devices because it is not always possible to change the incorporated amount of drug or to tune the morphology of the carrier. Such advanced membrane design giving tailored hydrophobicity over the structure and microstructure of the membrane impacts spatiotemporal release and will enable spatially and temporally controlled drug delivery for biomedical applications.

In the presented work, a model compound was used. The release kinetics observed cannot be quantitatively transferred to any active compound, as a specific drug has specific chemical and physical interactions with its carrier. The size of the drug can also influence its diffusion in the membrane. The use of the model compound gives the trends of the impact of the strategies studied to engineer nanofibrous membranes. In the work described, further advances and improvments could be performed. For example, the electrospinning of other materials in the acidic solvent system could be studied. Changes in the morphology and dimensions of the particles and in the aggregation degree, dimensions and polydispersity of the aggregated domains will influence the self-organization process. Indeed, tuning the size of the aggregated domains will lead to a fine tuning of the size of the honeycomb-like patterns. Controlling the polydispersity of the size of the aggregated domains of particles will impact the evolution of the growth of the pattern size and thus control the kinetic of the growth of the membranes thickness. For the drug delivery aspect, further experiments could be performed to study for example the impact of the thickness of the hydrophobic layer in the amphiphilic membrane. Another study would deal with the fabrication of amphiphilic multilayered

sandwich-like structures for drug loaded nanoparticles with a hydrophobic upper layer and a hydrophilic lower layer for directional delivery. To conclude the thesis, micropatterned electrospun membranes were successfully fabricated for controlled drug delivery for biomedical applications. The approaches studied were novel and published in relevant peer-reviewed journals. The control of the morphology of polyester nanofibers using in-situ hydrolytic degradation was presented for the first time. The combination of particles and fibers to create hierarchical microstructures or to tailor locally the hydrophobicity of electrospun membranes was an innovative strategy based on the fine control of the interaction of electrospinning and electrospraying technologies. Biocompatible and biodegradable membranes were elaborated for biomedical applications as tissue engineering, in which an active compound can be encapsulated and delivered.

ACKNOWLEDGEMENTS

First of all, I would like to thank my PhD supervisors for their great advices and support provided all over the last three years: Ana-Maria Popa, Anne Hébraud, Linda Thöny-Meyer, René M. Rossi and Guy Schlatter.

I would also like to thank the members of the jury for their interest and for the time taken to review my work: Prof. G. Schlatter, Prof. K. De Clerck, Prof. F. Bossard, Prof. P. Schaaf, Prof. L. Thöny-Meyer and Dr. R. Rossi.

I want to acknowledge all the people who helped and supported me in the lab: Barbara, Elisabeth, Fiona, Leonie, Noemie, Katherine, Stefi, Davide, Fabio, Karl, Gagik, Luciano, Matthias, Patrick and many others.

Then, I would like to give a special tribute to the friends with I spent my last three years here at Empa and outside Empa: Marek, Matthias, Gagik, Andrej, Matthew and Fiona.

My last thanks go of course to all my family, my Mum, my Father, Aurélie, Louise and my friends in Paris and Strasbourg.

REFERENCES

Chapter 1

1. Reneker, D. H.; Yarin, A. L., Electrospinning jets and polymer nanofibers. Polymer 2008, 49 (10), 2387-2425.

2. Reneker, D. H.; Chun, I., Nanometre diameter fibres of polymer, produced by electrospinning. Nanotechnology 1996, 7 (3), 216-223.

3. Greiner, A.; Wendorff, J. H., Electrospinning: A fascinating method for the preparation of ultrathin fibres. Angew Chem Int Edit 2007, 46 (30), 5670-5703.

4. Popa, A. M.; Eckert, R.; Crespy, D.; Rupper, P.; Rossi, R. M., A new generation of ultralight thermochromic indicators based on temperature induced gas release. J Mater Chem 2011, 21 (43), 17392-17395.

5. Guex, A. G.; Kocher, F. M.; Fortunato, G.; Korner, E.; Hegemann, D.; Carrel, T. P.; Tevaearai, H. T.; Giraud, M. N., Fine-tuning of substrate architecture and surface chemistry promotes muscle tissue development. Acta Biomater 2012, 8 (4), 1481-1489.

6. Sill, T. J.; von Recum, H. A., Electro spinning: Applications in drug delivery and tissue engineering. Biomaterials 2008, 29 (13), 1989-2006.

7. Wang, B. C.; Wang, Y. Z.; Yin, T. Y.; Yu, Q. S., Applications of Electrospinning Technique in Drug Delivery. Chem Eng Commun 2010, 197 (10), 1315-1338.

8. Huang, S.; Fu, X. B., Naturally derived materials-based cell and drug delivery systems in skin regeneration. J Control Release 2010, 142 (2), 149-159.

9. Szentivanyi, A.; Chakradeo, T.; Zernetsch, H.; Glasmacher, B., Electrospun cellular microenvironments: Understanding controlled release and scaffold structure. Adv Drug Deliver Rev 2011, 63 (4-5), 209-220.

10. Jaworek, A., Electrospray droplet sources for thin film deposition. J Mater Sci 2007, 42 (1), 266-297.

11. Morota, K.; Matsumoto, H.; Mizukoshi, T.; Konosu, Y.; Minagawa, M.; Tanioka, A.; Yamagata, Y.; Inoue, K., Poly(ethylene oxide) thin films produced by electrospray deposition: morphology control and additive effects of alcohols on nanostructure. J Colloid Interf Sci 2004, 279 (2), 484-492.

12. Lavielle, N.; Popa, A. M.; de Geus, M.; Hebraud, A.; Schlatter, G.; Thony-Meyer, L.; Rossi, R. M., Controlled formation of poly(Ɛ-caprolactone) ultrathin electrospun nanofibers in a hydrolytic degradation-assisted process. Eur Polym J 2013, 49 (6), 1331-1336.

13. Bock, N.; Dargaville, T. R.; Woodruff, M. A., Electrospraying of polymers with therapeutic molecules: State of the art. Prog Polym Sci 2012, 37 (11), 1510-1551.

14. Valo, H.; Peltonen, L.; Vehvilainen, S.; Karjalainen, M.; Kostiainen, R.; Laaksonen, T.; Hirvonen, J., Electrospray Encapsulation of Hydrophilic and Hydrophobic Drugs in Poly(L-lactic acid) Nanoparticles. Small 2009, 5 (15), 1791-1798.

15. Yoo, H. S.; Kim, T. G.; Park, T. G., Surface-functionalized electrospun nanofibers for tissue engineering and drug delivery. Adv Drug Deliver Rev 2009, 61 (12), 1033-1042.

16. Martins, A.; Duarte, A. R. C.; Faria, S.; Marques, A. P.; Reis, R. L.; Neves, N. M., Osteogenic induction of hBMSCs by electrospun scaffolds with dexamethasone release functionality. Biomaterials 2010, 31 (22), 5875-5885.

17. Luu, Y. K.; Kim, K.; Hsiao, B. S.; Chu, B.; Hadjiargyrou, M., Development of a nanostructured DNA delivery scaffold via electrospinning of PLGA and PLA-PEG block copolymers. J Control Release 2003, 89 (2), 341-353.

18. Luong-Van, E.; Grondahl, L.; Chua, K. N.; Leong, K. W.; Nurcombe, V.; Cool, S. M., Controlled release of heparin from poly(Ɛ-caprolactone) electrospun fibers. Biomaterials 2006, 27 (9), 2042-2050.

19. Sy, J. C.; Klemm, A. S.; Shastri, V. P., Emulsion as a Means of Controlling Electrospinning of Polymers. Adv Mater 2009, 21 (18), 1814-+.

20. Venugopal, G.; Krause, S.; Wnek, G. E., Morphological Variations in Polymer Blends Made in Electric-Fields. Chem Mater 1992, 4 (6), 1334-1343.

21. Xu, X. L.; Yang, L. X.; Xu, X. Y.; Wang, X.; Chen, X. S.; Liang, Q. Z.; Zeng, J.; Jing, X. B., Ultrafine medicated fibers electrospun from W/O emulsions. J Control Release 2005, 108 (1), 33-42.

22. Wang, C.; Yan, K. W.; Lin, Y. D.; Hsieh, P. C. H., Biodegradable Core/Shell Fibers by Coaxial Electrospinning: Processing, Fiber Characterization, and Its Application in Sustained Drug Release. Macromolecules 2010, 43 (15), 6389-6397.

23. Chakraborty, S.; Liao, I. C.; Adler, A.; Leong, K. W., Electrohydrodynamics: A facile technique to fabricate drug delivery systems. Adv Drug Deliver Rev 2009, 61 (12), 1043-1054.

24. Sun, X. Y.; Shankar, R.; Borner, H. G.; Ghosh, T. K.; Spontak, R. J., Field-driven biofunctionalization of polymer fiber surfaces during electrospinning. Adv Mater 2007, 19 (1), 87-+.

25. Sun, X. Y.; Nobles, L. R.; Borner, H. G.; Spontak, R. J., Field-driven surface segregation of biofunctional species on electrospun PMMA/PEO microfibers. Macromol Rapid Comm 2008, 29 (17), 1455-1460.

26. Huang, Z. M.; He, C. L.; Yang, A. Z.; Zhang, Y. Z.; Hang, X. J.; Yin, J. L.; Wu, Q. S., Encapsulating drugs in biodegradable ultrafine fibers through co-axial electrospinning. J Biomed Mater Res A 2006, 77A (1), 169-179.

27. Cui, W. G.; Li, X. H.; Zhou, S. B.; Weng, J., Degradation patterns and surface wettability of electrospun fibrous mats. Polym Degrad Stabil 2008, 93 (3), 731-738.

28. Cleland, J. L.; Lim, A.; Barron, L.; Duenas, E. T.; Powell, M. F., Development of a single-shot subunit vaccine for HIV-1 .4. Optimizing microencapsulation and pulsatile release of MN rgp120 from biodegradable microspheres. J Control Release 1997, 47 (2), 135-150.

29. Siepmann, J.; Gopferich, A., Mathematical modeling of bioerodible, polymeric drug delivery systems. Adv Drug Deliver Rev 2001, 48 (2-3), 229-247.

30. Liang, D.; Hsiao, B. S.; Chu, B., Functional electrospun nanofibrous scaffolds for biomedical applications. Adv Drug Deliver Rev 2007, 59 (14), 1392-1412.

31. Baker, B. M.; Nerurkar, N. L.; Burdick, J. A.; Elliott, D. M.; Mauck, R. L., Fabrication and Modeling of Dynamic Multipolymer Nanofibrous Scaffolds. J Biomech Eng-T Asme 2009, 131 (10).

32. Bottino, M. C.; Thomas, V.; Janowski, G. M., A novel spatially designed and functionally graded electrospun membrane for periodontal regeneration. Acta Biomater 2011, 7 (1), 216-224.

33. Piras, A. M.; Chiellini, F.; Chiellini, E.; Nikkola, L.; Ashammakhi, N., New multicomponent bioerodible electrospun nanofibers for dual-controlled drug release. J Bioact Compat Pol 2008, 23 (5), 423-443.

34. Okuda, T.; Tominaga, K.; Kidoaki, S., Time-programmed dual release formulation by multilayered drug-loaded nanofiber meshes. J Control Release 2010, 143 (2), 258-264.

35. Bonani, W.; Motta, A.; Migliaresi, C.; Tan, W., Biomolecule Gradient in Micropatterned Nanofibrous Scaffold for Spatiotemporal Release. Langmuir 2012, 28 (38), 13675-13687.

36. Wylie, R. G.; Ahsan, S.; Aizawa, Y.; Maxwell, K. L.; Morshead, C. M.; Shoichet, M. S., Spatially controlled simultaneous patterning of multiple growth factors in three-dimensional hydrogels. Nat Mater 2011, 10 (10), 799-806.

37. Xie, J. W.; Li, X. R.; Xia, Y. N., Putting Electrospun Nanofibers to Work for Biomedical Research. Macromol Rapid Comm 2008, 29 (22), 1775-1792.

38. Biondi, M.; Ungaro, F.; Quaglia, F.; Netti, P. A., Controlled drug delivery in tissue engineering. Adv Drug Deliver Rev 2008, 60 (2), 229-242.

39. Silva, E. A.; Mooney, D. J., Effects of VEGF temporal and spatial presentation on angiogenesis. Biomaterials 2010, 31 (6), 1235-1241.

40. Cao, L.; Mooney, D. J., Spatiotemporal control over growth factor signaling for therapeutic neovascularization. Adv Drug Deliver Rev 2007, 59 (13), 1340-1350.

41. Li, D.; Ouyang, G.; McCann, J. T.; Xia, Y. N., Collecting electrospun nanofibers with patterned electrodes. Nano Lett 2005, 5 (5), 913-916.

42. Katta, P.; Alessandro, M.; Ramsier, R. D.; Chase, G. G., Continuous electrospinning of aligned polymer nanofibers onto a wire drum collector. Nano Lett 2004, 4 (11), 2215-2218.

43. Yan, H.; Liu, L. Q.; Zhang, Z., Alignment of electrospun nanofibers using dielectric materials. Appl Phys Lett 2009, 95 (14).

44. Kuo, C. C.; Wang, C. T.; Chen, W. C., Highly-Aligned Electrospun Luminescent Nanofibers Prepared from Polyfluorene/PMMA Blends: Fabrication, Morphology, Photophysical Properties and Sensory Applications. Macromol Mater Eng 2008, 293 (12), 999-1008.

45. Carnell, L. S.; Siochi, E. J.; Holloway, N. M.; Stephens, R. M.; Rhim, C.; Niklason, L. E.; Clark, R. L., Aligned mats from electrospun single fibers. Macromolecules 2008, 41 (14), 5345-5349.

46. Wu, Y. Q.; Carnell, L. A.; Clark, R. L., Control of electrospun mat width through the use of parallel auxiliary electrodes. Polymer 2007, 48 (19), 5653-5661.

47. Zhang, D. M.; Chang, J., Electrospinning of Three-Dimensional Nanofibrous Tubes with Controllable Architectures. Nano Lett 2008, 8 (10), 3283-3287.

48. Murugan, R.; Ramakrishna, S., Design strategies of tissue engineering scaffolds with controlled fiber orientation. Tissue Eng 2007, 13 (8), 1845-1866.

49. Lavielle, N.; Hebraud, A.; Mendoza-Palomares, C.; Ferrand, A.; Benkirane-Jessel, N.; Schlatter, G., Structuring and Molding of Electrospun Nanofibers: Effect of Electrical and Topographical Local Properties of Micro-Patterned Collectors. Macromol Mater Eng 2012, 297 (10), 958-968.

50. Deitzel, J. M.; Kleinmeyer, J.; Harris, D.; Tan, N. C. B., The effect of processing variables on the morphology of electrospun nanofibers and textiles. Polymer 2001, 42 (1), 261-272.

51. Thandavamoorthy, S.; Gopinath, N.; Ramkumar, S. S., Self-assembled honeycomb polyurethane nanofibers. J Appl Polym Sci 2006, 101 (5), 3121-3124.

52. Ye, X. Y.; Huang, X. J.; Xu, Z. K., Nanofibrous mats with bird's nest patterns by electrospinning. Chinese J Polym Sci 2012, 30 (1), 130-137.

53. Yan, G. D.; Yu, J.; Qiu, Y. J.; Yi, X. H.; Lu, J.; Zhou, X. S.; Bai, X. D., Self-Assembly of Electrospun Polymer Nanofibers: A General Phenomenon Generating Honeycomb-Patterned Nanofibrous Structures. Langmuir 2011, 27 (8), 4285-4289.

54. Ahirwal, D.; Hebraud, A.; Kadar, R.; Wilhelm, M.; Schlatter, G., From self-assembly of electrospun nanofibers to 3D cm thick hierarchical foams. Soft Matter 2013, 9 (11), 3164-3172.

55. Huaqiong Li, Y. S. W., Feng Wen, Kee Woei Ng, Gary Ka Lai Ng, Subbu S. Venkatraman, Freddy Yin Chiang Boey, Lay Poh Tan, Human Mesenchymal Stem-Cell Behaviour On Direct Laser Micropatterned Electrospun Scaffolds with Hierarchical Structures. Macromol. Biosci. 2013, 13, 299-310.

56. Chen, J. T.; Chen, W. L.; Fan, P. W., Hierarchical Structures by Wetting Porous Templates with Electrospun Polymer Fibers. Acs Macro Lett 2012, 1 (1), 41-46.

57. Sundararaghavan, H. G.; Metter, R. B.; Burdick, J. A., Electrospun Fibrous Scaffolds with Multiscale and Photopatterned Porosity. Macromol Biosci 2010, 10 (3), 265-270.

58. Cipitria, A.; Skelton, A.; Dargaville, T. R.; Dalton, P. D.; Hutmacher, D. W., Design, fabrication and characterization of PCL electrospun scaffolds-a review. J Mater Chem 2011, 21 (26), 9419-9453.

59. Dong, Y. X.; Liao, S.; Ngiam, M.; Chan, C. K.; Ramakrishna, S., Degradation Behaviors of Electrospun Resorbable Polyester Nanofibers. Tissue Eng Part B-Re 2009, 15 (3), 333-351.

60. Rutledge, G. C.; Lowery, J. L.; Datta, N., Effect of fiber diameter, pore size and seeding method on growth of human dermal fibroblasts in electrospun poly(Ɛ-caprolactone) fibrous mats. Biomaterials 2010, 31 (3), 491-504.

61. Smith, L. A.; Ma, P. X., Nano-fibrous scaffolds for tissue engineering. Colloid Surface B 2004, 39 (3), 125-131.

62. Del Gaudio, C.; Grigioni, M.; Bianco, A.; De Angelis, G., Electrospun bioresorbable heart valve scaffold for tissue engineering. Int J Artif Organs 2008, 31 (1), 68-75.

63. Lee, K. H.; Kim, H. Y.; Khil, M. S.; Ra, Y. M.; Lee, D. R., Characterization of nano-structured poly(Ɛ-caprolactone) nonwoven mats via electrospinning. Polymer 2003, 44 (4), 1287-1294.

64. Moghe, A. K.; Hufenus, R.; Hudson, S. M.; Gupta, B. S., Effect of the addition of a fugitive salt on electrospinnability of poly(epsilon-caprolactone). Polymer 2009, 50 (14), 3311-3318.

65. Luo, C. J.; Stride, E.; Edirisinghe, M., Mapping the Influence of Solubility and Dielectric Constant on Electrospinning Polycaprolactone Solutions. Macromolecules 2012, 45 (11), 4669-4680.

66. Van der Schueren, L.; De Schoenmaker, B.; Kalaoglu, O. I.; De Clerck, K., An alternative solvent system for the steady state electrospinning of polycaprolactone. Eur Polym J 2011, 47 (6), 1256-1263.

Chapter 2

1. Reneker DH, Yarin AL. Electrospinning jets and polymer nanofibers. Polymer 2008;49(10): 2387-2425.

2. Reneker DH, Chun I. Nanometre diameter fibres of polymer, produced by electrospinning. Nanotechnology 1996;7(3): 216-223.

3. Greiner A, Wendorff JH. Electrospinning: A Fascinating Method for the Preparation of Ultrathin Fibers. Angew Chem Int Edit 2007;46(30): 5670-5703.

4. Popa AM, Eckert R, Crespy D, Rupper P, Rossi RM. A new generation of ultralight thermochromic indicators based on temperature induced gas release. J Mater Chem 2011;21(43): 17392-17395.

5. Guex AG, Kocher FM, Fortunato G, Körner E, Hegemann D, Carrel TP, Tevaearai HT, Giraud MN. Fine-tuning of substrate architecture and surface chemistry promotes muscle tissue development. Acta Biomat 2012;8(4): 1481-1489.

6. Sill TJ, von Recum HA. Electrospinning: Applications in drug delivery and tissue engineering. Biomaterials 2008;29(13): 1989-2006.

7. Cipitria A, Skelton A, Dargaville TR, Dalton PD, Hutmacher DW. Design, fabrication and characterization of PCL electrospun scaffolds - a review. J Mater Chem 2011;21(26): 9419-9453.

8. Lowery JL, Datta N, Rutledge GC. Effect of fiber diameter, pore size and seeding method on growth of human dermal fibroblasts in electrospun poly(ε-caprolactone) fibrous mats. Biomaterials 2010;31(3): 491–504.

9. Smith LA, Ma PX. Nano-fibrous scaffolds for tissue engineering . Colloid Surface B 2004;39(3): 125–131.

10. Del Gaudio C, Grigioni M, Bianco A, De Angelis G. Electrospun bioresorbable heart valve scaffold for tissue engineering. Int J Artif Organs 2008;31(1): 68–75.

11. Lee KH, Kim HY, Khil MS, Ra YM, Lee DR. Characterization of nano-structured poly(e-caprolactone) nonwoven mats via electrospinning. Polymer 2003;44(4): 1287-1294.

12. Moghe AK, Hufenus R, Hudson SM., Gupta BS. Effect of the addition of a fugitive salt on electrospinnability of poly(e-caprolactone). Polymer 2009;50(14): 3311-3318.

13. Luo CJ, Stride E, Edirisinghe M. Mapping the influence of solubility and dielectric constant on electrospinning polycaprolactone solutions. Macromolecules 2012;45(11): 4669-4680.

14. Van der Schueren L, De Schoenmaker B, Kalaoglu OI, De Clerck K. An alternative solvent system for the steady state electrospinning of polycaprolactone. Eur Polym J 2011;47(6): 1256-1263.

15. Grubisic Z, Rempp P, and Benoit H. A universal calibration for gel permeation chromatography. J Polym Sci Pol Phys 1996;34(10): 1707-1713.

16. Schindler A, Hibionada YM, Pitt CG. Aliphatic Polyesters. 111. Molecular Weight and Molecular Weight Distribution in Alcohol-Initiated Polymerizations of e-Caprolactone. J Polym Sci Pol Chem 1982;20(2): 319-326.

17. Yu H, Huang N, Wang C, Tang Z. Modeling of poly(L-lactide) thermal degradation: Theoretical prediction of molecular weight and polydispersity index. J of Appl Polym Sci 2003;88(11): 2557–2562.

18. Pitt CG, Gu Z. Modification of the rates of chain cleavage of poly(ϵ-caprolactone) and related polyesters in the solid state. J Controlled Release 1987;4(4): 283-292.

19. Lyu S, Sparer R, Untereker D. Analytical solutions to mathematical models of the surface and bulk erosion of solid polymers. J Polym Sci Polym Phys 2005;43(4): 383-397.

20. Simha R. Kinetics of Degradation and Size Distribution of Long Chain Polymers. J Appl Phys 1941;12(7): 569-578.

21. Antheunis H, Van der Meer JC, De Geus M, Heise A, Koning CE. Autocatalytic Equation Describing the Change in Molecular Weight during Hydrolytic Degradation of Aliphatic Polyesters. Biomacromolecules 2010;11(4): 1118-1124.

22. Gupta P, Elkins C, Long TE, Wilkes GL. Electrospinning of linear homopolymers of poly(methyl methacrylate): exploring relationships between fiber formation, viscosity, molecular weight and concentration in a good solvent. Polymer 2005;46(13): 4799-4810.

23. Koski A, Yim K, Shivkumar S. Effect of molecular weight on fibrous PVA produced by electrospinning. Mater Lett 2004;58(3-4): 493-497.

24. Fong H, Chun I, Reneker DH. Beaded nanofibers formed during electrospinning. Polymer 1999;40(16): 4585-4592.

25. McKee MG, Wilkes GL, Colby RH, Long TE. Correlations of Solution Rheology with Electrospun Fiber Formation of Linear and Branched Polyesters. Macromolecules 2004;37(5): 1760-1767.

Chapter 3

1. Reneker, D. H.; Yarin, A. L., Electrospinning jets and polymer nanofibers. Polymer 2008, 49 (10), 2387-2425.

2. Reneker, D. H.; Chun, I., Nanometre diameter fibres of polymer, produced by electrospinning. Nanotechnology 1996, 7 (3), 216-223.

3. Greiner, A.; Wendorff, J. H., Electrospinning: A fascinating method for the preparation of ultrathin fibres. Angew Chem Int Edit 2007, 46 (30), 5670-5703.

4. Popa, A. M.; Eckert, R.; Crespy, D.; Rupper, P.; Rossi, R. M., A new generation of ultralight thermochromic indicators based on temperature induced gas release. J Mater Chem 2011, 21 (43), 17392-17395.

5. Guex, A. G.; Kocher, F. M.; Fortunato, G.; Korner, E.; Hegemann, D.; Carrel, T. P.; Tevaearai, H. T.; Giraud, M. N., Fine-tuning of substrate architecture and surface chemistry promotes muscle tissue development. Acta Biomater 2012, 8 (4), 1481-1489.

6. Sill, T. J.; von Recum, H. A., Electro spinning: Applications in drug delivery and tissue engineering. Biomaterials 2008, 29 (13), 1989-2006.

7. Szentivanyi, A.; Chakradeo, T.; Zernetsch, H.; Glasmacher, B., Electrospun cellular microenvironments: Understanding controlled release and scaffold structure. Adv Drug Deliver Rev 2011, 63 (4-5), 209-220.

8. Bottino, M. C.; Thomas, V.; Janowski, G. M., A novel spatially designed and functionally graded electrospun membrane for periodontal regeneration. Acta Biomater 2011, 7 (1), 216-224.

9. Bonani, W.; Motta, A.; Migliaresi, C.; Tan, W., Biomolecule Gradient in Micropatterned Nanofibrous Scaffold for Spatiotemporal Release. Langmuir 2012, 28 (38), 13675-13687.

10. Okuda, T.; Tominaga, K.; Kidoaki, S., Time-programmed dual release formulation by multilayered drug-loaded nanofiber meshes. J Control Release 2010, 143 (2), 258-264.

11. Katta, P.; Alessandro, M.; Ramsier, R. D.; Chase, G. G., Continuous electrospinning of aligned polymer nanofibers onto a wire drum collector. Nano Lett 2004, 4 (11), 2215-2218.

12. Li, D.; Ouyang, G.; McCann, J. T.; Xia, Y. N., Collecting electrospun nanofibers with patterned electrodes. Nano Lett 2005, 5 (5), 913-916.

13. Murugan, R.; Ramakrishna, S., Design strategies of tissue engineering scaffolds with controlled fiber orientation. Tissue Eng 2007, 13 (8), 1845-1866.

14. Lavielle, N.; Hebraud, A.; Mendoza-Palomares, C.; Ferrand, A.; Benkirane-Jessel, N.; Schlatter, G., Structuring and Molding of Electrospun Nanofibers: Effect of Electrical and Topographical Local Properties of Micro-Patterned Collectors. Macromol Mater Eng 2012, 297 (10), 958-968.

15. Zhang, D. M.; Chang, J., Electrospinning of Three-Dimensional Nanofibrous Tubes with Controllable Architectures. Nano Lett 2008, 8 (10), 3283-3287.

16. Huaqiong Li, Y. S. W., Feng Wen, Kee Woei Ng, Gary Ka Lai Ng, Subbu S. Venkatraman, Freddy Yin Chiang Boey, Lay Poh Tan, Human Mesenchymal Stem-Cell Behaviour On Direct Laser Micropatterned Electrospun Scaffolds with Hierarchical Structures. Macromol. Biosci. 2013, 13, 299-310.

17. Chen, J. T.; Chen, W. L.; Fan, P. W., Hierarchical Structures by Wetting Porous Templates with Electrospun Polymer Fibers. Acs Macro Lett 2012, 1 (1), 41-46.

18. Sundararaghavan, H. G.; Metter, R. B.; Burdick, J. A., Electrospun Fibrous Scaffolds with Multiscale and Photopatterned Porosity. Macromol Biosci 2010, 10 (3), 265-270.

19. Deitzel, J. M.; Kleinmeyer, J.; Harris, D.; Tan, N. C. B., The effect of processing variables on the morphology of electrospun nanofibers and textiles. Polymer 2001, 42 (1), 261-272.

20. Thandavamoorthy, S.; Gopinath, N.; Ramkumar, S. S., Self-assembled honeycomb polyurethane nanofibers. Journal of Applied Polymer Science 2006, 101 (5), 3121-3124.

21. Ye, X. Y.; Huang, X. J.; Xu, Z. K., Nanofibrous mats with bird's nest patterns by electrospinning. Chinese J Polym Sci 2012, 30 (1), 130-137.

22. Yan, G. D.; Yu, J.; Qiu, Y. J.; Yi, X. H.; Lu, J.; Zhou, X. S.; Bai, X. D., Self-Assembly of Electrospun Polymer Nanofibers: A General Phenomenon Generating Honeycomb-Patterned Nanofibrous Structures. Langmuir 2011, 27 (8), 4285-4289.

23. Ahirwal, D.; Hebraud, A.; Kadar, R.; Wilhelm, M.; Schlatter, G., From self-assembly of electrospun nanofibers to 3D cm thick hierarchical foams. Soft Matter 2013, 9 (11), 3164-3172.

24. Ladd, M. R.; Lee, S. J.; Stitzel, J. D.; Atala, A.; Yoo, J. J., Co-electrospun dual scaffolding system with potential for muscle-tendon junction tissue engineering. Biomaterials 2011, 32 (6), 1549-1559.

25. Hong, Y.; Fujimoto, K.; Hashizume, R.; Guan, J. J.; Stankus, J. J.; Tobita, K.; Wagner, W. R., Generating elastic, biodegradable polyurethane/poly(lactide-co-glycolide) fibrous sheets with controlled antibiotic release via two-stream electrospinning. Biomacromolecules 2008, 9 (4), 1200-1207.

26. Bonani, W.; Maniglio, D.; Motta, A.; Tan, W.; Migliaresi, C., Biohybrid nanofiber constructs with anisotropic biomechanical properties. J Biomed Mater Res B 2011, 96B (2), 276-286.

27. Jaworek, A., Electrospray droplet sources for thin film deposition. J Mater Sci 2007, 42 (1), 266-297.

28. Morota, K.; Matsumoto, H.; Mizukoshi, T.; Konosu, Y.; Minagawa, M.; Tanioka, A.; Yamagata, Y.; Inoue, K., Poly(ethylene oxide) thin films produced by electrospray

deposition: morphology control and additive effects of alcohols on nanostructure. J Colloid Interf Sci 2004, 279 (2), 484-492.

29. Lavielle, N.; Popa, AM.; de Geus, M.; Hebraud, A.; Schlatter, G.; Thony-Meyer, L.; Rossi, RM., Controlled formation of poly(Ɛ-caprolactone) ultrathin electrospun nanofibers in a hydrolytic degradation-assisted process. Eur Polym J 2013, 49 (6), 1331-1336.

30. Bock, N.; Dargaville, T. R.; Woodruff, M. A., Electrospraying of polymers with therapeutic molecules: State of the art. Prog Polym Sci 2012, 37 (11), 1510-1551.

31. Ekaputra, A. K.; Prestwich, G. D.; Cool, S. M.; Hutmacher, D. W., Combining electrospun scaffolds with electrosprayed hydrogels leads to three-dimensional cellularization of hybrid constructs. Biomacromolecules 2008, 9 (8), 2097-2103.

32. Gupta, D.; Venugopal, J.; Mitra, S.; Dev, V. R. G.; Ramakrishna, S., Nanostructured biocomposite substrates by electrospinning and electrospraying for the mineralization of osteoblasts. Biomaterials 2009, 30 (11), 2085-2094.

33. Stankus, J. J.; Soletti, L.; Fujimoto, K.; Hong, Y.; Vorp, D. A.; Wagner, W. R., Fabrication of cell microintegrated blood vessel constructs through electrohydrodynamic atomization. Biomaterials 2007, 28 (17), 2738-2746.

34. Valo, H.; Peltonen, L.; Vehvilainen, S.; Karjalainen, M.; Kostiainen, R.; Laaksonen, T.; Hirvonen, J., Electrospray Encapsulation of Hydrophilic and Hydrophobic Drugs in Poly(L-lactic acid) Nanoparticles. Small 2009, 5 (15), 1791-1798.

35. Chu, X. L.; Wasan, D. T., Attractive interaction between similarly charged colloidal particles. J Colloid Interf Sci 1996, 184 (1), 268-278.

36. Stankus, J. J.; Guan, J. J.; Fujimoto, K.; Wagner, W. R., Microintegrating smooth muscle cells into a biodegradable, elastomeric fiber matrix. Biomaterials 2006, 27 (5), 735-744.

37. Van der Schueren, L.; De Schoenmaker, B.; Kalaoglu, O. I.; De Clerck, K., An alternative solvent system for the steady state electrospinning of polycaprolactone. Eur Polym J 2011, 47 (6), 1256-1263.

38. Bichoutskaia, E.; Boatwright, A. L.; Khachatourian, A.; Stace, A. J., Electrostatic analysis of the interactions between charged particles of dielectric materials. J Chem Phys 2010, 133 (2).

39. Stace, A. J.; Boatwright, A. L.; Khachatourian, A.; Bichoutskaia, E., Why like-charged particles of dielectric materials can be attracted to one another. J Colloid Interf Sci 2011, 354 (1), 417-420.

40. Baker, B. M.; Gee, A. O.; Metter, R. B.; Nathan, A. S.; Marklein, R. A.; Burdick, J. A.; Mauck, R. L., The potential to improve cell infiltration in composite fiber-aligned electrospun scaffolds by the selective removal of sacrificial fibers. Biomaterials 2008, 29 (15), 2348-2358.

41. Ionescu, L. C.; Lee, G. C.; Sennett, B. J.; Burdick, J. A.; Mauck, R. L., An anisotropic nanofiber/microsphere composite with controlled release of biomolecules for fibrous tissue engineering. Biomaterials 2010, 31 (14), 4113-4120.

42. Eap, S.; Ferrand, A.; Palomares, C. M.; Hebraud, A.; Stoltz, J. F.; Mainard, D.; Schlatter, G.; Benkirane-Jessel, N., Electrospun nanofibrous 3D scaffold for bone tissue engineering. Bio-Med Mater Eng 2012, 22 (1-3), 137-141.

43. Vitale-Brovarone, C.; Baino, F.; Verne, E., Feasibility and Tailoring of Bioactive Glass-ceramic Scaffolds with Gradient of Porosity for Bone Grafting. J Biomater Appl 2010, 24 (8), 693-712.

44. Karageorgiou, V.; Kaplan, D., Porosity of 3D biornaterial scaffolds and osteogenesis. Biomaterials 2005, 26 (27), 5474-5491.

45. Bruil A, Feijen J, Wenzel-Rejda T. (NPBI Nederlands Produktielaboratorium voor Bloedtransfusieapparatuur en Infusievloeistoffen B.V.). EP0406485 A1, January 9, 1991

Chapter 4

1. Reneker, D. H.; Chun, I., Nanometre diameter fibres of polymer, produced by electrospinning. Nanotechnology 1996, 7 (3), 216-223.

2. Reneker, D. H.; Yarin, A. L., Electrospinning jets and polymer nanofibers. Polymer 2008, 49 (10), 2387-2425.

3. Greiner, A.; Wendorff, J. H., Electrospinning: A fascinating method for the preparation of ultrathin fibres. Angew Chem Int Edit 2007, 46 (30), 5670-5703.

4. Popa, A. M.; Eckert, R.; Crespy, D.; Rupper, P.; Rossi, R. M., A new generation of ultralight thermochromic indicators based on temperature induced gas release. J Mater Chem 2011, 21 (43), 17392-17395.

5. Guex, A. G.; Kocher, F. M.; Fortunato, G.; Korner, E.; Hegemann, D.; Carrel, T. P.; Tevaearai, H. T.; Giraud, M. N., Fine-tuning of substrate architecture and surface chemistry promotes muscle tissue development. Acta Biomater 2012, 8 (4), 1481-1489.

6. Sill, T. J.; von Recum, H. A., Electro spinning: Applications in drug delivery and tissue engineering. Biomaterials 2008, 29 (13), 1989-2006.

7. Wang, B. C.; Wang, Y. Z.; Yin, T. Y.; Yu, Q. S., Applications of Electrospinning Technique in Drug Delivery. Chem Eng Commun 2010, 197 (10), 1315-1338.

8. Liang, D.; Hsiao, B. S.; Chu, B., Functional electrospun nanofibrous scaffolds for biomedical applications. Adv Drug Deliver Rev 2007, 59 (14), 1392-1412.

9. Szentivanyi, A.; Chakradeo, T.; Zernetsch, H.; Glasmacher, B., Electrospun cellular microenvironments: Understanding controlled release and scaffold structure. Adv Drug Deliver Rev 2011, 63 (4-5), 209-220.

10. Xu, W. J.; Atala, A.; Yoo, J. J.; Lee, S. J., Controllable dual protein delivery through electrospun fibrous scaffolds with different hydrophilicities. Biomed Mater 2013, 8 (1).

11. Biondi, M.; Ungaro, F.; Quaglia, F.; Netti, P. A., Controlled drug delivery in tissue engineering. Adv Drug Deliver Rev 2008, 60 (2), 229-242.

12. Bottino, M. C.; Thomas, V.; Janowski, G. M., A novel spatially designed and functionally graded electrospun membrane for periodontal regeneration. Acta Biomater 2011, 7 (1), 216-224.

13. Thakur, R. A.; Florek, C. A.; Kohn, J.; Michniak, B. B., Electrospun nanofibrous polymeric scaffold with targeted drug release profiles for potential application as wound dressing. Int J Pharmaceut 2008, 364 (1), 87-93.

14. Bonani, W.; Motta, A.; Migliaresi, C.; Tan, W., Biomolecule Gradient in Micropatterned Nanofibrous Scaffold for Spatiotemporal Release. Langmuir 2012, 28 (38), 13675-13687.

15. Okuda, T.; Tominaga, K.; Kidoaki, S., Time-programmed dual release formulation by multilayered drug-loaded nanofiber meshes. J Control Release 2010, 143 (2), 258-264.

16. Chen, D. W. C.; Liao, J. Y.; Liu, S. J.; Chan, E. C., Novel biodegradable sandwich-structured nanofibrous drug-eluting membranes for repair of infected wounds: an in vitro and in vivo study. Int J Nanomed 2012, 7, 763-771.

17. Lee, M. W.; An, S.; Joshi, B.; Latthe, S. S.; Yoon, S. S., Highly Efficient Wettability Control via Three-Dimensional (3D) Suspension of Titania Nanoparticles in Polystyrene Nanofibers. Acs Appl Mater Inter 2013, 5 (4), 1232-1239.

18. Lavielle, N.; Popa, AM.; de Geus, M.; Hebraud, A.; Schlatter, G.; Thony-Meyer, L.; Rossi, RM., Controlled formation of poly(Ɛ-caprolactone) ultrathin electrospun nanofibers in a hydrolytic degradation-assisted process. Eur Polym J 2013, 49 (6), 1331-1336.

19. Lavielle, N.; Hebraud, A.; Schlatter, G.; Thony-Meyer, L.; Rossi, RM., Popa, AM., Simultaneous electrospinning and electrospraying: A straightforward approach for fabricating hierarchically structured composite membranes. Acs Appl Mater Inter 2013, online.

20. Gau, H.; Herminghaus, S.; Lenz, P.; Lipowsky, R., Liquid morphologies on structured surfaces: From microchannels to microchips. Science 1999, 283 (5398), 46-49.

21. Abbott, N. L.; Folkers, J. P.; Whitesides, G. M., Manipulation of the Wettability of Surfaces on the 0.1-Micrometer to 1-Micrometer Scale through Micromachining and Molecular Self-Assembly. Science 1992, 257 (5075), 1380-1382.

22. Shull, K. R.; Karis, T. E., Dewetting Dynamics for Large Equilibrium Contact Angles. Langmuir 1994, 10 (1), 334-339.

23. Cui, W. G.; Li, X. H.; Zhu, X. L.; Yu, G.; Zhou, S. B.; Weng, J., Investigation of drug release and matrix degradation of electrospun poly(DL-lactide) fibers with paracetanol inoculation. Biomacromolecules 2006, 7 (5), 1623-1629.

24. Slowing, I. I.; Vivero-Escoto, J. L.; Wu, C. W.; Lin, V. S. Y., Mesoporous silica nanoparticles as controlled release drug delivery and gene transfection carriers. Adv Drug Deliver Rev 2008, 60 (11), 1278-1288.

25. Elzoghby, A. O.; Samy, W. M.; Elgindy, N. A., Albumin-based nanoparticles as potential controlled release drug delivery systems. J Control Release 2012, 157 (2), 168-182.

26. Wang, F.; Li, Z. Q.; Tamama, K.; Sen, C. K.; Guan, J. J., Fabrication and Characterization of Prosurvival Growth Factor Releasing, Anisotropic Scaffolds for Enhanced Mesenchymal Stem Cell Survival/Growth and Orientation. Biomacromolecules 2009, 10 (9), 2609-2618.